2019

OXIDATIVE DEGRADATION OF LIGNIN AND INVESTIGATION OF UTILIZATION OF LIGNIN-DERIVED MATERIALS AS BUILDING BLOCKS FOR EPOXY RESINS

Zhen Fang
University of Kentucky, kongkong10086@gmail.com
Author ORCID Identifier:
https://orcid.org/0000-0001-7695-9427
Digital Object Identifier: https://doi.org/10.13023/etd.2019.025

STUDENT AGREEMENT:

I represent that my thesis or dissertation and abstract are my original work. Proper attribution has been given to all outside sources. I understand that I am solely responsible for obtaining any needed copyright permissions. I have obtained needed written permission statement(s) from the owner(s) of each third-party copyrighted matter to be included in my work, allowing electronic distribution (if such use is not permitted by the fair use doctrine) which will be submitted to UKnowledge as Additional File.

I hereby grant to The University of Kentucky and its agents the irrevocable, non-exclusive, and royalty-free license to archive and make accessible my work in whole or in part in all forms of media, now or hereafter known. I agree that the document mentioned above may be made available immediately for worldwide access unless an embargo applies.

I retain all other ownership rights to the copyright of my work. I also retain the right to use in future works (such as articles or books) all or part of my work. I understand that I am free to register the copyright to my work.

REVIEW, APPROVAL AND ACCEPTANCE

The document mentioned above has been reviewed and accepted by the student's advisor, on behalf of the advisory committee, and by the Director of Graduate Studies (DGS), on behalf of the program; we verify that this is the final, approved version of the student's thesis including all changes required by the advisory committee. The undersigned agree to abide by the statements above.

Zhen Fang, Student

Dr. Mark S. Meier, Major Professor

Dr. Mark A. Lovell, Director of Graduate Studies

OXIDATIVE DEGRADATION OF LIGNIN AND INVESTIGATION OF UTILIZATION OF LIGNIN-DERIVED MATERIALS AS BUILDING BLOCKS FOR EPOXY RESINS

DISSERTATION

A dissertation submitted in partial fulfillment of the
requirements for the degree of Doctor of Philosophy in the
College of Arts and Sciences
at the University of Kentucky

By

Zhen Fang

Lexington, Kentucky

Director: Dr. Mark S. Meier, Professor of Chemistry

Lexington, Kentucky

2019

ABSTRACT OF DISSERTATION

OXIDATIVE DEGRADATION OF LIGNIN AND INVESTIGATION OF UTILIZATION OF LIGNIN-DERIVED MATERIALS AS BUILDING BLOCKS FOR EPOXY RESINS

Lignin, the second most abundant biopolymer on earth, is potentially a replaceable source for bulky fuels and chemical feedstocks. There have been numerous reports on methods for the oxidative cleavage of β-O-4 linkages but relatively few reports of how those methods affect other linkages that are present in lignin. We investigated how the β-1 and β-5 linkages respond under oxidative conditions proposed for lignin deconstruction based on their effect on β-O-4 linkages. Mechanochemical treatment of lignin can greatly improve the yield of monomer products and we applied a mechanochemical approach, using powerful ring-and-puck milling to promote lignin degradation. Along with similar production of monomers in a much shorter period than what we observed in previous ball-milling process, much more unexpected reactions were taking place during the current mechanochemical process.

Lignin is a promising feedstock for epoxy resins since lignin-derived aromatic monomers usually bear hydroxyl and carboxyl groups. We are working on utilizing these mono-aromatic compounds and highly-functionalized-lignin as precursors for preparation of epoxy thermosets. We are interested in investigating the properties of thermosets by utilizing the actual isolated monomer streams from raw lignin. We expect to observe attractive thermal and mechanical properties from these lignin-derived epoxy thermosets compare to that of the commercialized but currently limited-used BPA-based epoxy resins.

KEYWORDS: *Oxidative degradation, β-1 and β-5 model compounds, mechanical milling, epoxy resins, kraft lignin*

Zhen Fang

02/23/2019

OXIDATIVE DEGRADATION OF LIGNIN AND INVESTIGATION OF UTILIZATION OF LIGNIN-DERIVED MATERIALS AS BUILDING BLOCKS FOR EPOXY RESINS

By
Zhen Fang

Mark S. Meier
Director of Dissertation

Mark A. Lovell
Director of Graduate Studies

02/23/2019
Date

ACKNOWLEDGEMENTS

I would express my sincere appreciation to my advisor, professor Mark S. Meier, as this dissertation was completed under his excellent guidance and patient help. After spending over 4 years with Dr. Meier, I have greatly improved my knowledge and experimental skills. He is not only an outstanding professor but also a great friend. I also would like to thank Dr. Mark Crocker at CAER as he shared lots of brilliant ideas and helped me a lot as well. Collaborating with the catalysis group and attending bi-weekly co-group meetings really benefit me so much.

I would like to express my sincere gratitude to my committee members, Dr. Robert B. Grossman and Dr. Y. T. Cheng for their supportive and brilliant suggestions in my graduate study, as well as Dr. Michael Sama from AEN program for serving as the Outside Examiner.

I appreciate all the kind people in the department for their academic and professional support. I would like to thank Dr. Sean Parkin for his talented skills in identifying my unexpected di-ketone product, John Layton and Dr. A. F. Miller for their excellent training for the NMR technique, Dr. John Selegue for his maintenance and calibration of the DSC instrument, Dr. Matt Weisenberger from CAER for his insights in designing the single-cantilever DMA test, Art Sebesta, Charles Tipton and Jim Hover (CAER) for their design, cutting and polishing the sample bars for DMA experiment, Ashley Morris and Tristana Duvallet from CAER for their training in DMA and TGA test, and Dr. Mark Watson who also shared supportive insights for my laboratory work.

Moreover, I feel so grateful and lucky to have my wife Mingjian Pan and my parents being so supportive to my career. And I would thank our financial support. This work was financially supported by the National Science Foundation under awards NSF-EFRI-0937657 and NSF-IIA-1355438.

Table of Contents

List of Tables

List of Figures

List of Schemes

List of Abbreviations

^{13}C NMR	carbon-13 nuclear magnetic resonance
^{1}H NMR	proton nuclear magnetic resonance
^{31}P NMR	Phosphorus-31 nuclear magnetic resonance
aq.	aqueous
atm	atmosphere
BADGE	bisphenol A diglycidyl ether
BF_3•OEt_2	boron trifluoride diethyl etherate
BMKL	ball milled kraft lignin
BP	The British Petroleum Company plc and BP Amoco plc
BPA	Bisphenol A
BPF	Bisphenol F
B-V	Baeyer-Villiger
CAER	Center for Applied Energy Research
DCE	dichloromethane
DCM	dichloromethane
DDQ	2,3-dicholoro-5,6-dicyano-1,4-benzoquinone
DMA	dynamic mechanical analysis
DMF	dimethyl formamide
DMSO	dimethyl sulfoxide
DOE	Department of Energy
DSC	Differential scanning calorimetry

eq	equivalent
EA/EtOAc	ethyl acetate
EPON 826	BPA-based epoxy resin
EPON 862	BPF-based epoxy resin
G	guaiacyl
GC-MS	gas chromatography-mass spectrometry
GE-EAS	glycidyl ether of ethyl acetate soluble portion
GGE	gallon gasoline equivalent
H	hydroxyphenyl
HSQC	heteronuclear single quantum coherence
Hz	hertz
KL	kraft lignin
m-CPBA	meta-Chloroperoxybenzoic acid
MHz	megahertz
MWL	milled wood lignin
OSMKL	Oxidized shatterbox milled kraft lignin
PCC	pyridinium chlorochromate
Porp	porphyrin
S	syringyl
SMKL	shatterbox milled kraft lignin
t-BuOOH	tert-butylhydroperoxide
TEMPO	2,2,6,6-tetramethylpiperidine 1-oxyl

TGA	Thermogravimetric analysis
THF	tetrahydrofuran
TPPFeCl	tetraphenylporphyrin iron chloride
USDA	United States Department of Agriculture
δ	chemical shift

Chapter 1 Background Introduction

1.1 Renewables and Biomass

Non-renewable fossil fuels have provided most of the energy supply in the past century, and petroleum products have significantly contributed to human development. The necessities of human life like food, fuels and chemicals are dependent on petroleum-based industries. As of 2014, the world's proven oil reserves of 1.7 trillion barrels can only meet the next 52.5 years of global needs.[1] According to a report from BP,[1] in 2015 over 92 million barrels of crude oil were consumed every day to satisfy the energy needs of the world, and that demand will increase to 116 million barrels by 2030.[2] On the other hand, utilization of petroleum products has caused increasing environmental issues that could threaten the survival of humanity. The combination of severe concerns over the depletion of fossil fuel as energy source and global warming driven by fossil fuel consumption means that there is an urgent need for the development of renewable and environmentally-friendly energy resources. Only 19% of energy consumption in 2011 was supplied by renewable sources (such as wind, solar and biomass) and approximately 78% came from fossil fuels,[3] which illustrates that the role of renewables can grow substantially.

Biomass and its derivatives are considered one of the most promising substitutes for fossil fuels,[4] as they are easily generated in large amounts via biological photosynthesis from water, sunlight and CO_2. Terrestrial plants have shown great potential, and as carbon-neutral materials they will not adversely affect the global carbon balance because forests will absorb CO_2 to grow.[5] Between 80-164 billion tons of dry matter is produced annually[6] and utilization of this material could greatly mitigate the environmental and climate change caused by use of

fossil fuels, while at the same time reducing the societal dependence on fossil-based materials, as shown in Figure 1.1. For example, about 341 million tons of dry lignocellulosic biomass was available in the US in 2012,[7] 30% of which came from biomass that was generated from forest residue and the remaining 70% from agricultural residue. An ambitious goal has been set by the USDA and USDE[7] that 25% of chemicals and materials and 20% of liquid transportation fuel are to be produced from biomass by 2022. The European Union has also set similar mandatory goals to replace 30% of transportation fuels and 25-40% of products and fuels from fossil feedstock by biomass-derived materials.[8] In addition, use of renewable biomass can cut the cost of waste disposal, for example an estimate of 10 million dollars in land fill fees was paid annually for the disposal of apple dregs in US.[9] These benefits have attracted more interest and attention to the expansion of techniques and strategies to process biomass.

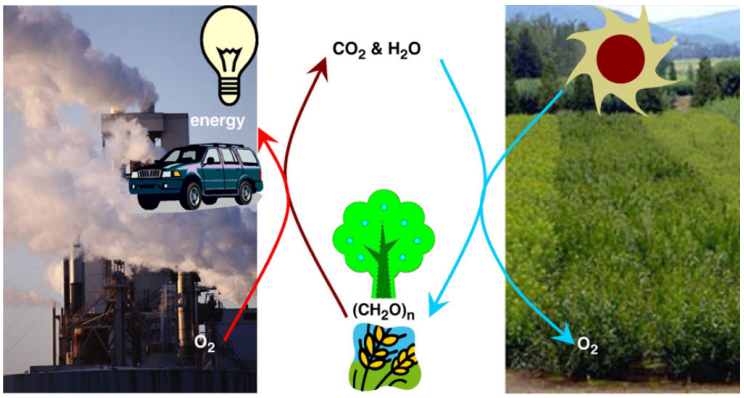

Figure 1. 1 Terrestrial plants absorb CO_2 from atmosphere, H_2O mostly from soil and energy from sunlight to produce biomass as well as O_2. Then O_2 can be reacted with biomass to produce energy, CO_2 and H_2O. No net CO_2 and H_2O is produced in this cyclic process.[5]

1.2 Why lignin?

More than 170 billion tons[5] of lignocellulose biomass, the most abundant bio-renewable resource on earth, is produced annually. Lignocellulose is composed of 20-30%

hemicellulose and 40-50% cellulose and lignin, wherein lignin contributes 15-30% by weight and up to 40% by energy of lignocellulosic biomass.[5, 8] Lignin is the second most abundant biopolymer and as a main byproduct of paper and pulp industry, an estimated production of 50 million tons of lignin was isolated in 2010[10] but only 2% of that lignin was used in low-value application for heat or power supply while the remaining 98% was simply burned as a low-value fuel.[11] These uses do not take full advantage of lignin to produce high-value products which stimulates the desire to find not only to isolate lignin from biomass but also to increase the commercial value of lignin-based products. The "money equivalent" of lignin that is directly used as fuels is only $0.18/kg and is about $1.08/kg when lignin can be converted into useful chemicals.[12] This difference leads to the development of techniques and strategies to convert lignin into value added and price-competitive chemicals. It has been suggested that if 60%-80% of lignin can be specifically converted into adipic acid and 1,4-butanediol, the minimum fuel selling price can be reduced to $3/GGE (gallon gasoline equivalent) from the current (2018) price of $5.10/GGE.[13]

Lignin is still primarily considered as the promising feedstock of aromatic chemicals due to its aromatic skeleton. Since lignin behaves as a resin that fills the spaces between hemicellulose and cellulose (which are both polymers of C5 and C6 sugars[14]) to supply the rigidity to the overall plant structure (shown in Figure 1.2), separation of lignin will make the hemicellulose and cellulose fractions more accessible to biological and chemical digestion.[14]

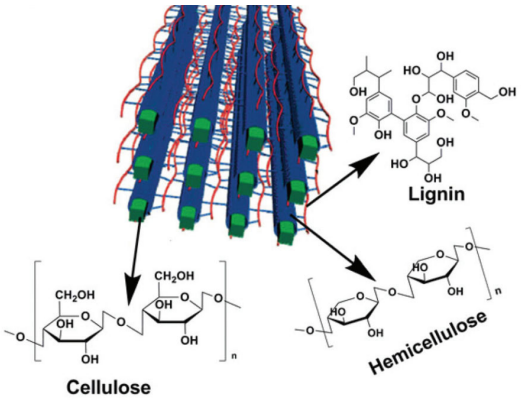

Figure 1. 2 Schematic analysis of the location and structure of lignin in lignocellulosic material[15]

1.3 Structure and Property of Lignin

1.3.1 Building units

Lignin can be defined as a highly methoxylated 3-dimensional cross-linked amorphous polymer composed of three primary monolignols: sinapyl, coniferyl, and p-coumaryl alcohols, also known as syringyl (S), guaiacyl (G), and p-hydroxyphenyl (H) units, respectively, as shown in Figure 1.3.

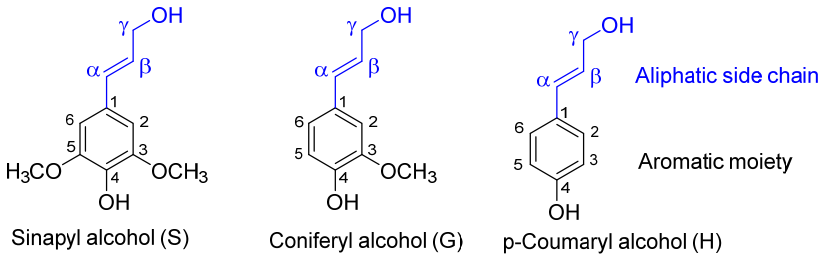

Figure 1. 3 Three monolignol monomers, primary building units of lignin[16]

These three monolignols all consist of a propyl side chain and a phenyl group but differ in the number of methoxy groups that are attached to the aromatic ring: *p*-coumaryl, coniferyl, and sinapyl alcohols carry none, one, and two methoxy groups, respectively. The carbon atoms on the aromatic rings are labeled as 1 to 6 while those in the aliphatic branches are labeled as α, β and γ in order to get those various linkage types categorized (Figure 1.3).

Lignin can be classified into four different types: type-G lignin (softwood lignin, which has more guaiacyl species), type-G-S (hardwood lignin, which contains both guaiacyl and syringyl units), type-H-G-S (grass lignin, which contains all of the three blocks), and type-H-G lignin based on the diversity of monomer abundance.[17] Due to the variety of monomer content, the linkages formed during polymerization by random phenyl radical-radical coupling reactions will also differ, which makes it quite difficult to determine the exact structure of each isolated lignin. Scheme 1.1 shows several resonance forms of a phenoxyl radical formed from coniferyl alcohol via a one-electron oxidation, and radical coupling reactions can occur in any of several different positions due to the delocalization of the unpaired electron.[18]

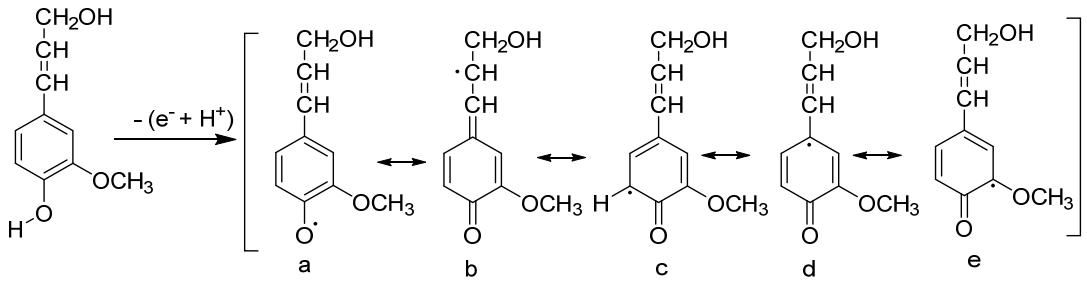

Scheme 1. 1 Resonance forms of the coniferyl alcohol radical[18]

1.3.2 Linkage Types

Lignin monolignols are linked by either C-O-C or C-C bonds, wherein the most common linkages are ether bonds (C-O-C) which comprises almost two thirds of the linkage structures of lignin. Some of the examples of C-O-C and C-C linkages are shown in Figure 1.4.

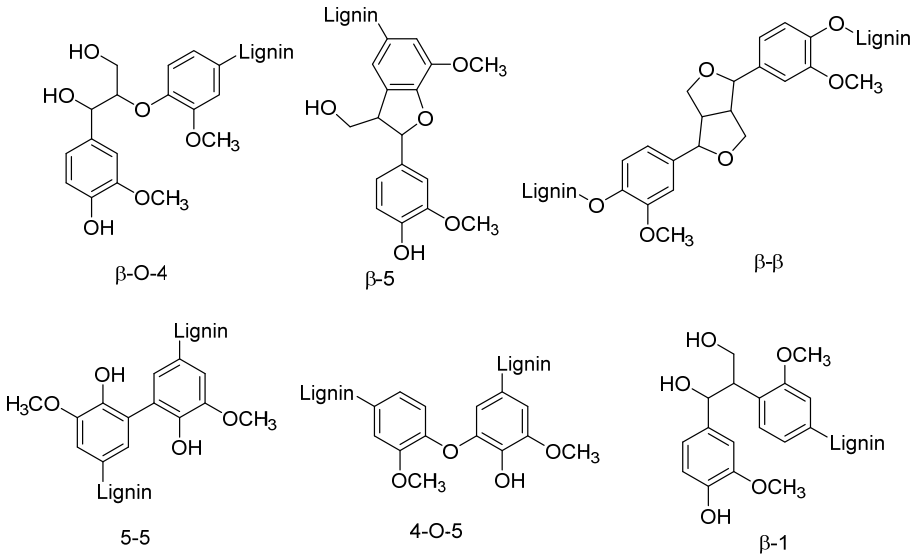

Figure 1. 4 Examples of C-O and C-C linkages in lignin[10]

The relative abundance of some typical linkages is shown in Table 1.1, and it should be noticed that some common functional groups[19] (i.e. methoxyl, aliphatic and phenolic hydroxyl) usually present as well. As seen in Table 1-1, the β-O-4 linkage is dominant, making up almost half of the linkage structures of lignin,[20] and hardwood lignin has a larger fraction of β-O-4 linkages than does softwood lignin. Hardwood lignin (Type-S-G lignin) contains fewer β-5 and 5-5 linkages than does softwood lignin (Type-G lignin), which is consistent with the fact that Type-G monolignols possess an available C_5 position for radical coupling while that coupling reaction is blocked in Type-S monolignols due to a methoxy group (see Figure 1.3). These data also varies due to some factors like growing area, environment or analysis techniques, even for the same plant substrates.[21]

Table 1. 1 Relative abundance of different linkages[19]

Linkage type	Softwood (spruce) [%]	Hardwood (birch) [%]
β-*O*-4-Aryl ether	46	60
α-*O*-4-Aryl ether	6–8	6–8
4-*O*-5-Diaryl ether	3.5–4	6.5
β-5-Phenylcoumaran	9–12	6
5-5-Biphenyl	9.5–11	4.5
β-1-(1,2-Diarylpropane)	7	7
β-*β*-(Resinol)	2	3
Others	13	5

A schematic overview of typical softwood lignin structures with dominant linkages is shown below in Figure 1.5. It should be notable that this is not an "observed" structure of lignin but a model that illustrates most bonding patterns.

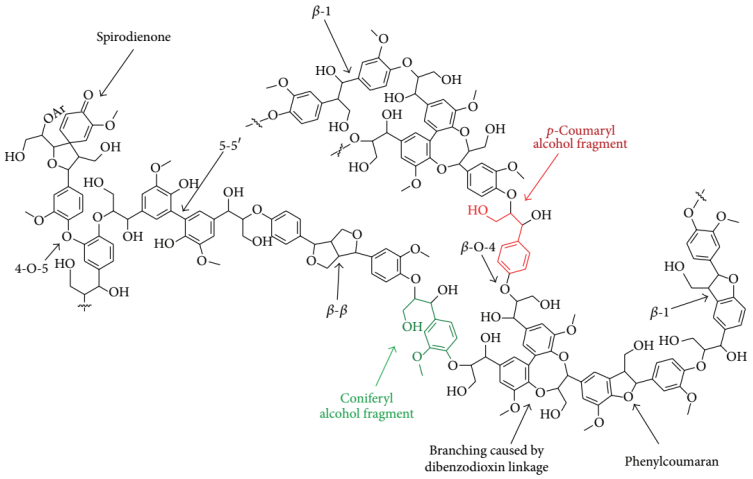

Figure 1. 5 Schematic representation of common linkages in a lignin fragment[22]

The complicated, heterogeneous nature of the lignin macropolymer yields difficulty into direct applications.[23] The high molecular weight (for example, molecular weight of kraft lignin was reported to reach 200,000 g/mol)[12] limits the solubility as well as the accessibility of parts of the structure and the reactivity with many reagents. Tremendous efforts[10, 16] have been made to better utilize lignin - to convert the macropolymer into chemicals with low molecular mass and better solubility. Depolymerization strategies are typically either

acid/base catalyzed, oxidative, reductive, or thermal approaches. Model compounds containing the linkages that are found in real lignin are widely used in the development of methods for lignin deconstruction due to the complex, heterogeneous nature of native lignin. The low molecular weight and simple structures of lignin model compounds makes the analysis and characterization of products obtained from their reactions relatively easy.[8] Research on the utilization of lignin has primarily focused on the development of sustainable, cost-effective, environmental friendly and technical-selective strategies to produce small molecules from the polymer, and the most widely used approaches are described below.

1.4 Current approach for lignin degradation

1.4.1 Oxidative cleavages

Oxidation is one of the dominate strategies for deconstructing lignin into chemical fuels and other value-added aromatic monomers. Reductive approaches tend to afford simple phenolic compounds by removing or simplifying the functionalities during lignin degradation while transition metal-based catalysts, high temperature and high pressure of H_2 is usually required and most reductive methods can not cleave C-C linkages. Oxidative approaches tend to produce more complex aromatics as oxidation can insert oxygen-containing functional groups. Oxidative cleaving reactions include breaking ether bonds, C-C bonds, or other linkages in lignin - even cleaving aromatic rings.[16] Commonly used oxidants such as nitrobenzene, O_2, H_2O_2 and metal oxides have been employed industrially.[24] Aerobic catalytic oxidative deconstruction of lignin is especially attractive as cheap atmospheric oxygen is readily available. Catalysts are required and the specific reactivity of the catalyst is critical in

these oxidations, otherwise the reaction can lack activity and selectivity, and lead to over-oxidation or lower conversion and poor yields of desired products.[25, 26]

Recently, primarily three types of products (dicarboxylic acids, low-molecular weight phenols and benzoquinones) have drawn the bulk of interest in different groups.[23] Since lignin is a macropolymer composed of aromatic subunits, deconstruction of lignin into phenolic products that have lower molecular weight is sensible. Early oxidative cleavage of lignin utilized transition metal-based oxidants such as CuO, MnO_2 or metal ions (Cu^{2+}, Co^{2+} and Mn^{3+}).[23] Those powerful oxidants can efficiently oxidize alcohols to acids, and are usually employed in stoichiometric or even excess amounts; therefore, stoichiometry sometimes needs to be carefully controlled to prevent formation of over-oxidation. For instance, $KMnO_4$ is a very common strong oxidant[27] especially under acidic conditions that can oxidize alcohols to acids and sometimes can oxidatively cleave rings. Oxidative cleavage on native lignin by $KMnO_4$ to veratric acids has been reported[18] but in a low yield (only 8%), and the low solubility of $KMnO_4$ in nonpolar solvents[28] has also limited its application. Methods for using catalytic amounts of $KMnO_4$ would be needed for deconstructing lignin in a practical manner. Stark[29] reported a method to oxidatively decompose lignin to aromatic aldehydes, phenols and other aromatic products through $Mn(NO_3)_2$ as the catalyst in an ionic liquid at 100 °C under 8.4 MPa air for 24h and produced up to a 66.3% conversion. Partenheimer[30] reported that lignin was oxidized to aromatic aldehydes/acids by using a Co/Mn/Zr/Br catalyst system in air with a 10.9 wt% yield.

Despite these inorganic metal-based oxidants, many organic catalysts that utilize oxygen as the ultimate oxidant has been reported. For example DDQ (2,3-dichloro-5,6-

dicyano-1,4-benzoquinone) was discovered to behave as an efficient oxidant for numerous reactions.[31, 32] DDQ can be widely used in oxidations of alcohols,[33, 34] in removal of protecting groups,[35, 36] in oxidative couplings[37, 38] and in cyclizations,[39, 40] as well as application in decomposition of lignin models and raw lignin.[41] Westwood's group has reported that DDQ can not only oxidize benzylic alcohols to the corresponding ketones in β-O-4 linkages,[42] but also modify β-β linkages in kraft lignin.[41] Interestingly, treatment of the β-β model compound eudesmin with 1 eq. of DDQ produced an alkene while when the amount of DDQ increased to 3 eq., an unusual pyran-4-one was formed (Scheme 1.2). Oxidations of alcohols to ketones at room temperature by catalytic amount of DDQ in the presence of AcOH with $NaNO_2$ as a co-catalyst and O_2 as the ultimate oxidant was reported (Scheme 1.3).[43] Benzyl alcohols with unprotected phenols can be cleanly converted to corresponding aldehydes in 90% yield in 5h wherein the phenolic hydroxyl groups were not affected,[43] a process which is specifically attractive in oxidative degradation of lignin since large amount of free phenols existing in lignin are always problematic under oxidative systems.

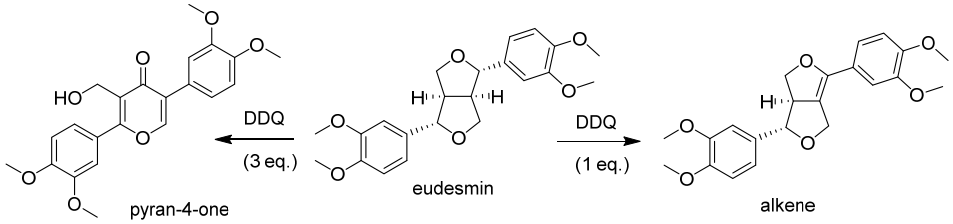

Scheme 1. 2 Different products formed when eudesmin was treated with different amount of DDQ

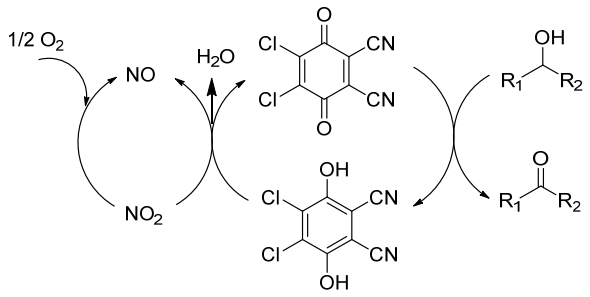

Scheme 1. 3 Proposed catalytic cycle for the aerobic oxidation of alcohols catalysed by DDQ

TEMPO (2,2,6,6-tetra-methyl-piperidin-1-oxy) is a stable nitroxyl radical that has previously been employed as a co-catalyst in aerobic metal-catalytic alcohol oxidations[44-46] to improve the selectivity under mild conditions. These metal-based methodologies either rely on expensive transition metals[47, 48] or produce hazardous heavy metal waste.[49] More importantly, in some cases[50] the presence of even trace amount of water will cause the deactivation of metal catalysts. Therefore, the exploration of metal-free catalysts for the aerobic alcohol oxidations has been stimulated.

Despite the direct oxidative cleavage of lignin models or lignin itself, several groups have reported a two-step strategy to cleave lignin model compounds. Since β-O-4 linkages are the most common of the lignin linkages, this approach primarily focused on the oxidation of benzylic hydroxy groups to the corresponding benzylic ketones, followed by hydrolysis of resulting products from sequent catalytic oxidative systems to cleave the C_β-O bond, in some cases the C_α-C_β bond. Stahl's group reported chemoselective aerobic oxidation of benzylic hydroxy groups in β-O-4 models, using a system that is totally metal-free and consisting of inexpensive mineral acids and TEMPO. The resulting ketones can be easily cleaved with H_2O_2 into veratric acid and guaiacol (Scheme 1.4).[51] They also achieved cleavage of these oxidized β-O-4 linkages within aqueous formic acid solution in mild condition wherein

monomeric products can be isolated in 70%-90% yield.[52] Moreover, following this method, over 60wt% yield of low molecular weight monomers can be obtained from an oxidized aspen lignin.[52] No C-O bond cleavage occurred when a non-oxidized β-O-4 model was treated with formic acid, indicating that the benzylic ketone is critical in success of the deconstruction. Westwood[42] and co-workers reported that benzylic oxidation of β-O-4 models with catalytic DDQ was easily achieved, and the resulting oxidized β-O-4 linkages were cleaved with Zn/NH_4Cl. This strategy focused on ether bond cleavages, and compared to other methods they can obtain highly selective products over 80% yield in one-pot in 15 min.

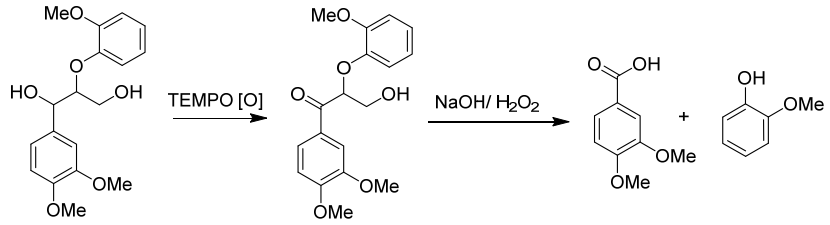

Scheme 1. 4 Monomers obtained from a β-O-4 model compound via benzylic oxidation with TEMPO and hydrolysis with H_2O_2 in basic condition

Wang's group[53] reported that benzylic oxidation of the β-O-4 alcohols to corresponding ketones can makes the C_β-O more fragile by lowering the C_β-O bond energy from 247.9 kJ/mol to 161.1 kJ/mol (see Scheme 1.5). While the C_α-C_β bond energy increased from 264.3 kJ/mol to 294.2 kJ/mol. Additionally, instead of working on cleavage of the C_β-O bond, they employed a specific copper/1,10-phenanthroline catalyst that can lower the activation energy of the C_α-C_β bond energy by about 100 kJ/mol. They obtained aromatic monomers in over 80% yield in this approach.

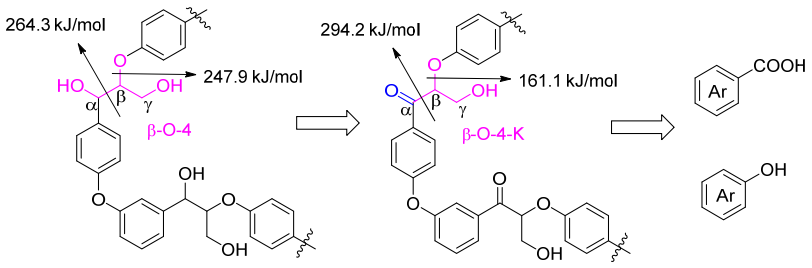

Scheme 1. 5 Two-step strategy for cleavage of β-O-4 linkage and changes in bond energy

1.4.2 Acid-catalyzed cleavages

Early in 1924, Hagglund and Bjorkman[54] reported the acid pulping of lignin by treating with 12% aqueous HCl, with 1,3,5-benzenetriol, barbituric acid, and thiobarbituric acid obtained. As ether bond linkages dominate in lignin biomass,[55] hydrolytic cleavage of β-aryl and α-aryl ether bonds also dominates[56] in acid-catalyzed decomposition since the phenolic ether bond and carbon-carbon bond between aromatic blocks are relatively stable.[57] The rates of hydrolysis of α-aryl ether bonds are 100 times faster than those of β-aryl linkages.[58] A series of phenolic and nonphenolic β-O-4 models were synthesized and subjected to hydrolysis by hydrochloric acid by Jia in order to study the mechanism.[59] Sarkanen proposed a mechanism that involved a dehydration reaction to yield the enol aryl ether (the rate-determine step), and the resulting enol aryl ether can be hydrolyzed very rapidly to α-ketocarbinol (finally transformed to a mixture of "Hibbert's ketones" due to the allylic rearrangement)[60] and guaiacol, as shown in Scheme 1.6. Additionally, though the prominent intermediate in acid-catalyzed bond cleavage is the benzylic carbenium ion, the prevailing pathway relies on the specific acid used (see Scheme 1.7). Utilization of HCl or HBr leads to the formation of intermediate (a) and H_2SO_4 yields the formation of intermediate (b).[61-63] Monomeric products obtained from subsequent hydrolysis of intermediate (a) can be seen in Sarkanen's work[60] (Scheme 1.6); further hydrolysis of intermediate (b) produces

aldehyde (c) and other phenolic monomers.[64] Despite of mineral acids, lewis acids,[65, 66] organic acids,[67] and acidic ionic liquids[68, 69] have also been applied for hydrolysis of model compounds and real lignin.

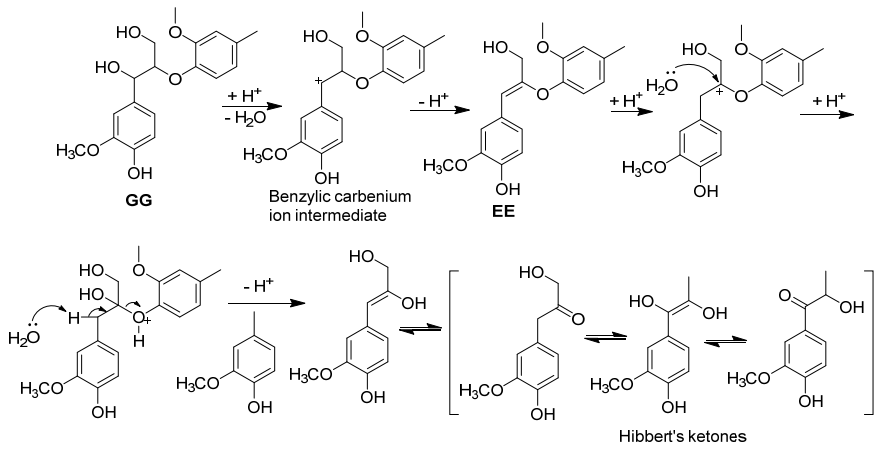

Scheme 1. 6 Mechanism of cleavage of β-phenyl ether linkages of lignin model through acid-catalyzed hydrolysis[60]

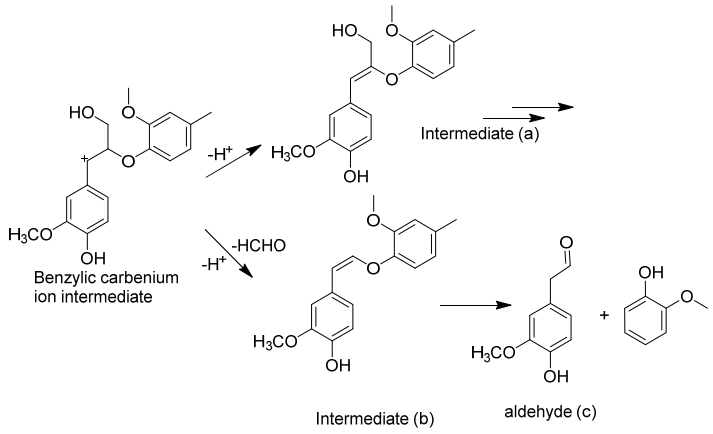

Scheme 1. 7 Formation of different intermediates from the benzylic carbenium ion

Jia and co-workers employed series of Lewis acids ($AlCl_3$, $CuCl_2$ and $FeCl_3$) that can achieve C_β-O-C_{aryl} ether bond cleavage of two β-O-4 model compounds into guaiacol in as high as 49% yield in ionic liquids.[70] Westwood and co-workers reported synthesis of new model compounds (see Figure 1.6) that consisted of both β-O-4 and β-5.[71] They introduced ethylene glycol to "trap" the released formaldehyde from the β-O-4 and β-5 moieties so the

amount the formed formaldehyde can be quantified. Additionally, they screened different types of metal triflates and up to 19.3% of monomeric products were obtained when $Fe(OTf)_3$ was used.[72]

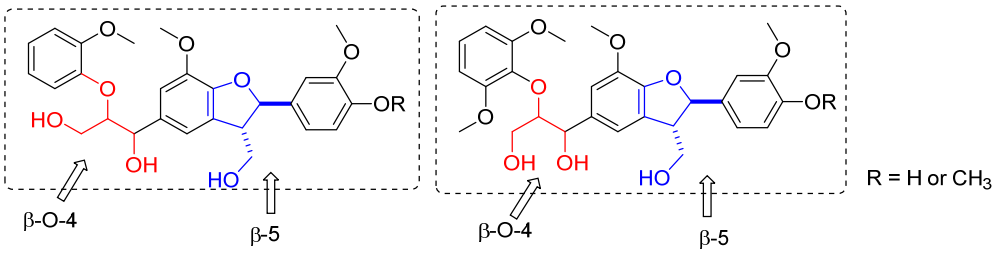

Figure 1. 6 Models that combined β-O-4 and β-5 linkages

1.4.3 Base-catalyzed cleavages

Lignin is significantly more soluble in alkaline conditions than in water due to deprotonation of phenolic hydroxyl groups.[64] Not only can alkaline conditions can extract lignin from biomass by breaking the lignin-carbohydrate bonds, but these conditions also enable fragmentation and deconstruction of lignin via cleavage of the β-O-4 moieties, where fragments that are formed can be solubilized in alkaline media.[64] Types and yields of formed monomers heavily vary with the pressure, temperature, reaction time and especially the specific bases used.[73] Generally longer reaction time and higher temperature leads to higher yields of monomers; stronger bases tend to favor higher conversion as mechanisms and kinetics of the depolymerization reactions are governed by the those strong bases.[74, 75] At low temperature (≤ 300 °C), substituted and unsubstituted methoxyphenols are the prevalent products while catechol or alkylcatechols become the predominate products when temperature is higher than 300 °C.[64] Base-catalyzed degradation of lignin, which occurs primarily at the β-O-4 portions and cleavage of ether bonds, can be categorized into two types.[76-78]

(1) α-aryl ether bonds with free phenolic hydroxy groups on the *para*- position, so cleavage occurs readily through a quinone methide intermediate, wherein transformation of the quinone methide intermediate to guaiacol and coniferyl alcohol can occur with further treatment of the aqueous alkaline solution with a nucleophile such as H_2S, as shown in Scheme 1.8**.** Clearly, carbon-carbon bonds can be formed via the competition reactions between the reactive quinone methide and *in situ* formed lignin nucleophile, eventually leads to repolymerization, demonstrating that inhibition of repolymerization is critical in improving the generation of monomeric products. For example, Lercher and coworkers obtained monomers in 15wt% yield within less than 5 min from a hardwood lignin that was treated with NaOH at 300 ºC in water, but at longer times the yield dramatically decreased due to repolymerization.[73]

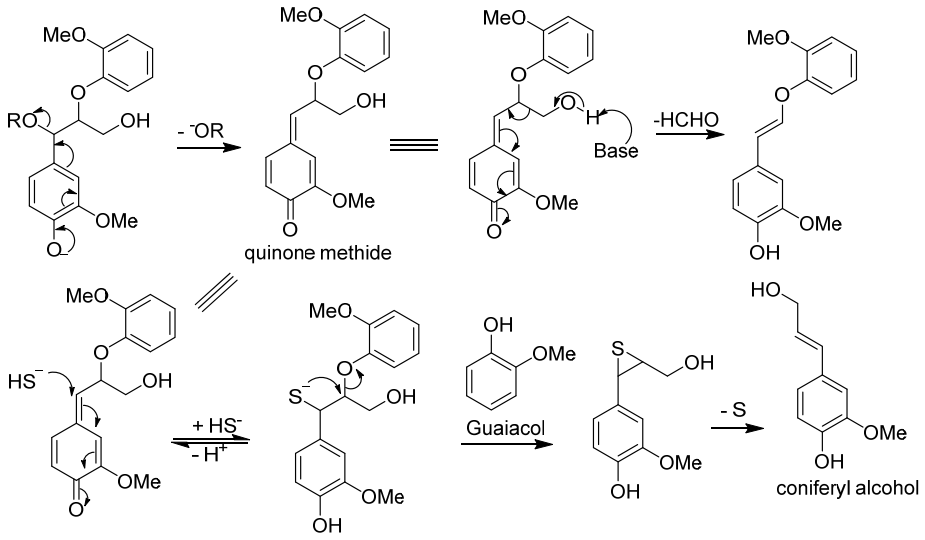

Scheme 1. 8 Cleavage of α-aryl ether bonds in phenolic models[76, 79]

(2) β-aryl ether bonds in nonphenolic models that possess free alcoholic OH groups in the α-position of the aliphatic side chain, as shown in Scheme 1.9.

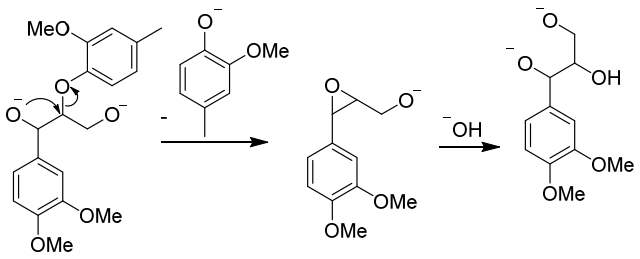

Scheme 1. 9 Cleavage of β-aryl ether bond in nonphenolic models

Conventional strategies in depolymerization of lignin can not deconstruct more robust linkages other than β-O-4 linkages further. Additional tactics, including less-traditional chemical processing (i.e. mechanochemical) is needed in depolymerization of lignin as breaking the most abundant β-O-4 linkages does not guarantee success in breaking other linkages. In order to achieve more reaction sites and higher monomer yield, combination of mechanical pre-treatment and chemical processes comes to sight. Recently, researchers combined base-catalyzed lignin degradation strategies and mechanical processing together which can improve generation of monomeric chemicals and oligomers. Details about mechanochemical process of lignin are discussed below.

1.4.4 Mechanochemical treatment of lignin

Due to its nature as a complex three-dimensional amorphous polymer, the isolation and extraction of lignin from raw biomass as well as subsequent conversion into valuable chemicals is a significant challenge.[80]

Pre-treatment to isolate the primary components from biomass is essential in biorefinery operations.[8] Mechanical milling is an effective pre-treatment method for lignocellulosic materials and can increase the efficiency of enzymatic hydrolysis[81] and maximize lignin extraction;[82] this is due to reduction of particle size[83] and crystallinity,[84] as

well as to the disruption of cell walls.[85] Extraction of ball-milled lignin in neutral solutions (water/dioxane, 1/9 v/v) was developed by Björkman[86] and milled wood lignin (MWL) is considered to represent the intact lignin. This is because the extraction can be conducted under mild conditions and in neutral solutions, although issues such as possible depolymerization and low extraction yield still exist.[87] It should be noticed that more phenolic hydroxyls are generated after ball milling and these eventually contribute to the growth of α-carbonyl content due to side-chain oxidation.[88] Ikeda and co-workers reported that more structure changes were taking place in a vibratory ball mill within solvent-free system while fewer changes in lignin structure occur when toluene was used as a solvent.[89]

Chemical modification of lignin itself during the milling process has been observed, including the growth of carbonyl and phenolic hydroxyl content, cleavage of β-O-4 linkages, and reduction of molecular weight.[82, 85, 90, 91] For example, Qu[92] demonstrated that wet ball-milling can dramatically decrease the polydispersity and increase the phenolic hydroxyl content. High yields of lignin degradation products have been obtained by using a combination of mechanical and chemical pre-treatment.[93] A combination of ball-milling with enzymatic and mild acid hydrolysis can increase the isolated yield of lignin up to 50% (w/w) but the required milling time can be quite prolonged (25 days).[85] Other reports have employed milling times from 5 hours[90] to as much as 20 hours.[94] It has been reported that milling in the presence of strong bases can effectively cleave the common β-O-4 ether bonds in harsh conditions.[74, 95] Indeed, the addition of a solid base, such as NaOH into the milling progress has proven to significantly increase the yield of monomeric products. Cleavage of 76% of the β-O-4 linkages occurred during the ball-milling process (12h) in the presence of NaOH.[96] In

this case, though guaiacol can be isolated in relatively good yields, a host of unidentified by-products formed when model compounds with propyl chains were treated under this mechanochemical process.

Ball milling, the typical technique in mechanochemical processing of lignin, is generally associated with high energy cost. It has been demonstrated that with growth of biomass scale (from 1g to 1000g), energy cost per kg will drop dramatically, indicating that ball mills can be potentially suitable on an industry scale.[97]

Utilization of lignin-derived monomeric products such as phenols, aromatic acids and other oligomers have been reported in many areas.[98] These products possess a broad range of bioactivities which have been used in discovery of Pharmaceuticals.[98] Pharmaceuticals are value-added products from lignin while requirement of substantial synthetic work are unlikely to use up the potential large supply of lignin products. On the other hand, usage of these products as fuels are low value, but they can be consumed in very large volume. Degradation of lignin into lower molecular weight, more soluble phenolic compounds requires significant energy. Methods and applications that employ lignin as a sustainable source to create new products with minimal further additional processing or deconstructing will be both environmentally and economic attractive. The large number of aliphatic and phenolic OH's components in lignin could serve as linkers in producing lignin-based macromonomers. In practice, lignin has been introduced into polyesters, polyurethanes and epoxide resins as a macromonomer.[10]

1.5 Lignin as a building block to create polymers

The rigidity of the aromatic units in lignin can help improve stiffness of lignin-based polyurethanes. In addition, functionalized lignin has been used in the preparation of new materials as well; not only more functionalities and reactive sites could be generated but also make the original poorly-accessible reactive sites more accessible. For example, Duong and co-workers synthesized a polyurethane using kraft lignin as a reactant, and produced a material with a high molecular weight (up to 912,000 g/mol) in only 3 hours (see Scheme 1.10).[99] Xue employed up to about 39 wt% lignin in the synthesis of a series of lignin-based polyurethane foams.[100] Lewis acid catalysed demethylation of methoxy groups - a simple functionalization approach - was achieved by Chung and co-workers.[101] An average of 28% more OH groups were generated and the cross-link density of the resulting polyurethane was significantly improved by using the demethylated lignin.

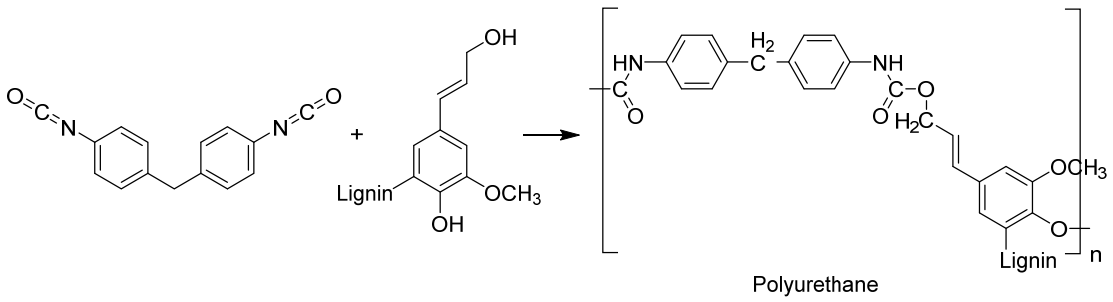

Scheme 1. 10 Schematic preparation of polyurethane from lignin

In addition to the synthesis of polyurethanes, many lignin-based polyesters were reported.[10] For example Binh and co-workers synthesized polyesters that had a T_g of 70 ºC and molecular weights of 39,000 g/mol under basic conditions via condensation of kraft lignin and sebacoyl chloride (Scheme 1.11).[102]

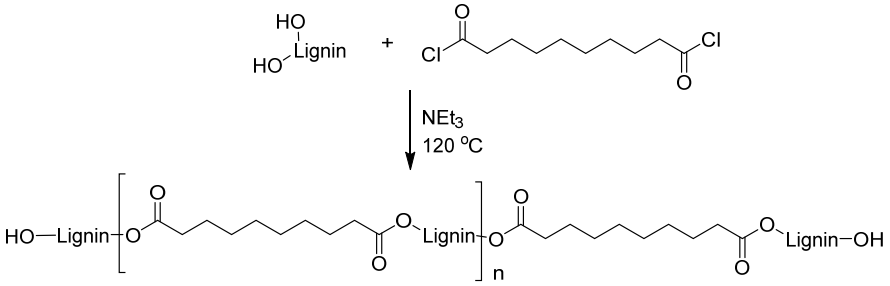

Scheme 1. 11 Synthesis of polyester from kraft lignin and sebacoyl chloride under basic conditions

Among all of the lignin-based macromonomers, lignin-based epoxide resins are very interesting. Epoxy resins have been widely used as structural adhesives, protective coatings, composite materials, and in other areas due to their excellent thermal stability and mechanical performance. Bisphenol A (BPA) is the most common used building block in the epoxy resin industry[103] but recently concerns of potential toxicity associated with BPA has limited its application since BPA is suspected to be an endocrine disruptor[104] and exposure can increase incidence of obesity, heart disease, diabetes and other diseases.[105] Therefore, replacement of BPA-based epoxy resins with other monomers, especially from sustainable and renewable resources (such as lignin) is strongly desired, as the current production of BPA heavily relies on petroleum-derived products.[106] Structures of BPA and bisphenol A diglycidyl ether (BADGE) were shown in Figure 1.7.

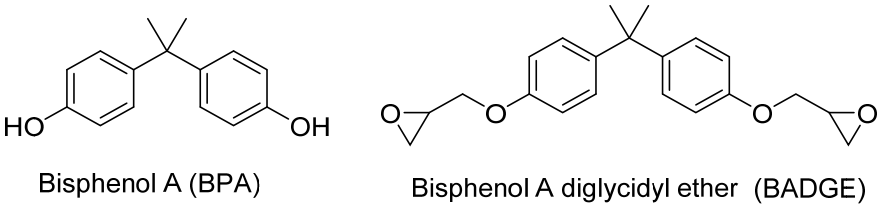

Figure 1. 7 Structures of BPA and BADGE

Engelmann and co-workers employed 1,3-glycerol diglycidyl ether along with up to 50wt% lignin in synthesis of a series of epoxide resins.[107] The resulting resins with high wt%

of lignin content behaves more thermally stable than those prepared from pyrogallol. No epoxide groups exist in native lignin so lignin cannot behave as a sole cross-linker in resin synthesis; therefore, the system usually requires addition of another cross-linking reagent. Epoxide groups are usually introduced either directly into lignin molecular structures, or into the macromonomeric structures to create better desirable epoxide resins. Epichlorohydrin is widely used in introduction of epoxide groups in lignin under basic conditions (Scheme 1.12).[10]

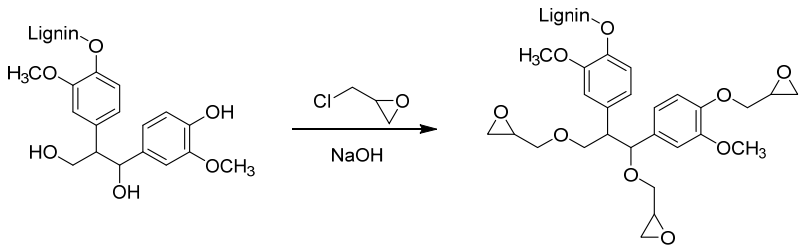

Scheme 1. 12 Introduction of epoxide groups in lignin by using epichlorohydrin

Over and co-workers prepared epoxy thermosets consisting of up to 42wt% organosolv lignin, and the resulting resin had higher cross-linking density, increased stiffness and T_g when content of lignin located between 8%-33wt%, compared to non-lignin based polymers.[108] In addition, increasing hydroxy content (generally phenolic moieties) can significantly improve the degree of epoxidation.[10]

From our survey of the literature it is clear that lignin is used in small fractions, at best, in preparation of these polymers and the bulk of the material still comes from petroleum-derived chemicals. Limitations of applications of lignin without degradation are also obvious, as properties of formed materials may depend on the source of lignin and extraction progress.[109]

1.6 Lignin-derived aromatics as building blocks for epoxy resins

Low molecular weight compounds (generally are well-known phenolic compounds) generated from mild lignin degradation methodologies can usually retain aromaticity and other functionalities, which could be utilized to synthesize materials that possess valuable properties such as structural rigidity or thermal stability. A plethora of low molecular weight aromatic chemicals can be obtained from lignin deconstruction, but usually in relatively small quantities. Currently, vanillin is the only lignin-derived aromatic chemical that can be produced on industrial scale, so at this time only lignin-to-vanillin derived chemicals (i.e. vanillic acid and vanillic alcohol) can be potentially commercialized. Though 85% of vanillin is still produced from petroleum, lignin-derived vanillin contributes 15% of the whole production.[110]

Vanillin and its derivatives are employed in synthesis of different kinds of polymers. For instance, Fache[111] developed 22 derivatives of vanillin that carry epoxide, allyl, carboxylic acid, alcohol and amine moieties for the synthesis of polyurethane, polyester and epoxy resins. In particular, three biobased non-aliphatic amine-functionalized derivatives that each bear two reactive primary amine groups are of great potential in epoxy synthesis (Figure 1.8). Additionally, another set of phenolic aromatic monomers were first pre-treated with Dakin oxidation to improve their phenolic functionality and converted into epoxides with epichlorohydrin subsequently.[112] Zhao and co-workers employed vanillin and other lignin-derived aldehydes (*para*-hydroxybenzaldehyde, syringaldehyde) and guaiacols in synthesis of triphenylmethane-type polyphenols (Scheme 1.13).[113] Treated those polyphenols with epichlorohydrin yielded mono, tri and penta-epoxy products. Epoxy thermosets from these

glycidyl ethers exhibited outstanding T_g (167 ^oC) and glassy modulus (12.3 Gpa). In this work demethylation was conducted first to generate more reactive sites. Aouf and co-workers reported that vanillic acid was allylated with allyl bromide, and epoxide groups were introduced with epoxidation of the allylic double bonds with *m*-CPBA instead of employing epichlorohydrin in the synthetic process.[114] By carefully controlling the ratio of oxidant and double bonds, a set of mono, di, tri and penta-epoxidized products were obtained.

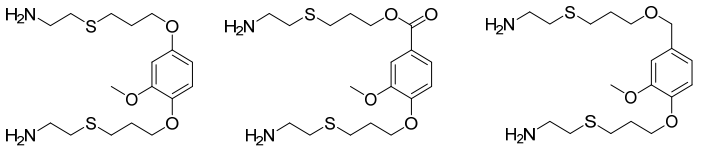

Figure 1. 8 Amine-functionalized derivatives from vanillin

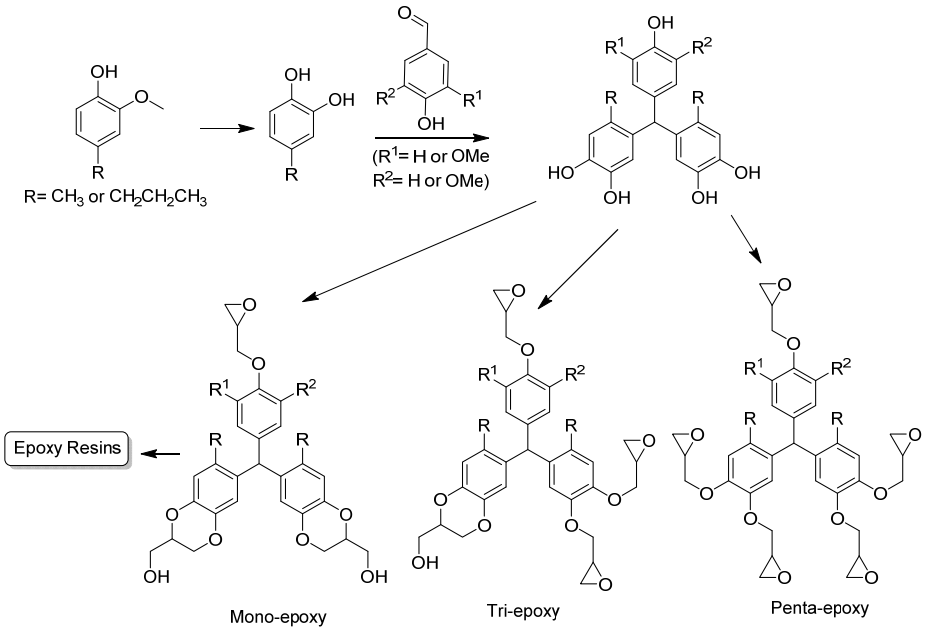

Scheme 1. 13 Synthesis route of fully renewable triphenylmethane-type polyphenols and corresponding polymers

1.7 Motivation of our work

Our overall goal is to investigate different approaches (primarily oxidative, acid/base catalyzed approaches) to deconstruct the complex lignin polymer to produce small high-value

aromatic compounds such as substituted phenols, vanillin, vanillic acids, and other compounds, and then to demonstrate that some of these products can be as building blocks for commercially important polymers, specifically in epoxy resins. Deconstructing lignin through a 2-step oxidation approach will be discussed in chapter 2 and 3. Utilization of lignin products as replacements for some of the components in a commercial epoxy resin system will be discussed in chapter 4.

Chapter 2. Cleavage of β-1 and β-5 Lignin Model Compounds via oxidation and other approaches

Disclaimer: Portions of this chapter were taken from the following paper:
Z. Fang and M. S. Meier. Toward the oxidative deconstruction of lignin: oxidation of β-1 and β-5 linkages. *Org. Biomol. Chem.*, 2018**, 16,** 2330-2341.

2.1 Introduction

Oxidation is an attractive technique to isolate aromatics from lignin biomass since plenty of hydroxyl groups are present in the lignin polymer, as indicated in Figure 1.5. We are specifically interested in the possibility of cleavage of the C_α-C_β bond through a two-step oxidation process, starting with oxidation of the benzylic alcohols to ketones and following with Baeyer-Villiger oxidation of the resulting ketones to produce esters. Products with reduced molecular weights, or oligomers that are small enough for refining to high-value chemicals, can be obtained from hydrolysis of the resulting esters. A schematic approach is shown in Scheme 2.1.

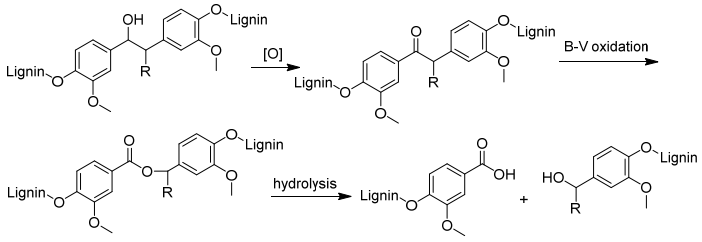

Scheme 2. 1 The two-step oxidation strategy to deconstruct lignin

Other types of C-C linkages, such as the β-1 and β-5 linkages, should also be targets of interest since they constitute significant portions in lignin biomass (see Table 1.1). Successful cleavage of the C_α-C_β bond in the β-O-4 linkage from our previous study[115] stimulates us to focus on the same two-step oxidation process in β-1 and β-5 linkages (Scheme 2.2).

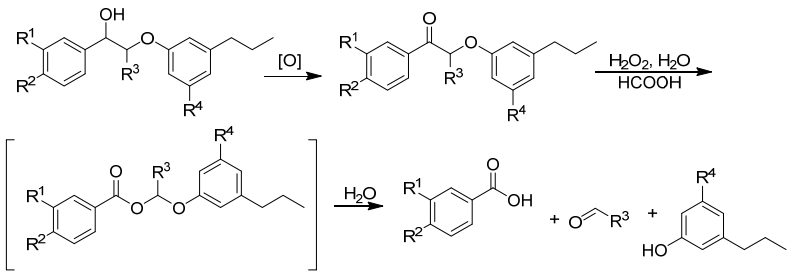

Scheme 2. 2 Cleavage of β-O-4 model compounds via the two-step oxidative approach

The motivation behind this project was not to produce optimized procedures for a given lignin linkage, since such optimized procedures would not be useful in the deconstruction of lignin which contains many different kinds of linkages. We applied the same procedures that had been established for the common β-O-4 linkage and asked the question "under these conditions, what happens to the β-1 and β-5 linkages that are inevitably present in lignin?". We set out to determine the outcomes by applying DDQ-based, TEMPO-based and other several catalytic aerobic catalytic systems with our β-1 and β-5 models in conventional organic solvents, as well as to determine the compatibility of unprotected phenolic hydroxyl groups during oxidation with these systems. If necessary, undesired reactions involving phenols may compel us to investigate different oxidation systems. Stoichiometric amounts of powerful oxidants such as $KMnO_4$ and Co(III) were examined in the oxidative systems as well to establish the common oxidative products from the β-1 and β-5 linkages. We also explored the possibility of opening the dihydrofuran ring in β-5 linkages, since cleavage of the C_α-O-C_{aryl} ether bond in β-5 linkages affords compounds that have β-1 linkages (Scheme 2.3). Corresponding β-1 linkages tend to be more labile and fragile than the β-5 linkages under those oxidative conditions. The types and yields of resulting products will give us ideas in further development of oxidative cleavage approaches.

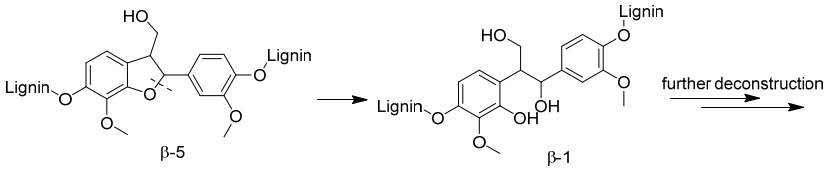

Scheme 2. 3 Cleavage of the C_α-O-C_{aryl} ether bond in β-5 linkages

As mentioned in Chapter 1, lignin is an amorphous polymer produced by the enzyme-mediated phenoxyl radical coupling polymerization of three different lignol monomers,

resulting in a complex crosslinked-structure.[10, 116] β-O-4 Linkages (Figure 2.1) are the most common linkages between monolignols, comprising almost half of the linkages in lignin[20] (~46% in softwood lignin and ~60% in hardwood lignin)[22]. Cleavage of β-O-4 linkages has drawn a great deal of attention as a way to disassemble lignin because of their frequency and fragility. It has been suggested that most β-ethers are destroyed during lignin processing and/or isolation - for example the β-O-4 content is very low after the kraft process.[117]

Crosslinking nature of lignin would mandate that many linkages be broken for monomers to be liberated. In practice, breaking β-O-4 linkages does not liberate large quantities of monomers, indicating that conditions optimized for cleaving this specific linkage do not cleave all other linkages. These other types of linkages, such as β-1 and β-5 linkages, should be of interest since they constitute significant portions of lignin biomass. These two linkages contribute 7-9% and 9-12% in lignin, respectively, depending on processing methods and lignin sources.[8] Rather than involving an ether linkage, in β-1 and β-5 linkages the two aromatic units are linked via a two-carbon bridge (see Figure 2.1).

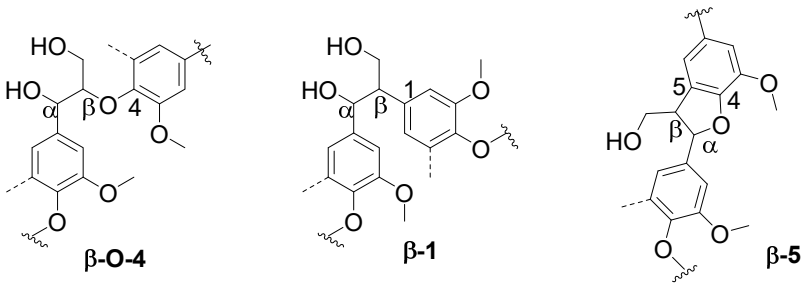

Figure 2. 1 Structures of β-O-4, β-1 and β-5 linkages

Model compounds containing the linkages that found in real lignin are important to use in the development of lignin valorization due to the complicated and heterogeneous nature of lignin. The low molecular weight and simple structures of lignin model compounds makes the analysis and characterization of products obtained from their reactions relatively easy.[8] β-

O-4 linkages model compounds and reactions based on the functional groups and their reactivity in these compounds have been studied and reported in numerous literature reports (i.e. Crestini,[118] Amen-Chen,[119] Kim,[120] *etc*) since β-O-4 is the most abundant linkage in lignin. Patil[121] in our group has demonstrated that cleavage of C_α-C_β bond in β-O-4 model compounds can be achieved via a two-step oxidation process by applying aerobic DDQ and TEMPO-based catalytic oxidations to the benzylic alcohol, followed with a Baeyer-Villiger oxidation. Potentially useful aromatic compounds can be obtained through hydrolysis of the resulting ester.

To study the chemistry of the β-1 and β-5 linkages we prepared four model compounds, including β-1 models (1,2-diaryl-1,3-propanediols) **II-1** and **II-2** and β-5 models (phenylcoumarans) **II-3** and **II-4** (see Figure 2.2). Hydroxyl groups are introduced in α and γ positions in β-1 model compounds **II-1** and **II-2** to compare the compatibility and selectivity with various oxidation conditions, wherein electron-donating methoxy groups on the aromatic rings can enhance the probability of oxidations. In addition, the free phenolic hydroxyl groups (abundant in real lignin) in **II-2** and **II-4** can test the compatibility with diverse oxidants and other reagents. We investigated how these model compounds behave not only under oxidative systems and but also other conditions such as strong acidic and alkaline conditions.

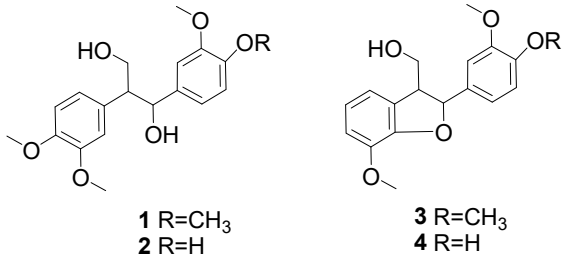

Figure 2. 2 Structures of β-1 and β-5 model compounds

2.2 Results and Discussion

2.2.1 Preparation of lignin model compounds

Preparation of β-1 model compounds **II-1** and **II-2** followed the methods reported by Cho.[122] Aldol condensation of ester **II-5** with aldehyde **II-6** produced ester **II-7**, which was reduced with $LiAlH_4$ to give **II-1** (R_2=OCH_3) and **II-2** (R_2=OH) (see Scheme 2.4).

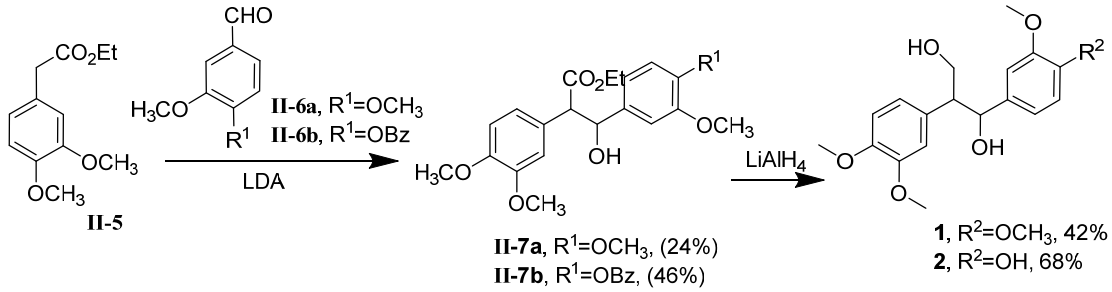

Scheme 2. 4 Preparation of **II-1** and **II-2**

Following the method of Brunow,[123] compounds **II-3** and **II-4**, models for the β-5 linkage, were prepared by aldol condensation between o-vanillin and acetophenone **II-8** to produce chalcone **II-9**. After protection of the phenolic hydroxyl, epoxide **II-10** was formed by treatment with H_2O_2 in a phase-transfer system. 1,3-propanediol **II-11** was obtained by rearrangement of epoxide **II-10** with boron trifluoride diethyl etherate and subsequent $NaBH_4$ reduction. Palladium-catalyzed debenzylation with H_2 and acid-catalyzed ring closure produced **II-3** and **II-4** (see Scheme 2.5).

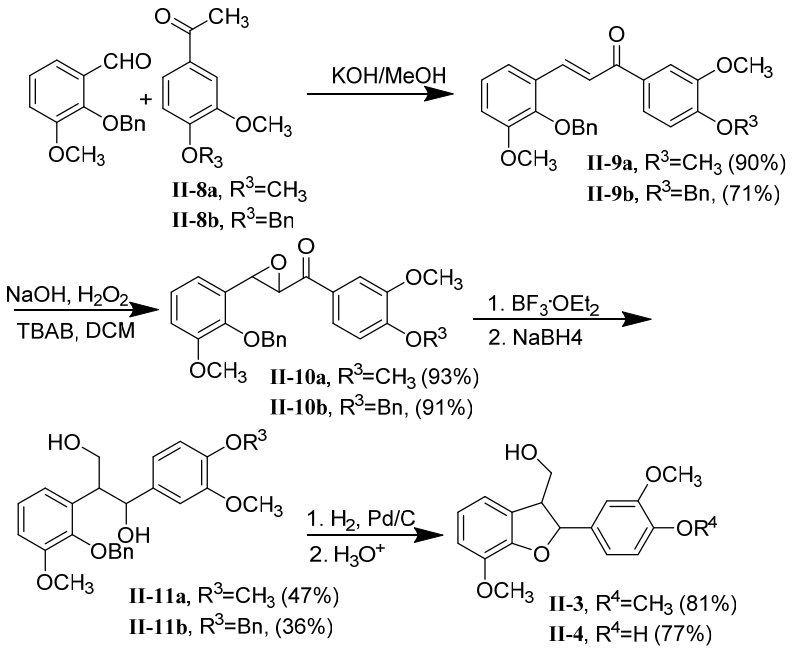

Scheme 2. 5 Preparation of **II-3** and **II-4**

2.2.2 Oxidative Cleavage of Lignin Models II-1 - II-4

Oxidation of alcohols into carbonyl compounds is one of the most important conversions in organic synthesis,[124] while selective oxidation of the benzylic alcohols into ketones is extremely essential in decomposition of lignin. Stoichiometric amounts of traditional oxidants like PCC[125,126] or MnO_2[127] have been used, but the spectre of production of large environmental harmful toxic waste[128] has precluded their applications in lignin degradation. Realizing oxygen is the most economic and readily available oxidant, oxidation of lignin by using gaseous oxygen and catalysts becomes more promising. While oxidations without catalysts are less selective and can potentially lead to over-oxidation,[129] therefore we might investigate stoichiometric reactions in an effort to find effective chemistry, and finally utilization of a catalytic system with O_2 as the ultimate oxidant is essential.

Using oxygen as an abundant, cheap oxidant, many transition metal catalysts have been reported[130-132] to achieve the aerobic catalytic oxidation of alcohols under oxygen

atmosphere. Usage of expensive transitional metals such as Pd, Au, and Ru as well as dependence on complex ligands[43] makes such methods less attractive. Therefore, the investigation of effective, metal-free catalysts to accomplish oxidations of alcohols with molecular oxygen in mild conditions is extremely meaningful and attractive.

These three linkages (β-O-4, β-1 and β-5) can behave differently under the same oxidative conditions. For example, catalytic vanadium oxidative cleavage methods are highly efficient for β-O-4 linkages but ineffective for cleavage of β-1 linkages.[133] Sedai[134] reported copper and vanadium-catalyzed aerobic oxidations of a 1:1 mixture of β-1 and β-O-4 models and determined that vanadium-catalyzed oxidation of the β-O-4 model was slightly faster than oxidation of the β-1 model while with the copper catalyst, oxidation of β-1 model was faster than oxidation of the β-O-4 model.

Therefore, we examined the effect of established β-O-4 oxidation strategies on the more robust β-1 and β-5 linkages, in an effort to understand how these structures respond under oxidative conditions proposed for lignin deconstruction based on their effect on β-O-4 linkages. We investigated the yields and selectivities of these oxidation methods on β-1 and β-5 linkages, using both stoichiometric and catalytic systems that have been previously applied to other linkages. Thus, we performed oxidations under conditions used previously so that the relative reactivity of the different linkages can be compared. Accordingly, product yields are not fully optimized for β-1 and β-5 linkages but the results shed light on what may happen to these linkages in lignin under conditions optimized for reaction of the more common β-O-4 linkages.

a) Stoichiometric oxidations of II-1 - II-4

2.2.2.1 $KMnO_4$ Oxidation of II-1 - II-4

With models **II-1 - II-4** in hand we examined the oxidation of these compounds under conventional stoichiometric oxidation conditions. We began with oxidation using $KMnO_4$, as this reagent has been used for oxidative degradation and analysis of different lignins.[135] In these analyses, monomeric benzoic acids are produced, providing the ratio of monolignols in the lignin. When **II-1** was treated with $KMnO_4$ under acidic conditions, the expected benzoic acid **II-12** was the major product (85%). Oxidation of **II-2** produced benzoic acid **II-12** (15 %) and benzaldehyde **II-13** (12%) as well as material that was not chromatographically mobile, which we suspect is the result of phenolic oxidative coupling.[136] We did not detect vanillic acid (**II-14**) after running at 120 °C for 19h, consistent with oxidative polymerization of the unprotected phenol in **II-2** and in products derived from the phenolic ring of **II-2** (see Scheme 2.6).

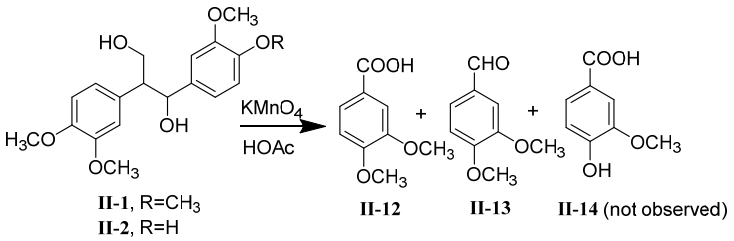

Scheme 2. 6 $KMnO_4$ oxidation of **II-1** and **II-2**

When carried out on β-5 model **II-3**, $KMnO_4$ oxidation produced acid **II-12** (19%) and aldehyde **II-13** (17%), as well as **II-15** (12%), a β-1 structure that was determined NMR (including HMBC experiments). A trace amount of aldehyde **II-16** was also isolated (see Scheme 2.7).

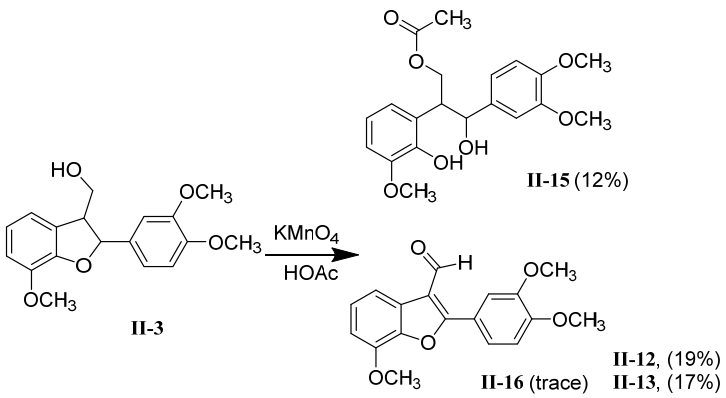

Scheme 2. 7 $KMnO_4$ oxidation of **II-3**

As with the oxidation of **II-2**, $KMnO_4$ oxidation of **II-4** (which bears an unprotected phenolic hydroxyl) resulted in the formation of chromatographically immobile material, which we believe to be the polymeric products of phenolic oxidative coupling. No small molecule products were observed.

2.2.2.2 $Co(OAc)_3$ Oxidation of II-1 - II-4

Stoichiometric and catalytic oxidation of β-1 and β-O-4 lignin model compounds with $Co(OAc)_3$ have been reported by DiCosimo.[137] Oxidation of dihydroanisoin **II-17** and of 1,2-bis(4-methoxyphenyl) propane-1,3-diol **II-18** with stoichiometric amounts of Co(III) acetate produced anisaldehyde by cleavage of the C_α-C_β bond (Scheme 2.8) via a single electron transfer oxidation progress, but only acid-catalyzed dehydration occurred under catalytic conditions.

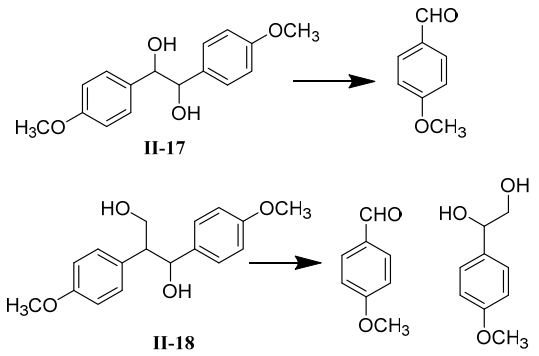

Scheme 2. 8 Examples of oxidations of β-1 models using stoichiometric amounts (2 eq.) of Co(III), reported by Cosimo[137]

Co(III)-based homogeneous oxidation catalysts are often synthesized by *in situ* oxidation of commercially available Co(II) compounds.[138] In our hands, oxidation of **II-1** with stoichiometric amounts of $Co(OAc)_2$ under one atmosphere of O_2 produced aldehyde **II-13** in 82% yield. Oxidation of **II-2** was more complicated, as stilbene **II-19** (9%) and diacetate **II-20** (2%) were isolated, in addition to acetates **II-21** (28%) and **II-22** (7%) (see Scheme 2.9). The β-5 models **II-3** and **II-4** proved largely resistant to oxidation under these conditions, simply producing the γ-acetates **II-23** from **II-3** (88%) and **II-24** from **II-4** (70%), with no apparent oxidation in either case (see Figure 2.3).

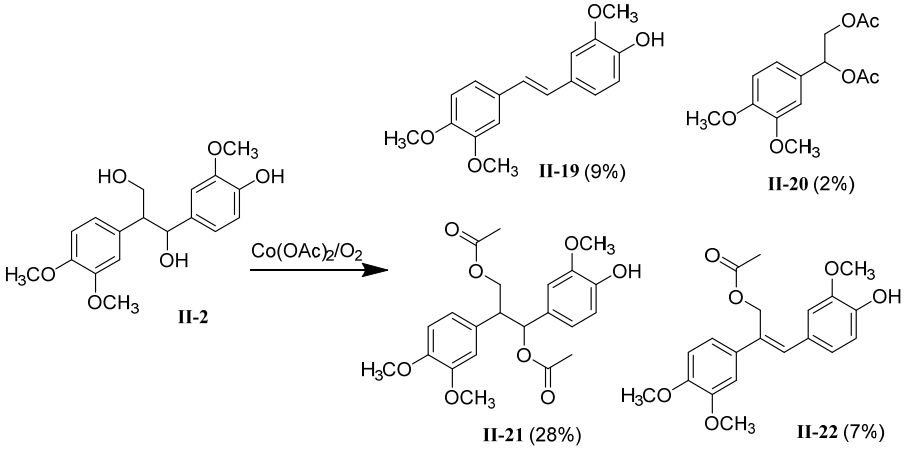

Scheme 2. 9 $Co(OAc)_2/O_2$ oxidation of **II-2**

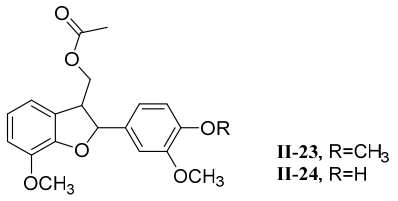

Figure 2. 3 Structures of γ-acetates **23** and **24**

b) Catalytic oxidations of II-1 - II-4

Utilization of waste lignin as a source of value-added materials, such as fuels and feedstock chemicals, requires very inexpensive treatment methods. Consumption of reagents in stoichiometric oxidations is unlikely to be cost-effective, so the development of catalytic methods that rely on O_2 as the only consumed oxidant is essential.

2.2.2.3 DDQ oxidation of II-1 - II-4

Oxidations of alcohols by applying catalytic amounts of DDQ (0.2 eq.) with $Mn(OAc)_3$ as co-oxidant (6 eq.) in dichloromethane at 22 ºC was reported by Cosner,[139] but large amounts of byproducts were produced as well due to the large amount of $Mn(OAc)_3$ used. Adhering to the strategy to avoid using metal-related oxidants but using abundant inexpensive oxygen as the ultimate oxidant, Shen[140] and coworkers reported a DDQ/tert-butyl nitrite catalyst system that can effectively oxidize alcohols to corresponding ketones at 80 ºC in DCE under 0.2 MPa O_2. Zhang[141] reported that oxidative dehydrogenation of 9,10-dihydro-anthracene to anthracene can be achieved by applying catalytic metal-free DDQ/$NaNO_2$ system in the presence of O_2. In this report, $NaNO_2$ is used as a shuttle between oxygen and DDQH, as shown in Scheme 2.10.

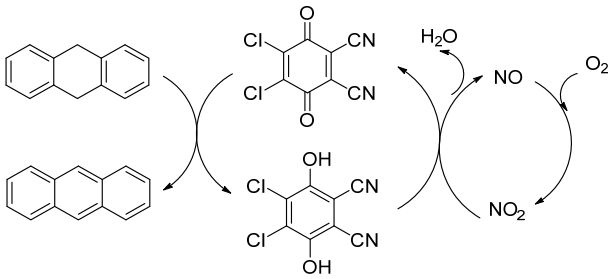

Scheme 2. 10 A proposed catalytic cycle for oxidative dehydrogenation of 9,10-dihydroanthracene to anthracene

However, stoichiometric or even excess amounts of DDQ have to be used[142] which increases the concern for cost and purification issues due to the formation of byproduct DDHQ. Wang[43] reported that alcohols can be oxidized to corresponding ketones at room temperature, with yields up to 97%, by use of a catalytic amount of DDQ in the presence of AcOH with $NaNO_2$ as a co-catalyst and O_2 as the ultimate oxidant. AcOH catalyses the decomposition[143] of $NaNO_2$ to NO and therefore is crucial to the catalytic cycle. Recently, investigation of reactivity of β-O-4, β-β and Hibbert's ketones (keto-containing structures formed in acidolysis of lignin) in birch lignin under both stoichiometric and catalytic DDQ oxidation systems has been reported,[144] and results from HSQC NMR spectra suggested that as increasing amounts of DDQ were used a significant number of the benzylic hydroxyl groups of the β-O-4 linkages were oxidized.

In earlier work, we found that under the DDQ/$NaNO_2$/AcOH system, oxidations of β-O-4 models proceeded in low yields in a standard reaction time of 19 hours and in all cases, the bulk of the starting materials were recovered unchanged.[115] In contrast, the benzylic hydroxyl groups in β-1 model compounds **II-1** and **II-2** were selectively oxidized to the corresponding ketones in high yields in the same 19 hour reaction time, and it is particularly notable that clean oxidation of compound **II-2** was achieved in 84% yield (see Scheme 2.11).

The presence of the unprotected phenolic hydroxyl in **II-2** is problematic in the TEMPO-based oxidations (see below). Chromatographically immobile material was not observed in DDQ-catalyzed reactions, suggesting that polymerization did not occur with this oxidation system.

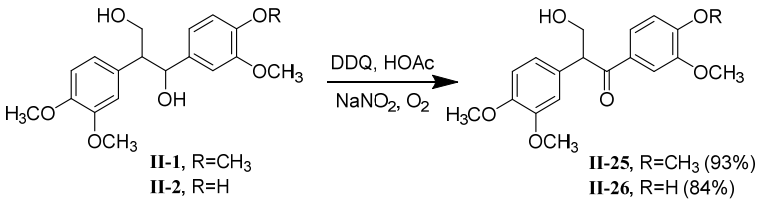

Scheme 2. 11 DDQ oxidation of **II-1** and **II-2**

Not surprisingly, benzofuran derivatives were produced from oxidations of compounds **II-3** and **II-4** with DDQ-based oxidations. In DDQ oxidations of compound **II-3** we found that further oxidation of the γ-hydroxyl also occurs; producing aldehyde **II-16** in 56% yield along with benzofuran alcohol **II-27** in only 18% yield. The γ hydroxyl group in compound **II-4** remained unaffected under these oxidation conditions, and 43% of starting material **II-4** was recovered (see Scheme 2.12).

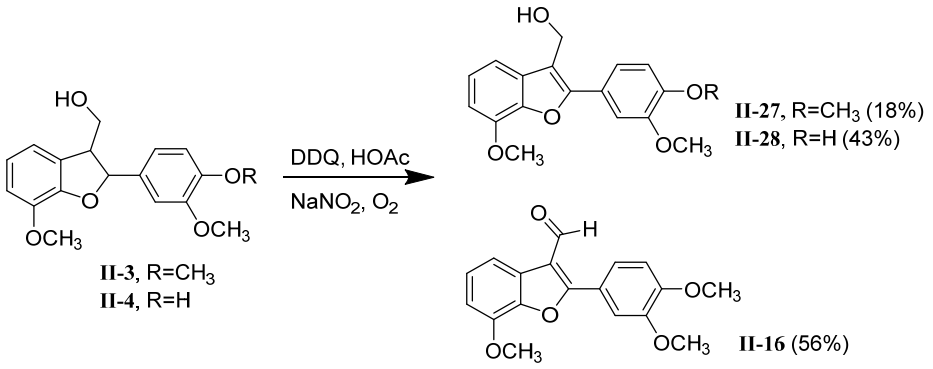

Scheme 2. 12 DDQ oxidation of **II-3** and **II-4**

Compatibility with unprotected phenols is a highly desirable characteristic of the DDQ oxidation of **II-2**, which produced ketone **II-26** in high yield without any phenolic

oxidative coupling products, suggesting that the oxidation proceeded without generation of a phenolic radical.

2.2.2.4 Vanadium-catalyzed oxidation of II-1 - II-4

Aerobic oxidations of benzylic alcohols,[145, 146] phenols[147] and diols[148] by vanadium complexes have been reported. Son,[149] Hanson[150] and Chan[151] reported vanadium-catalyzed oxidation of β-O-4 lignin models, in which elimination products as well as benzylic alcohol oxidation products, were observed (see Scheme 2.13). Hanson and co-workers reported that oxidation of phenolic β-O-4 lignin models with a combination of 0.1 eq. of NEt_3 and vanadium complexes at 80 °C afforded unexpected $C_{(phenyl)}$-$C_{(alkyl)}$ cleavage products.[150]

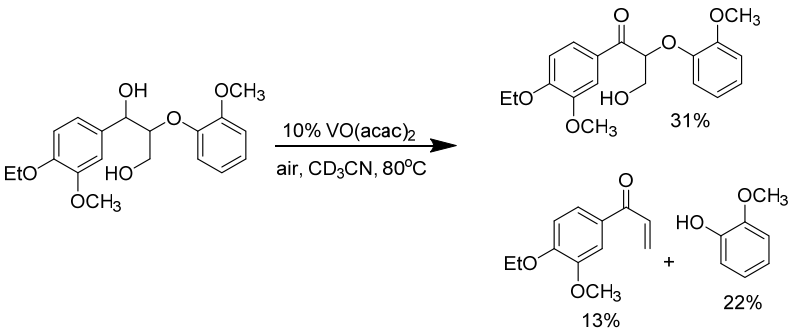

Scheme 2. 13 C-O Bond cleavage and benzylic alcohol oxidation using catalytic $VO(acac)_2$ reported by Son[149]

Ma[152] has reported an acetic acid promoted oxidative C-C bond cleavage of a β-O-4 model catalyzed by commercial available $VO(acac)_2$ using molecular oxygen as ultimate oxidant (Scheme 2.14).

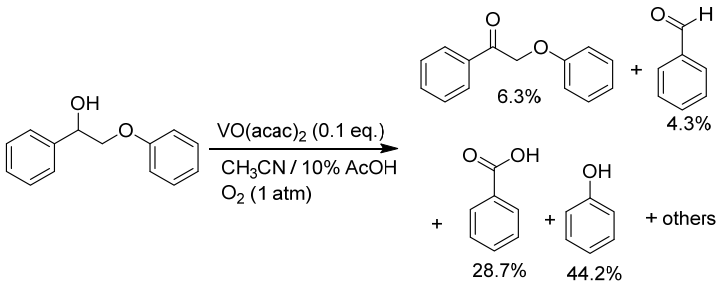

Scheme 2. 14 Acid-promoted oxidation of a β-O-4 model with catalytic $VO(acac)_2$ reported by Ma[152]

Application of the $VO(acac)_2/O_2$ oxidation system to the oxidation of nonphenolic β-1 model **II-1** gave C_α-C_β bond cleavage products **II-12** (19%) and **II-13** (31%), along with diketone **II-29** (4%) (see Figure 2.4), and 56% recovered **II-1**. Prolonging the reaction time did not increase the yield of C-C cleavage products.

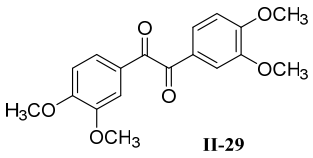

II-29

II-12 (19%)
II-13 (31%)

Figure 2. 4 Vanadium oxidation products from **II-1**

Chromatographically immobile materials were the major products formed from $VO(acac)_2/O_2$ oxidation of phenolic model **II-2**, along with small amounts of acid **II-12** (trace), aldehyde **II-13** (4%), vanillin (5.4%), and 25% recovered starting material. Little evidence of reaction was observed when nonphenolic β-5 model **II-3** was treated under same conditions, even when the mixture was stirred at 100 ^oC for 48h.

Interestingly, when **II-4** (which, like **II-2**, has an unprotected phenol) was treated with $VO(acac)_2/O_2$, no chromatographically immobile products were observed. Other than recovered starting material, the only identifiable products resulted from acetylation of the phenolic hydroxyl group (3%) and trace amount of aromatization of **II-4** to produce 2, 3-dihydrobenzofuran derivative **II-28**.

2.2.2.5 TEMPO oxidation of II-1 - II-4

Liu[153] has reported oxidations of benzylic alcohols to corresponding ketones in high yield within 2h by applying a TEMPO/Br_2/$NaNO_2$ system with 0.4 MPa air at 80 ºC in DCM, wherein NO (generated from $NaNO_2$) is critical to activate molecular oxygen. However, bromination of the aromatic rings occurred when this method was applied to highly electron-rich compounds. In order to avoid using hazardous Br_2 directly, a revised approach was reported by Xie[154] from the same group by using TEMPO/HBr/ *tert*-Butyl nitrite (which acts as a source of NO) system with 0.6 MPa O_2 at 80 ºC. Recently, Wang[49] introduced hydrochloric acid into the $NaNO_2$/TEMPO system, and alcohol oxidations were observed in extremely high conversion yield and selectivity at room temperature with an O_2 balloon. In this work, they assumed that H^+ was donated to $NaNO_2$ to produce NO and oxidizing species such as NOCl was generated from the reaction of halide anions with NO_2, wherein NOCl promoted the oxidation[155, 156] of TEMPO/TEMPOH to $TEMPO^+$, as shown in Scheme 2.15. Selectively oxidation of the benzylic hydroxyl in a β-O-4 lignin model by applying this methodology was reported by Rahimi,[51] wherein γ-hydroxy group remained unaffected, and carbon-carbon bond was cleaved with a subsequent oxidation, as shown in Scheme 2.16. This result also stimulates our interest to investigate the oxidation on β-1 and β-5 models since γ-alcohols also exist in these models.

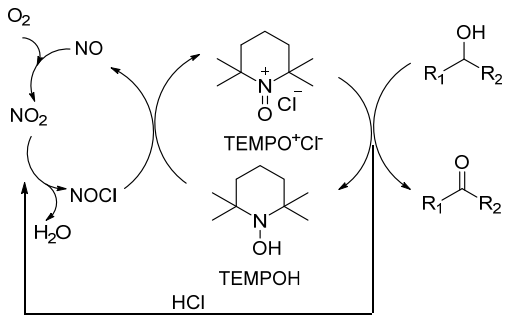

Scheme 2. 15 Proposed mechanism for TEMPO/HCl/$NaNO_2$-catalyzed aerobic oxidation of alcohols

---

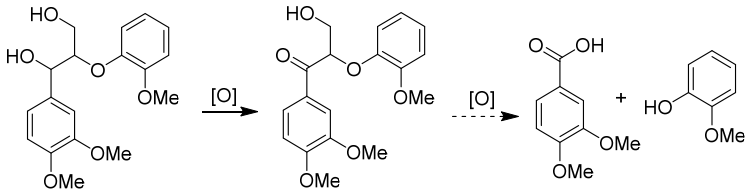

Scheme 2. 16 Selective alcohol oxidation of lignin model compounds

Aerobic oxidation of lignin β-O-4 model compounds with a Cu(I)-TEMPO system have been reported by number of groups[51, 157-162] and these reactions resulted in C-O and C-C bond cleavage products. A $Fe(NO_3)_3$/TEMPO system[163] was used to catalyze aerobic oxidation of alcohols to aldehydes/ketones and benzylic alcohol oxidation was obtained in 78% yield in β-O-4 lignin models.[51] Sedai[134] also reported aerobic oxidation of phenolic and non-phenolic β-1 lignin models with a CuOTf/TEMPO catalytic system, wherein C-C cleavage products were observed. These results are particularly significant, because in our hands,[115] oxidation of lignin models with unprotected phenolic hydroxyl groups produced significant amounts of chromatographically immobile products.

A variety of different TEMPO-based oxidation systems have been developed, in which different cocatalysts are employed. To enable a direct comparison between these different systems, we compared the yields of oxidation products at a standard reaction time of 19 hours.

The benzylic hydroxyl group in **II-1** was selectively oxidized to ketone **II-25** under $NaNO_2$/HCl/TEMPO system and we again isolated the unexpected 1,2-diketone product **II-29** in 12% yield. A small amount of 1,2-diketone **II-29** (see Scheme 2.17) was isolated when **II-1** was treated with $VO(acac)_2/O_2$ as well. Diketone **II-29** could result from one of several pathways, including benzylic oxidation of **II-30** (see Scheme 2.17), which is the *retro*-aldol condensation product of **II-25**. An authentic sample of **II-30** was prepared by acylation of veratrole with dimethoxyphenylacetic acid, and then subjected to TEMPO/O_2/HCl/$NaNO_2$ oxidation and to $VO(acac)_2/O_2$ oxidation, but neither of these reactions produced **II-29**. Accordingly, we suspect that **II-29** results from autoxidation of the benzylic C-H in **II-25**, followed by the loss of CH_2O and water (see Scheme 2.17). This hypothesis was supported by the observation that exposing **II-25** to the $NaNO_2$/HCl/TEMPO oxidation system resulted in formation of **II-29**. Oxidation of **II-1** afforded acid **II-12** (27%), aldehyde **II-13** (75%) and diketone **II-29** (19%) when treated with a CuCl/TEMPO/O_2 system, while ketone **II-25** (46%) and aldehyde **II-13** (31%) were the only products observed when **II-1** was treated with the $Fe(NO_3)_3$/TEMPO/O_2 system (see Table 2.1).

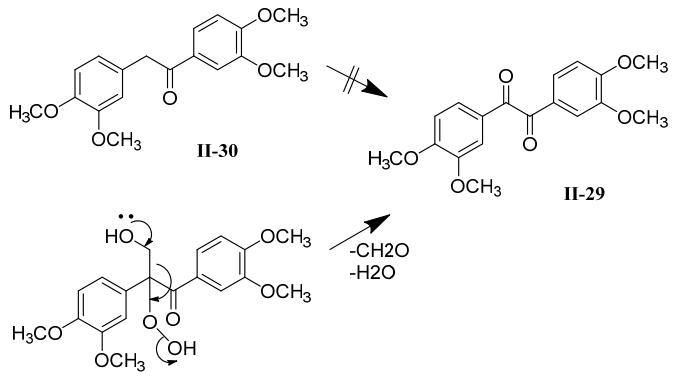

Scheme 2.17 Possible routes to produce **II-29** from the autoxidation product of **II-25**

Table 2. 1 TEMPO-based oxidation of **II-1**

	II-12	**II-13**	**II-25**	**II-29**
TEMPO, O_2, $HCl/NaNO_2$	0%	0%	46%	12%
TEMPO, $O_2/Fe(NO_3)_3$	0%	31%	46%	0%
TEMPO, O_2/CuCl	27%	75%	0%	19%

All TEMPO-based oxidations of β-5 model **II-3** produced benzofuran carboxaldehyde **II-16**, with few other minor side products. Of the three methods we examined, the TEMPO/O_2/$NaNO_2$/HCl method was the most efficient, producing a 50% yield of **II-16** after the standard reaction time. The other methods did not produce above a 16% yield of **II-16** after the same reaction time.

We find that TEMPO-based oxidations are generally not compatible with unprotected phenolic hydroxyls. In all TEMPO-based oxidations of **II-4**, we only obtained chromatographically immobile material, again presumably polymer. In reactions of **II-2**, we obtained immobile material in most cases, although small amounts of acid **II-12,** aldehyde **II-13** and ketone **II-26** were observed (see Table 2.2). It is notable that more C-C bond cleavage products acid **II-12** and aldehyde **II-13** were produced by the CuCl/TEMPO/O_2 system than by the other two systems, suggesting that Cu(I)/O_2 is an active oxidant of **II-2** and does more than just reoxidize TEMPO.

Table 2. 2 TEMPO oxidation of **II-2**

	II-12	**II-13**	**II-26**
TEMPO, O_2, $HCl/NaNO_2$	0%	0%	0%
TEMPO, $O_2/Fe(NO_3)_3$	0%	trace	16%
TEMPO, O_2/CuCl	19%	11%	19%

2.2.2.6 TPPFeCl/t-BuOOH Oxidation of II-1 - II-4

We previous found that the benzylic OH in the β-O-4 model **II-31** was oxidized to corresponding ketone **II-32** with a porphyrin/t-BuOOH oxidation system[164] but under same conditions we find that C-C bond cleavage dominated in the oxidation of the nonphenolic β-1 model **II-1**. The primary products of this reaction were 3,4-dimethoxybenzoic acid **II-12** (15%) and 3,4-dimethoxybenzaldehyde **II-13** (50%). Only 8% of the corresponding ketone **II-25** was formed, and 11% of starting material was recovered. The same porphyrin-based oxidation of the nonphenolic β-5 model **II-3** generated a 22% yield of aromatized aldehyde **II-16**, a 3% yield of alcohol **II-27**, and surprisingly a 16% yield of 3,4-dimethoxy benzaldehyde **II-13** was obtained, resulting from opening of the dihydrofuran ring. Starting material **II-3** (28%) was also recovered (Scheme 2.18).

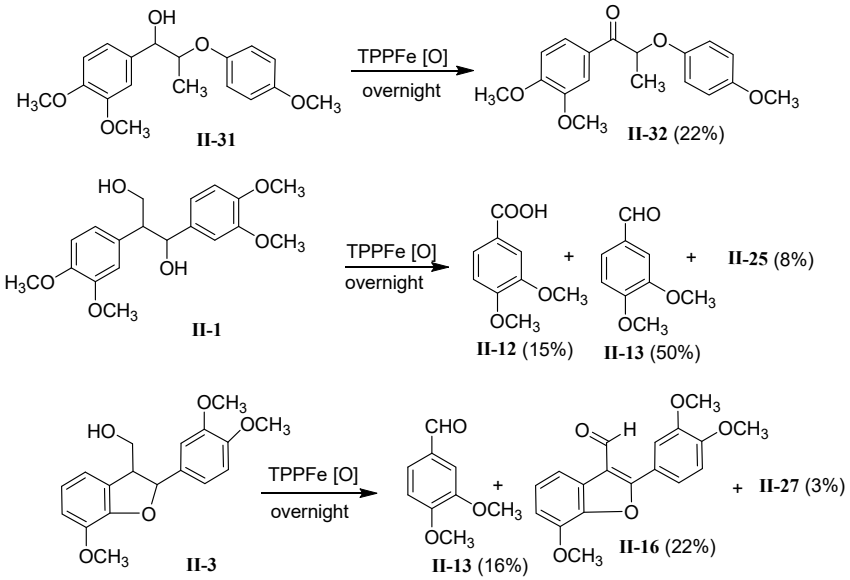

Scheme 2. 18 Porphyrin oxidations of β-O-4, β-1 and β-5 models

Oxidative coupling reactions usually occur due to a large amount of free phenols existing in the lignin polymer, causing formation of char or other insoluble components. Therefore, searching for other strategies that can produce simple aromatics under mild

conditions is also significant. Considering the dominant C-O-C linkages and unprotected phenolic hydroxyl groups in lignin, acid-catalyzed and base-catalyzed decomposition should be notable. Thus, we selectively treated specific model compound **II-3** under acid conditions and **II-4** under alkaline conditions to investigate how they behave under these treatments.

2.2.3 Acid-catalyzed Cleavage of Model Compound II-3

Strong acids with a nucleophilic conjugate base are capable of cleaving ethers.[165] Given the frequency of ether linkages in lignin, we wanted to see how strong acids affect the ethers in models for the β-5 linkage. We know that ring-opening of epoxy compounds involves protonating the ether and nucleophilic attacking on the adjacent carbon to this protonated ether. Hydrobromic acid is a notable option because it is a proton-donating source and nucleophile.

Boovanahalli[165] reported cleavage of 2,3-dihydrobenzofuran with hydrobromic acid in an ionic liquid solvent, although in low isolated yield. Prolonged heating did not increase the yield but did increase the formation of byproducts. Ionic liquids can be used as effective solvents, but they are expensive and hard to remove from the mixture. Therefore, in our experiments we used DCE instead of ionic liquids.

Treatment of **II-3** with HBr produced benzofuran **II-33** in 12.5% yield, as well as multiple byproducts. These byproducts may be formed as a result of cleavage of one or more of the methoxy groups, but none of these products have been identified. Prolonged heating did not improve yield of **II-33**. Ring-opened products were not present in significant amounts in the mixture, possibly because the intramolecular 5-member ring-closure (the reverse

reaction) preferred to occur due to tautomerization. A possible mechanism for the formation of **II-33** is shown in Scheme 2.19.

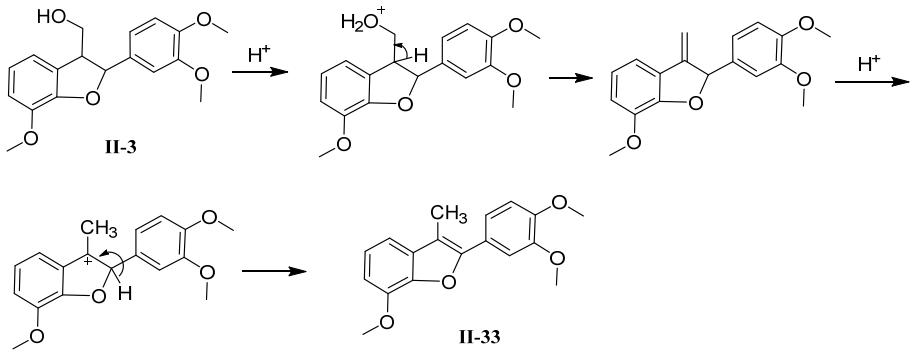

Scheme 2. 19 Proposed mechanism of formation of **II-33**

2.2.4 Basic-catalyzed Cleavage of Model Compound II-4

Hydrolysis of lignin in basic conditions usually generates relatively simple aromatics under mild conditions although in low yield.[16] Cleavage of ether bonds is an attractive and common approach in lignin decomposition, utilizing commercially available, inexpensive bases such as KOH and NaOH. Organic bases such as TBD (1,5,7-triazabicyclo[4.4.0]dec-5-ene) has also been used, in combination of an ionic liquid ([BDMIm]Cl), for delignification of lignin,[79] a process wherein over 40% of the β-O-4 ether bonds were cleaved.

Repolymerization issues should be considered in delignification process; therefore, inhibition of the repolymerization reactions is one of the key challenges in generation of mononuclear aromatic products from lignin. Introduction of capping reagents such as boric acid and phenol, which capture reactive species, have been reported[73, 166, 167] to solve this problem. Other approaches such as application of more selective catalysts in base-catalyzed hydrolysis[168, 169] has also been helpful. Though base-catalyzed deconstruction of lignin models can produce monomeric products in reasonable yields, we should notice that native lignin is extremely difficult to isolate from biomass[22] due to the complex physical and chemical

interactions between lignin and other compositions of plants, which makes it very hard to study the chemistry of these linkages when applying those same base-catalyzed systems to lignin itself.

When β-5 models that bear a phenolic hydroxyl are treated with base, the 2, 3-dihydrobenzofuran ring can be opened to a quinone methide intermediate. John[170] reported that a cyclization of this intermediate, a process that would re-aromatize the A-ring, is more favorable than elimination of a β-proton, so the ring-opening product (a stilbene) is a minor product. The presence of electron-withdrawing group in the γ position, an ester group (compound **II-34**) in John's case,[170] favors the elimination of the β-proton resulting in the aromatization of the A-ring (showed in Scheme 2.20).

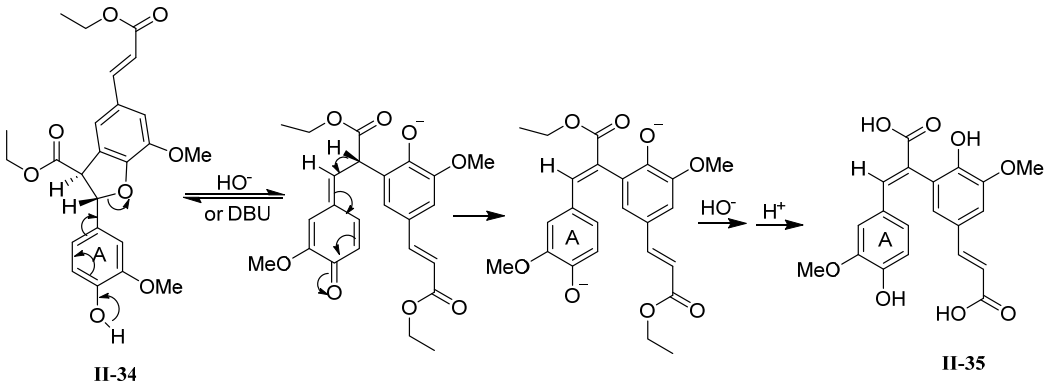

Scheme 2. 20 Mechanism for the formation of the stilbene **II-35** from basic treatment of the β-5-coupled dehydrodiferulate ester **II-34** in the cell wall

In our case, when **II-4** is treated with KOH in 1,4-dioxane at room temperature and stirred overnight, 72% of the starting material was recovered. However, we also isolate small amounts of stilbene **II-36**, resulting from loss of the γ hydroxymethyl group**.** Since the β-proton in **II-4** is adjacent to a weakly electron-withdrawing hydroxymethyl group, it is less acidic than the β-proton in the diester reported by John,[170] so elimination is slow and recyclization is the major pathway. Therefore, restriction of ring-closure reaction and

accelerate the elimination is essential to shift the equilibrium to the stilbene side. A possible mechanism of formation of stilbene **II-36** is shown below in Scheme 2.21.

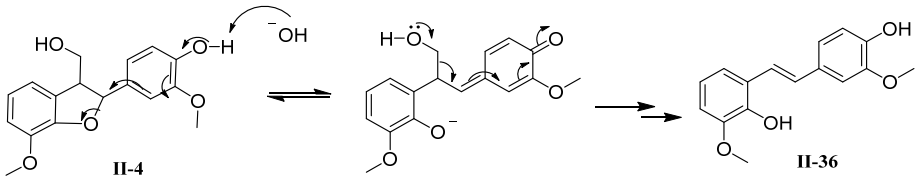

Scheme 2. 21 Proposed mechanism of formation of stilbene **II-36**

2.3 Conclusion

We have prepared several compounds as models for the β-1 and β-5 linkages in the biopolymer lignin, and we investigated the chemistry of these compounds under conditions that have been applied to the common β-O-4 linkage. We observed that in many cases benzylic hydroxyl groups can be selectively oxidized by several different oxidants. However, direct oxidative cleavage of C-C bonds in β-1 models was observed in metal-catalyzed TEMPO oxidation systems and with stoichiometric strong oxidants (i.e. $KMnO_4$ and Co(III) acetate), unlike the result of these reactions when applied to β-O-4 models. Interestingly, different TEMPO-based oxidation systems produced different arrays of products, suggesting that the reagents used to reoxidize TEMPO ($NaNO_2/O_2$, $Fe(NO_3)_3/O_2$, and $CuCl/O_2$) are not completely innocent - they play roles as oxidants beyond just the reoxidation of TEMPO.[134] Benzylic oxidation dominated in metal-free catalyzed TEMPO oxidation of both non-phenolic β-O-4 and β-1 compounds, while C-C bond cleavage was observed in copper or iron catalyzed TEMPO oxidation of non-phenolic β-1 models. Oxidative cleavage of β-O-4 model compounds does not occur in a significant extent under the same conditions.[51] In all cases, chromatographically immobile products (presumed to be polymers) were formed when

phenolic β-O-4, β-1 and β-5 models were treated under the same conditions. In addition, aromatization of the dihydrofuran ring in compound **II-3** took place in all TEMPO-based oxidations.

It is not surprising that the β-5 linkage proved to be more difficult to cleave than the β-1 linkage. Oxidation most often resulted in simple aromatization of the dihydrofuran. Reactions that opened the dihydrofuran ring in the β-5 model **II-3** were only observed when **II-3** were treated with $KMnO_4$ at elevated temperature.

Oxidative approaches to lignin depolymerization always risk the formation of intractable material by oxidative coupling of phenolic monomers that are liberated in the course of depolymerization. In most cases, here and elsewhere,[171, 172] the presence of unprotected phenols tends to lead to formation of insoluble and chromatographically immobile materials, presumably oxidative coupling products. We found that while some reagents produce immobile materials from oxidation of unprotected phenols **II-2** and **II-4**, several proved to be somewhat compatible with phenols. Oxidation of **II-2** with $KMnO_4$ and with $VO(acac)_2$ both produced mononuclear aromatic products though cleavage of the C_α-C_β bond, but most of the material from the phenol-bearing ring was lost. Most promising was the oxidation of **II-2** with DDQ, which produced benzylic ketone **II-26** in high yield. This reaction exhibits selectivity for the benzylic position as well as compatibility with phenols, characteristics that are highly desirable for a two-step, benzylic oxidation/Baeyer-Villiger route to cleavage of lignin.

Under most effective conditions for cleaving β-O-4 linkages, the β-1 linkages and the β-5 linkages break as well. When subjected to TPPFeCl/tBuOOH oxidation, β-1 models react

quite differently from β-O-4 models. The β-1 model **II-1** undergoes C-C bond cleavage, whereas the β-O-4 models studied earlier[164] produce benzylic ketones. This difference highlights the need to understand how different lignin linkages behave under oxidizing conditions. An effective approach to oxidative deconstruction of lignin will need to consider the effect of oxidation on each of the diverse array of linkages present in lignin.

2.4 Experimental Section

Column chromatography was performed using silica gel-60 (Supelco) and preparative TLC was carried out with 1 mm plates (Merck). ^{1}H and ^{13}CNMR spectra were obtained at room temperature on a Varian INOVA 400 MHz spectrometer, with chemical shifts (δ) referenced to the residual solvent signal. Following the method of Cho,[122] compounds **1** and **2** were prepared by the following procedure:

2.4.1 Synthesis of Model Compounds II-1 and II-2

Preparation of II-1

A solution of 1.3 mL 2.5M n-BuLi (3.28 mmol) was added to a stirred solution of diisopropylamine (0.46 mL, 3.28 mmol) in 3 mL dry THF at -78 ^{o}C under N_2 atmosphere. After 30 mins ethyl 3,4-dimethoxyphenyl acetate **II-5** (0.74 g, 3.28 mmol) was added dropwise and then the resulting solution was stirred for 1 h followed by addition of veratrylaldehyde **II-6a** (0.45 g, 2.73 mmol). After 3 h additional stirring at the same temperature, the mixture was diluted with 10 mL H_2O and extracted with ethyl acetate (3 x 10 mL). The combined organic layers were dried with Na_2SO_4 and evaporated in *vacuo*.

Purification by column chromatography on silica gel (hexane/ethyl acetate = 3:1) to give **II-7a** as a yellow oil (0.25 g, 0.64 mmol, 24%).

$LiAlH_4$ (0.043 g, 1.126 mmol) was added into as a solution of ester **II-7a** (0.22 g, 0.563 mmol) in 10 mL THF in ice bath. The mixture was stirred for 30 mins at 0 ^oC and then for 3 h at room temperature. The solution was diluted with 5 mL H_2O and acidified with 5 mL 1 M HCl solution then extracted with ethyl acetate (3 x 10 mL). The combined organic layers were dried with Na_2SO_4 and evaporated in *vacuo*. The crude product was purified by column chromatography on silica gel (hexane/ethyl acetate = 3:1) to produce **II-1** as a yellow oil (0.08 g, 0.23 mmol, 42%).

^{1}HNMR (400 MHz, $CDCl_3$): 6.89 - 6.73 (6 H, m), 4.93 (1 H, d, J = 4.5 Hz), 3.91 - 3.80 (12 H, m), 3.79 - 3.73 (2 H, m), 3.09 (1 H, d, J = 6.5 Hz); ^{1}CNMR (100 MHz, $CDCl_3$): 148.5, 148.5 148.1, 147.7, 135.5, 131.7, 120.3, 118.8, 111.9, 110.9, 110.4, 109.5, 79.3, 66.4, 55.8, 55.8, 55.7, 55.7, 54.4.

Preparation of II-2

Ethyl 3,4-dimethoxyphenyl acetate **II-5** (0.74 g, 3.28 mmol,) was added dropwise in solution of THF containing 2.5 M LDA (2.4 mL, 6.0 mmol) in 10 mL dry THF at -78 ^oC under N_2 atmosphere and stirred for 1h. The resulting solution was stirred for 1 h followed by addition of aldehyde **II-6b** (0.7 g, 2.73 mmol). After 3 h additional stirring at the same temperature, the mixture was diluted with 10 mL H_2O and extracted with ethyl acetate (3 x 10 mL). The combined organic layers were dried with Na_2SO_4 and evaporated in *vacuo* to produce a crude brown oil (1.4 g). Purification by column chromatography on silica gel (hexane/ethyl acetate = 2:1) to yield **II-7b** as a yellow oil (0.6 g, 1.25 mmol, 46%).

$LiAlH_4$ (0.1 g, 2.5 mmol) was added into as a solution of ester **II-7b** (0.6 g, 1.25 mmol) in 10 mL THF in ice bath. The mixture was stirred for 30 mins at 0 ^oC then for 3 h at room temperature. The solution was diluted with 5 mL H_2O and acidified with 5 mL 1M HCl solution then extracted with ethyl acetate (3 x 10 mL). The combined organic layers were dried with Na_2SO_4 and concentrated in *vacuo*. The crude was purified by column chromatography on silica gel (hexane/ethyl acetate = 1:1) to produce **II-2** as a yellow oil (0.21 g, 0.628 mmol, 68%).

^{1}HNMR (400 MHz, $CDCl_3$): 6.78 (2 H, d, *J* = 7.9 Hz), 6.70 - 6.66 (2 H, m), 6.64 (3 H, d, *J* = 1.2 Hz), 4.88 (1 H, d, *J* = 6.4 Hz), 3.90 - 3.82 (2 H, m), 3.82 (3 H, s), 3.76 (6 H, s), 3.03 (1 H, t, *J* = 6.5 Hz), 3.01 - 2.94 (1 H, m); ^{1}CNMR (100 MHz, $CDCl_3$): 148.7, 148.0, 146.5, 145.1, 133.9, 131.0, 121.0, 119.5, 114.0, 112.5, 111.1, 109.2, 75.5, 63.9, 55.8, 55.7, 55.7, 54.9.

Following the method of Brunow,[123] compounds **II-3** and **II-4** were prepared by the following procedure:

Preparation of II-3

A solution of 12 g KOH in 20 mL methanol was added dropwise to a stirred solution of 3,4-dimethoxyacetophenone **II-8a** (1.09 g, 6 mmol) and 2-(benzyloxy)-3-methoxybenzaldehyde (1.45 g, 6 mmol) in 20 mL methanol. After stirring for 24 h, the solution was neutralized by adding 4 M HCl. The yellow precipitate formed was isolated by vacuum filtration, and the filter cake was washed with methanol, then with water. The solid was dried and recrystallized from methanol to produce chalcone **II-9a** as a yellow oil (0.92 g, 2.35 mmol, 60%).

A solution of 5 mL 30% hydrogen peroxide and 6 mL 4% (w/v) aqueous NaOH was added dropwise to chilled solution of chalcone **II-9a** (0.818 g, 2 mmol) in DCM (10 mL, precooled to 0 ^{o}C in an ice bath). Phase transfer catalyst TBAB (0.1g, 0.31mmol) was added and then the mixture was stirred at ice bath for 30 mins and overnight at room temperature. Saturated aqueous $Na_2S_2O_3$ (10 mL) was added to quench the reaction. The solution was extracted with dichloromethane (3 x 20 mL) and the combined organic layers were dried with Na_2SO_4. Evaporation of the solvent gave **II-10a** as a yellow oil (0.78 g, 1.86 mmol, 93%).

Fresh BF_3-diethyl etherate (1.8 g, 13 mmol) was added dropwise into as solution of **II-10a** (0.55 g, 1.3 mmol) in 20 mL dry diethyl ether. The mixture was stirred at room temperature for 2.5 h and then quenched by adding water (20 mL). The organic layer was separated and extracted the aqueous layer with ethyl acetate (3 x 20 mL). All organic layers were combined and dried with Na_2SO_4. Evaporation of solvent gave a dark brown product that was used in the next step without purification.

The crude product was dissolved in 20 mL dioxane-H_2O (v/v=1:1), then $NaBH_4$ (0.4 g, 7.14 mmol) was added to the solution. The mixture was stirred for 24 h then acidified with 1M HCl to pH=7, and extracted with dichloromethane (3 x 20 mL). The combined organic layers were washed with saturated aqueous NaCl, dried with Na_2SO_4 and evaporation of solvent gave orange oil. Purification by column chromatography on silica gel (hexane/ethyl acetate = 3:1) gave **II-11a** as a yellow oil (1.3 g, 3.07 mmol, 47%).

A suspension of benzyl ether **II-11a** (0.2 g, 0.47 mmol) and 20 mg 10% Pd/C in 10 mL methanol was stirred under 1 atm H_2 (balloon). The hydrogenation consumption ceased after 3 h. The catalyst was filtered off and evaporation of solvent gave the 1,3-diol as a yellow

oil (0.15 g, 0.45 mmol, 92%), wherein (80 mg, 0.24 mmol) of the resulting 1,3-diol was then dissolved in 5 mL dioxane-H_2O (v/v=1:1) and was treated with 1.0 mL 0.2 M HCl at 50 ºC for 7 h. The solution was cooled, then neutralized with 1 M aqueous NaOH to pH=7 and extracted with ethyl acetate (3 x 10 mL). The combined organic layers were dried with Na_2SO_4. Evaporation of solvent gave **II-3** as a yellow oil (66 mg, 0.209 mmol, 88%).

^{1}HNMR (400 MHz, $CDCl_3$): 6.96 - 6.92 (2 H, m), 6.90 - 6.85 (1 H, m), 6.84 - 6.79 (3 H, m), 5.58 (1 H, d, *J* = 7.2 Hz), 3.99 - 3.93 (1 H, m), 3.90 (1 H, m, *J* = 5.5 Hz, 3.9 Hz), 3.88 (3 H, s), 3.85 (3 H, s), 3.83 (3 H, s), 3.66 - 3.60 (1 H, m); ^{13}CNMR (100 MHz, $CDCl_3$): 149.1, 148.9, 148.3, 144.5, 133.6, 127.7, 121.4, 118.6, 116.2, 112.0, 110.9, 109.3, 87.7, 64.0, 55.9, 55.9, 55.8, 53.6

Preparation of II-4

A solution of 5.6 g KOH in 20 mL methanol was added dropwise to a stirred solution of 1-(4-(benzyloxy)-3-methoxyphenyl)ethanone **II-8b** (2.7 g, 10.5 mmol) and 2-(benzyloxy)-3-methoxybenzaldehyde (2.5 g, 10.5 mmol) in 40 mL methanol. After stirring for 24 h, the solution was neutralized by adding 4 M HCl. The yellow precipitate formed was isolated by vacuum filtration, and the filter cake was washed with methanol, then with water. The solid was dried and recrystallized from methanol to produce chalcone **II-9b** (3.6 g, 7.5 mmol, 71%) as yellow plates which were used in the following step.

A solution of 7.8 mL 30% hydrogen peroxide and 11 mL 4% (w/v) aqueous NaOH was added dropwise to chilled solution of chalcone **II-9b** (3.5 g, 7.26 mmol) in DCM (20 mL, precooled to 0 ºC in an ice bath). Phase transfer catalyst TBAB (0.35g, 1.08 mmol) was added and then the mixture was stirred at ice bath for 30 mins and overnight at room temperature.

Saturated aqueous $Na_2S_2O_3$ (10 mL) was added to quench the reaction. The solution was extracted with dichloromethane (3 x 20 mL) and the combined organic layers were dried with Na_2SO_4. Evaporation of the solvent gave **II-10b** as a yellow oil (3.6 g, 7.25 mmol, 99%).

Fresh BF_3-diethyl etherate (10.26 g, 72 mmol) was added dropwise into as solution of **II-10b** (3.6 g, 7.2 mmol) in 50 mL dry diethyl ether. The mixture was stirred at room temperature for 2.5 h and then quenched by adding water (100 mL). The organic layer was separated and extracted the aqueous layer with ethyl acetate (3 x 20 mL). All organic layers were combined and dried with Na_2SO_4. Evaporation of solvent gave a dark brown product that was used in the next step without purification.

The crude product was dissolved in 50 mL dioxane-H_2O (v/v=1:1), then $NaBH_4$ (2.6 g, 46.4 mmol) was added to the solution. The mixture was stirred for 24 h then acidified with 1M HCl to pH=7, and extracted with dichloromethane (3 x 20 mL). The combined organic layers were washed with saturated aqueous NaCl, dried with Na_2SO_4 and evaporation of solvent gave orange oil. Purification by column chromatography on silica gel (CH_2Cl_2/ethyl acetate = 4:1) gave **II-11b** as a yellow oil (1.3 g, 2.6 mmol, 36%).

A suspension of benzyl ether **II-11b** (1.3 g, 2.6 mmol) and 0.1g 10% Pd/C in 30 mL methanol was stirred under 1 atm H_2 (balloon). The hydrogenation consumption ceased after 3 h. The catalyst was filtered off and evaporation of solvent gave the 1,3-diol as a yellow oil (0.76 g, 2.37 mmol, 92%) which was then dissolved in 30 mL dioxane-H_2O (v/v=1:1) and was treated with 10 mL 0.2 M HCl at 50 ^oC for 7 h. The solution was cooled, then neutralized with 1 M aqueous NaOH to pH=7 and extracted with ethyl acetate (3 x 20 mL). The

combined organic layers were dried with Na_2SO_4. Evaporation of solvent gave **II-4** as a yellow oil (0.6 g, 1.98 mmol, 84%).

^{1}HNMR (400 MHz, $CDCl_3$): 6.94 - 6.71 (6 H, m), 5.51 (1 H, d, *J* = 7.0 Hz), 3.86 (5 H, d, *J* = 7.3 Hz), 3.76 (3 H, s), 3.59 (1 H, d, *J* = 5.9 Hz); ^{13}CNMR (100 MHz, $CDCl_3$): 146.8, 146.5, 145.0, 131.2, 123.5, 122.3, 121.1, 114.8, 113.6, 111.7, 110.1, 106.5, 79.0, 56.0, 55.9, 55.8, 55.3.

2.4.2 Oxidation of Model Compounds II-1 - II-4

2.4.2.1 General Procedure for the $KMnO_4$-Catalyzed Oxidation of II-1 - II-4

A mixture of lignin model (1 eq.) and $KMnO_4$ (2 eq.) in AcOH (4 mL/mmol) was stirred at 120 ^oC for 19 h. The mixture was then cooled, diluted with water and extracted with ethyl acetate. The combined organic layers were washed with aqueous KOH, aqueous HCl, and water, then dried over Na_2SO_4 and concentrated under vacuum. The products were purified by column chromatography on silica gel.

$KMnO_4$ oxidation of II-1

A mixture of **II-1** (90 mg, 0.26 mmol) and $KMnO_4$ (164 mg, 0.52mmol) in AcOH (2 mL) was used. The products were purified by column chromatography on silica gel (hexane/ethyl acetate = 3:1) to give acid **12** (40 mg, 0.22 mmol, 85%) as white solid.

$KMnO_4$ oxidation of II-2

A mixture of **II-2** (36 mg, 0.11 mmol) and $KMnO_4$ (34 mg, 0.22mmol) in AcOH (1 mL) was used. The products were purified by column chromatography on silica gel (hexane/ethyl acetate = 3:1) to give acid **II-12** (3 mg, 0.016 mmol, 15%) and aldehyde **II-13** (2 mg, 0.013 mmol, 12%) as white solids. Chromatographically immobile was also observed.

$KMnO_4$ oxidation of II-3

A mixture of **II-3** (76 mg, 0.24 mmol) and $KMnO_4$ (76 mg, 0.48mmol) in AcOH (2 mL) was used. The products were purified by column chromatography on silica gel (hexane/ethyl acetate = 1:1) to give acid **II-12** (11 mg, 0.06 mmol, 19%), aldehyde **II-13** (9 mg, 0.05 mmol, 17%), and **II-15** (14mg, 0.04 mmol, 12%) as yellow oils. A trace amount of aldehyde **16** was also isolated. NMR spectra of **II-12** and **II-13** are identical to literature reports.[173, 174]

II-15: (2-(1-(3,4-dimethoxyphenyl)-1,3-dihydroxypropan-2-yl)-6-methoxyphenyl acetate): ^{1}HNMR (400 MHz, $CDCl_3$): 6.94 (2 H, d, *J* = 9.2 Hz), 6.89 (1 H, dd, *J* = 9.0 Hz, 5.9 Hz), 6.86 - 6.80 (3 H, m), 5.47 (1 H, d, *J* = 7.4 Hz), 4.43 (1 H, dd, *J* = 11.1 Hz, 5.6 Hz), 4.32 (1 H, dd, *J* = 11.1 Hz, 7.4 Hz), 3.90 (3 H, d, *J* = 1.4 Hz), 3.87 (3 H, s), 3.85 (3 H, s), 3.84 - 3.77 (1 H, m), 2.02 (3 H, s). ^{13}CNMR (100 MHz, $CDCl_3$): 170.8, 149.2, 149.1, 148.0, 144.5, 133.0, 127.4, 121.5, 118.8, 116.6, 112.2, 111.0, 109.3, 88.2, 65.5, 56.0, 55.9, 55.9, 50.4, 20.8. HRMS (ESI): *m*/*z* $[M + NH_4 - H_2O]^+$ calcd for $C_{20}H_{26}NO_6$ 376.1760, found 376.1754.

$KMnO_4$ oxidation of II-4

A mixture of **II-4** (240 mg, 0.80 mmol) and $KMnO_4$ (251 mg, 1.59 mmol) in 8 mL AcOH was used. An insoluble product (138 mg) was isolated, along with 86 mg of ethyl acetate-soluble and chromatography mobile (100% MeOH) material was also isolated but could only be identified as a complex mixture of products.

2.4.2.2 General Procedure for the Co(III) Catalyzed Oxidation of II-1 - II-4

A mixture of lignin model (1 eq.), $Co(OAc)_2 \cdot 4H_2O$ (2 eq.) and AcOH (2 mL/mmol) were stirred under an O_2 atmosphere (balloon) at 120 ^oC for 19h. The mixture was extracted

with DCM and the organic layer was washed with chilled water. The combined organic layers were dried over Na_2SO_4 and concentrated under vacuum. The crude products were purified by column chromatography on silica gel.

Co(III) oxidation of II-1

Products afforded from a mixture of **II-1** (90 mg, 0.26 mmol) and $Co(OAc)_2 \cdot 4H_2O$ (129 mg, 0.52 mmol) were purified by column chromatography on silica gel (hexane/ethyl acetate = 1:1) to give aldehyde **II-13** (35 mg, 0.21 mmol, 81.5%).

Co(III) oxidation of II-2

Products afforded from a mixture of **II-2** (90 mg, 0.27 mmol) and $Co(OAc)_2 \cdot 4H_2O$ (134 mg, 0.54 mmol) were purified column chromatography on silica gel (hexane/ethyl acetate = 1:1) (hexane/ethyl acetate = 3:1) to give a yellow solid stilbene (**II-19**) (7 mg, 0.024 mmol, 9.1%), a yellow oil diester (**II-20**) (1.8 mg, 0.006 mmol, 2.4%), a yellow oil isomeric diester (**II-21**) (31.5 mg, 0.075 mmol, 27.9%) and a yellow oil isomeric ester (**II-22**) (8.5 mg, 0.02 mmol, 7.5%).

II-19:**(E)-4-(3,4-dimethoxystyryl)-2-methoxyphenol.** ^{1}HNMR (400 MHz, $CDCl_3$): 7.04 (1 H, d, *J* = 1.9 Hz), 7.02 (2 H, dd, *J* = 4.9 Hz, 3.1 Hz), 7.00 - 6.98 (1 H, m), 6.91 - 6.87 (3 H, m), 6.84 (1 H, d, *J* = 8.2 Hz), 5.62 (1 H, s), 3.94 (3 H, s), 3.93 (3 H, s), 3.89 (3 H, s). ^{13}CNMR (100 MHz, $CDCl_3$): 149.1, 148.6, 146.7, 145.3, 130.7, 130.2, 126.8, 126.3, 120.1, 119.5, 114.5, 111.3, 108.6, 108.0, 55.9, 55.9, 55.8.

Diester II-20: **(1-(3,4-dimethoxyphenyl)-1,2-ethanediol-1,2-diacetate**). ^{1}HNMR (400 MHz, $CDCl_3$): 6.94 (1 H, ddd, *J* = 8.2 Hz, 2.0 Hz, 0.4 Hz), 6.90 (1 H, d, *J* = 2.0 Hz), 6.85 (1 H, d, *J* = 8.3 Hz), 5.97 (1 H, dd, *J* = 6.7 Hz, 5.4 Hz), 4.31 (1 H, s), 4.30 (1 H, s), 3.89

(3 H, s), 3.85 (3 H, s), 2.10 (3 H, s), 2.05 (3 H, s). ^{13}CNMR (100 MHz, $CDCl_3$): 170.4, 169.8, 149.2, 149.0, 128.9, 119.2, 111.1, 110.0, 73.0, 65.9, 55.8, 55.7, 20.9, 20.6.

Diester (**II-21**): ^{1}HNMR (400 MHz, $CDCl_3$, mixture of diastereomers): 6.83 - 6.77 (1 H, m), 6.77 - 6.73 (2 H, m), 6.72 (1 H, d, *J* = 2.5 Hz), 6.70 - 6.67 (1 H, m), 6.65 (2 H, dd, *J* = 7.8 Hz, 1.9 Hz), 6.61 (1 H, d, *J* = 1.9 Hz), 6.55 (1 H, dd, *J* = 8.2 Hz, 2.0 Hz), 6.45 (1 H, d, *J* = 2.0 Hz), 6.00 (1 H, d, *J* = 7.6 Hz), 5.90 (1 H, d, *J* = 8.7 Hz), 5.61 (1 H, s), 5.53 (1 H, s), 4.47 (1 H, dd, *J* = 11.1 Hz, 7.2 Hz), 4.32 (1 H, dd, *J* = 11.1 Hz, 5.3 Hz), 4.25 (1 H, dd, *J* = 11.2 Hz, 6.2 Hz), 4.08 (1 H, dd, *J* 11.2 Hz, 6.9 Hz), 3.84 (3 H, s), 3.80 (3 H, s), 3.79 (2 H, s), 3.77 (3 H, s), 3.72 (2 H, s), 3.69 (2 H, s), 3.41 – 3.35 (1 H, m), 3.32 (1 H, q, *J* = 6.9 Hz), 2.06 (2 H, s), 1.99 (2 H, s), 1.93 (3 H, s), 1.90 (3 H, s). ^{13}CNMR (100 MHz, $CDCl_3$, mixture of diastereomers): 170.9, 170.7, 169.9, 169.7, 148.5, 148.4, 148.1, 148.0, 146.2, 145.9, 145.6, 145.2, 130.2, 130.2, 130.1, 130.1, 121.1, 121.0, 120.2, 120.1, 114.2, 114.0, 112.1, 112.0, 110.8, 110.8, 110.1, 109.7, 76.3, 75.5, 64.6, 55.8, 55.8, 55.8, 55.8, 55.8, 55.7, 49.8, 49.5, 21.2, 21.0, 20.9, 20.8. HRMS (ESI, NH_4Cl buffer): *m*/*z* $[M + NH_4]^+$ calcd for $C_{22}H_{30}NO_8$ 436.1971, found 436.1965.

Ester II-22 (mixture of diastereomers): ^{1}HNMR (400 MHz, $CDCl_3$,): 7.08 - 7.02 (2 H, m), 6.99 (1 H, s), 6.93 (1 H, d, *J* = 8.1 Hz), 6.91 - 6.88 (2 H, m), 6.88 - 6.84 (2 H, m), 6.82 (1 H, dd, *J* = 8.2 Hz, 1.8 Hz), 6.77 (1 H, d, *J* = 1.8 Hz), 6.72 (1 H, d, *J* = 8.2 Hz), 6.64 (1 H, dd, *J* = 8.2 Hz, 2.0 Hz), 6.58 (1 H, s), 6.49 (1 H, d, *J* = 1.9 Hz), 5.66 (1 H, s), 5.53 - 5.51 (1 H, m), 5.15 (2 H, s), 4.87 (2 H, d, *J* = 1.2 Hz), 3.93 (3 H, s), 3.91 (3 H, s), 3.90 (3 H, s), 3.89 (3 H, s), 3.76 (3 H, s), 3.54 (3 H, s), 2.06 (3 H, s), 2.06 (2 H, s). ^{13}CNMR (100 MHz, $CDCl_3$, mixture of diastereomers): 171.0, 170.7, 149.1, 148.8, 148.8, 148.4, 146.3, 145.7, 145.3, 144.9, 134.2,

133.9, 133.2, 132.4, 131.0, 129.4, 129.0, 128.4, 123.3, 122.4, 121.1, 118.7, 114.4, 113.9, 112.2, 111.4, 111.3, 111.2, 111.1, 109.6, 69.6, 62.2, 55.9, 55.9, 55.9, 55.9, 55.8, 55.4, 29.7, 21.0. HRMS (ESI): *m*/*z* $[M\text{-}CH_3COO]^+$ calcd for $C_{18}H_{19}O_4$ 299.1283, found 299.1279.

Co(III) oxidation of II-3

Products afforded from a mixture of **II-3** (90 mg, 0.28 mmol) and $Co(OAc)_2 \cdot 4H_2O$ (142 mg, 0.57 mmol) were purified by column chromatography on silica gel (hexane/ethyl acetate = 1:1), gave the γ-acetate from **3** as a brown oil (90 mg, 0.25 mmol, 88%).

II-23:(**(2-(3,4-dimethoxyphenyl)-7-methoxy-2,3-dihydrobenzofuran-3-yl)methyl acetate**): ^{1}HNMR (400 MHz, $CDCl_3$): 6.95 - 6.79 (6 H, m), 5.45 (1 H, d, *J* = 7.5 Hz), 4.42 (1 H, dd, *J* = 11.2 Hz, 5.6 Hz), 4.30 (1 H, dd, *J* = 11.1 Hz, 7.4 Hz), 3.87 (3 H, s), 3.84 (6 H, d, *J* = 4.7 Hz), 3.82 - 3.76 (1 H, m), 2.00 (3 H, s). ^{13}CNMR (100 MHz, $CDCl_3$): 170.8, 149.1, 149.1, 148.0, 144.5, 133.0, 127.4, 121.5, 118.8, 116.6, 112.1, 110.9, 109.2, 88.2, 65.5, 56.0, 55.9, 55.9, 50.4, 20.8.

Co(III) oxidation of II-4

Products afforded from a mixture of **II-4** (63 mg, 0.21 mmol) and $Co(OAc)_2 \cdot 4H_2O$ (0.41 mg, 0.41 mmol) were purified by column chromatography on silica gel (hexane/ethyl acetate = 1:1) to give a phenyl acetate from **II-4** as a brown oil (49 mg, 0.13 mmol, 70%). Chromatographically immobile products were also observed.

II-24: 4-(3-(hydroxymethyl)-7-methoxy-2,3-dihydrobenzofuran-2-yl)-2-methoxyphenyl acetate: ^{1}HNMR (400 MHz, $CDCl_3$): 6.91 (1 H, d, *J* = 4.5 Hz), 6.88 (3 H, m), 6.85 - 6.82 (2 H, m), 5.67 (1 H, s), 5.45 (1 H, d, *J* = 7.5 Hz), 4.44 (1 H, dd, *J* = 11.1 Hz, 5.6 Hz), 4.32 (1 H, dd, *J* = 11.1 Hz, 7.5 Hz), 3.89 (3 H, s), 3.86 (3 H, s), 3.80 (1 H, dd, *J* =

10.9 Hz, 5.2 Hz), 2.02 (3 H, s). ^{13}CNMR (100 MHz, $CDCl_3$): 170.6, 147.7, 146.4, 145.5, 144.3, 132.2, 127.2, 121.3, 119.32, 116.3, 114.0, 111.9, 108.4, 88.1, 65.2, 55.7, 55.7, 50.2, 20.5.

2.4.2.3 General DDQ oxidation of II-1 - II-4

A mixture of substrate (1 eq.), DDQ (0.1 eq.), $NaNO_2$ (0.1 eq.), CH_2Cl_2 (20 mL/mmol) and acetic acid (2 mL/mmol) was stirred under an O_2 atmosphere (balloon) at room temperature for 22 h. The mixture was extracted with ethyl acetate and the organic layer was washed with saturated aqueous NaCl, dried over Na_2SO_4 and then concentrated under vacuum. The products were purified column chromatography on silica gel.

DDQ oxidation of II-1

A mixture of **II-1** (50 mg, 0.14 mmol), DDQ (3.3 mg, 0.014 mmol), $NaNO_2$ (0.93 mg, 0.014 mmol), CH_2Cl_2 (2 mL) and acetic acid (0.2 mL) was used. The products were purified column chromatography on silica gel (hexane/ethyl acetate = 1:1) to produce ketone **II-25** as a yellow oil (46 mg, 0.13 mmol, 93%).

II-25: (**1,2-bis(3,4-dimethoxyphenyl)-3-hydroxypropan-1-one**). ^{1}HNMR (400 MHz, $CDCl_3$): 7.54 (1 H, dd, *J* = 8.4 Hz, 2.0 Hz), 7.51 (1 H, d, *J* = 2.0 Hz), 6.82 – 6.75 (3 H, m), 6.74 (1 H, d, *J* = 1.7 Hz), 4.66 (1 H, dd, *J* = 8.3 Hz, 4.9 Hz), 4.22 (1 H, dd, *J* = 11.3 Hz, 8.3 Hz), 3.86 (3 H, s), 3.85 (3 H, s), 3.83 (1 H, m), 3.81 (3 H, s), 3.80 (3 H, s). ^{13}CNMR (100 MHz, $CDCl_3$): 198.4, 153.3, 149.3, 148.8, 148.4, 129.4, 129.2, 123.7, 120.7, 111.6, 111.0, 110.8, 110.0, 65.1, 55.9, 55.9, 55.8, 55.4.

DDQ oxidation of II-2

A mixture of **II-2** (93 mg, 0.28 mmol), DDQ (6.6 mg, 0.028 mmol), $NaNO_2$ (1.86 mg, 0.028 mmol), CH_2Cl_2 (6 mL) and acetic acid (0.4 mL) was used. The products were purified by column chromatography on silica gel (hexane/ethyl acetate = 1:1) to produce ketone **II-26** as an orange oil (78 mg, 0.23 mmol, 84%).

II-26: (**2-(3,4-dimethoxyphenyl)-3-hydroxy-1-(4-hydroxy 3-methoxyphenyl)propan-1-one**): ^{1}HNMR (400 MHz, $CDCl_3$): 7.56 - 7.50 (2 H, m), 6.86 - 6.83 (1 H, m), 6.82 - 6.79 (2 H, m), 6.76 (1 H, d, *J* =1.6 Hz), 6.07 (1 H, s), 4.67 (1 H, dd, *J* =8.3 Hz, 5.0 Hz), 4.24 (1 H, dd, *J* = 11.2 Hz, 8.4 Hz), 3.90 (3 H, s), 3.89 - 3.85 (1 H, m), 3.84 (3 H, s), 3.83 (3 H, s). ^{13}CNMR (100 MHz, $CDCl_3$): 198.5, 150.5, 149.4, 148.5, 146.5, 129.1, 129.1, 124.4, 120.7, 113.8, 111.7, 111.0, 110.5, 65.3, 55.9, 55.9, 55.8, 55.4. HRMS (ESI): *m*/*z* $[M - H]^+$ calcd for $C_{18}H_{19}O_6$ 331.1182, found 331.1172.

DDQ oxidation of II-3

A mixture of **II-3** (140 mg, 0.44 mmol), DDQ (10 mg, 0.044 mmol), $NaNO_2$ (3 mg, 0.044 mmol), CH_2Cl_2 (8 mL) and acetic acid (0.6 mL) was used. The products were purified by column chromatography (hexane/ethyl acetate = 3:1) to produce aldehyde **II-16** as a yellow solid (36 mg, 0.11 mmol, 56%) and benzofuran alcohol **II-27** as a yellow oil (12 mg, 0.038 mmol, 18%). Starting material **II-3** (35mg, 25%) was also recovered.

II-16: (**2-(3,4-dimethoxyphenyl)-7-methoxybenzofuran-3-carbaldehyde**). ^{1}HNMR (400 MHz, $CDCl_3$): 10.29 (1 H, s), 7.79 (1 H, d, *J* = 7.9 Hz), 7.42 (1 H, d, *J* = 8.3 Hz), 7.30 - 7.21 (1 H, m), 6.98 (1 H, d, *J* = 8.3 Hz), 6.87 (1 H, d, *J* = 8.1 Hz), 4.01 (3 H, s), 3.96 (3 H, s),

3.94 (3 H, s). ^{13}CNMR (100 MHz, $CDCl_3$): 186.6, 165.5, 151.7, 149.3, 144.9, 143.0, 127.3, 125.6, 123.0, 121.0, 116.9, 114.4, 111.5, 111.2, 107.9, 56.2, 56.1, 56.0

II-27: (**(2-(3,4-dimethoxyphenyl)-7-methoxybenzofuran-3-yl)methanol**): ^{1}HNMR (400 MHz, $CDCl_3$): 7.47 - 7.41 (2 H, m), 7.26 - 7.24 (1 H, m), 7.18 (1 H, t, *J* = 7.8 Hz), 6.95 (1 H, d, *J* = 8.9 Hz), 6.81 (1 H, dd, *J* = 7.9 Hz, 1.2 Hz), 4.91 (2 H, s), 4.02 (3 H, s), 3.96 (3 H, s), 3.92 (3 H, s). ^{13}CNMR (100 MHz, $CDCl_3$): 154.1, 149.8, 149.1, 145.2, 142.9, 131.1, 123.6, 122.9, 120.6, 113.9, 111.5, 111.1, 110.5, 106.7, 56.1, 56.0, 56.0, 55.6.

DDQ oxidation of II-4

A mixture of **II-4** (93 mg, 0.31 mmol), DDQ (7.3 mg, 0.031 mmol), $NaNO_2$ (2 mg, 0.031 mmol), CH_2Cl_2 (3 mL) and acetic acid (0.44 mL) was used. The products were purified by column chromatography on silica gel (hexane/ethyl acetate = 3:1) to produce a yellow oil **II-28** (40 mg, 0.13 mmol, 43%) and starting material **4** (40 mg, 43%) was recovered as well.

II-28: (**(2-(3,4-dimethoxyphenyl)-7-methoxybenzofuran-3-yl)methanol**): ^{1}HNMR (400 MHz, $CDCl_3$): 7.44 (1 H, d, *J* = 1.9 Hz), 7.41 (1 H, dd, *J* = 8.3 Hz, 2.0 Hz), 7.29 - 7.26 (1 H, m), 7.20 (1 H, t, *J* = 7.8 Hz), 7.02 (1 H, d, *J* = 8.3 Hz), 6.83 (1 H, dd, *J* = 7.8 Hz, 1.1 Hz), 5.83 (1 H, s), 4.93 (2 H, s), 4.04 (3 H, s), 3.99 (3 H, s). ^{13}CNMR (100 MHz, $CDCl_3$): 154.3, 146.7, 146.6, 145.3, 142.9, 131.1, 123.7, 122.4, 121.3, 114.7, 113.7, 111.5, 110.0, 106.7, 56.2, 56.1, 55.7. HRMS (ESI): *m/z* $[M - H]^+$ calcd for $C_{17}H_{15}O_5$ 299.0919, found 299.0914.

2.4.2.4 General $VO(acac)_2$ oxidation of II-1 - II-4

A mixture of lignin model (1 eq.), $VO(acac)_2$ (0.3 eq.), MeCN (30 mL/mmol) and 10% aqueous AcOH (0.3 mL) were stirred under an O_2 atmosphere (balloon) at 100 °C for 48h.

The mixture was extracted with EA and the organic layer was washed with chilled water. The combined organic layers were dried over Na_2SO_4 and concentrated under vacuum. The product mixtures were purified by column chromatography on silica gel.

VO(acac)$_2$ oxidation of II-1

A mixture of **II-1** (100 mg, 0.287 mmol), $VO(acac)_2$ (24.1 mg, 0.086 mmol) were used. The mixture products were purified by column chromatography on silica gel (hexane/ethyl acetate = 3:1) to give acid **II-12** (10 mg, 0.055 mmol, 19%), aldehyde **II-13** (15 mg, 0.09 mmol, 31.4%), a yellow solid diketone **II-29** (3.5mg, 0.01 mmol, 3.7%). Starting material **II-1** was also recovered (56 mg, 52.8%).

II-29: (**1,2-bis(3,4-dimethoxyphenyl)ethane-1,2-dione**). ^{1}HNMR (400 MHz, $CDCl_3$): 7.59 (1 H, s), 7.47 (1 H, d, *J* = 8.3 Hz), 6.88 (1 H, d, *J* = 8.5 Hz), 3.95 (6 H, s). ^{13}CNMR (100 MHz, $CDCl_3$): 193.4, 154.8, 149.5, 126.4, 126.3, 110.3, 56.2, 56.1.

VO(acac)$_2$ oxidation of II-2

A mixture of **II-2** (122 mg, 0.365 mmol), $VO(acac)_2$ (30.68 mg, 0.11 mmol) were used. The product mixture was purified by column chromatography on silica gel (hexane/ethyl acetate = 3:1) to give acid **II-12** (trace), aldehyde **II-13** (3 mg, 0.018 mmol, 5%), vanillin (3 mg, 0.0197 mmol, 5.4%). Starting material **II-2** was recovered (30 mg, 24.6%) as well. Chromatographically immobile material was also observed.

VO(acac)$_2$ oxidation of II-4

A mixture of **4** (82 mg, 0.27 mmol), $VO(acac)_2$ (22.8 mg, 0.08 mmol) were used. The products were purified by column chromatography on silica gel (hexane/ethyl acetate = 3:1)

to give the phenyl acetate and a yellow oil **28** (trace). Starting material was also recovered (50 mg, 60.9%).

2.4.2.5 General TEMPO/$NaNO_2$/NaCl/HCl oxidation of II-1 - II-4

A mixture of lignin model (1 eq.), TEMPO (0.15 eq.), $NaNO_2$ (0.25 eq.), 36% aqueous HCl (0.5 eq.), NaCl (0.5 eq.) and CH_2Cl_2 (20 mL/mmol) stirred under an O_2 atmosphere (balloon) at room temperature for 23 h. The mixture was extracted with ethyl acetate and the organic layer was washed with saturated aqueous $Na_2S_2O_3$, saturated aqueous $NaHCO_3$, then with water. The combined organic layers were dried over Na_2SO_4 and concentrated under vacuum. The product mixtures were purified by column chromatography on silica gel.

Oxidation of II-1

A mixture of **II-1** (50 mg, 0.145 mmol), TEMPO (3.4 mg, 0.021 mmol), $NaNO_2$ (2.5 mg, 0.0359 mmol), 36% aqueous HCl (6 μL, 0.0717 mmol), NaCl (4.2 mg, 0.0717 mmol) and DCM (2 mL) was used. The mixture products were purified by column chromatography on silica gel (hexane/ethyl acetate = 2:1) to give a yellow oil ketone **II-25** (23 mg, 0.06 mmol 46%) and diketone **II-29** (6 mg, 0.018 mmol, 12%).

Oxidation of II-2

A mixture of **II-2** (34 mg, 0.1 mmol), TEMPO (2.4 mg, 0.075 mmol), $NaNO_2$ (1.7 mg, 0.025 mmol), 36% aqueous HCl (4.3 μL, 0.05 mmol), NaCl (2.9 mg, 0.05 mmol) and CH_2Cl_2 (2 mL) was used. The product was chromatographically immobile.

Oxidation of II-3

A mixture of **II-3** (136 mg, 0.43 mmol), TEMPO (10 mg, 0.0645 mmol), $NaNO_2$ (7.5 mg, 0.1 mmol), 36% aqueous HCl (17 μL, 0.2 mmol), NaCl (12.6 mg, 0.2 mmol) and CH_2Cl_2 (2 mL) was used. The products were purified by column chromatography on silica gel (hexane/ethyl acetate = 3:1) to give aldehyde **II-16** as a yellow solid (40 mg, 0.13 mmol, 50%).

Oxidation of II-4

A mixture of **II-4** (95 mg, 0.314 mmol), TEMPO (7.6 mg, 0.047 mmol), $NaNO_2$ (5.4 mg, 0.078 mmol), 36% aqueous HCl (13 μL, 0.157 mmol), NaCl (9.1 mg, 0.157 mmol) and CH_2Cl_2 (2 mL) was used. The products were chromatographically immobile.

2.4.2.6 General $Fe(NO_3)_3$ /TEMPO oxidation of II-1 - II-4

A mixture of substrate (1 eq.), TEMPO (0.1 eq.), $Fe(NO_3)_3 \cdot 9H_2O$ (0.05 eq.), NaCl (0.1 eq.) and DCE (10 mL/mmol) stirred under an O_2 atmosphere (balloon) at room temperature for 19h. The mixture was extracted with ethyl acetate and the organic layer was washed with saturated aqueous $Na_2S_2O_3$, saturated aqueous $NaHCO_3$, then with water. The combined organic layers were dried over Na_2SO_4 and concentrated under vacuum. The products were purified by column chromatography on silica.

$Fe(NO_3)_3$ /TEMPO oxidation of II-1

A mixture of **II-1** (80 mg, 0.23 mmol), TEMPO (3.6 mg, 0.023 mmol), $Fe(NO_3)_3 \cdot 9H_2O$ (4.6 mg, 0.0115 mmol), NaCl (1.3 mg, 0.023 mmol) and DCE (2 mL) was used. The mixture products were purified by column chromatography on silica gel

(hexane/ethyl acetate = 3:1) to give aldehyde **II-13** (12 mg, 0.072 mmol, 31%) and ketone **II-25** (37 mg, 0.106 mmol, 46%).

$Fe(NO_3)_3$ /TEMPO oxidation of II-2

A mixture of **II-2** (37mg, 0.11 mmol), TEMPO (1.9 mg, 0.011 mmol), $Fe(NO_3)_3 \cdot 9H_2O$ (2.2 mg, 0.005 mmol), NaCl (0.6 mg, 0.011 mmol) and DCE (2 mL) was used. The mixture products were purified by column chromatography on silica gel (hexane/ethyl acetate = 3:1) to give aldehyde **II-13** (trace), and a yellow oil **II-26** (6mg, 0.018mmol, 16%). Chromatographically immobile material was also observed.

$Fe(NO_3)_3$ /TEMPO oxidation of II-3

A mixture of **II-3** (73 mg, 0.23 mmol), TEMPO (3.9 mg, 0.023 mmol), $Fe(NO_3)_3 \cdot 9H_2O$ (4 mg, 0.01 mmol), NaCl (1.3 mg, 0.023 mmol) and DCE (2 mL) was used. The mixture products were purified by column chromatography on silica gel (hexane/ethyl acetate = 3:1) to give aldehyde **II-16** (11 mg, 0.035 mmol, 15.2%). Starting material **II-3** was also recovered (53 mg, 73%).

$Fe(NO_3)_3$ /TEMPO oxidation of II-4

A mixture of **II-4** (100 mg, 0.33 mmol), TEMPO (5.1 mg, 0.033 mmol), $Fe(NO_3)_3 \cdot 9H_2O$ (6.6 mg, 0.0165 mmol), NaCl (2 mg, 0.033 mmol) and DCE (3 mL) was used. The reaction products were chromatographically immobile.

2.4.2.7 General CuCl /TEMPO oxidation of II-1 - II-4

A mixture of substrate (1 eq.), TEMPO (0.3 eq.), CuCl (0.2 eq.) and pyridine (10 mL/mmol) stirred under an O_2 atmosphere (balloon) at 100 ^oC for 19h. The mixture was extracted with ethyl acetate and the organic layer was washed with saturated aqueous $Na_2S_2O_3$,

saturated aqueous $NaHSO_4$, then with water. The combined organic layers were dried over Na_2SO_4 and concentrated under vacuum. The product mixtures were purified by column chromatography on silica gel.

CuCl /TEMPO oxidation of II-1

A mixture of **II-1** (100 mg, 0.287 mmol), TEMPO (13.4 mg, 0.086 mmol), CuCl (5.7 mg, 0.057 mmol) and pyridine (2 mL) was used. The products were purified by column chromatography on silica gel (hexane/ethyl acetate = 3:1) to give acid **II-12** (36 mg, 0.198 mmol, 75.4%), aldehyde **II-13** (14 mg, 0.084 mmol, 27%) and diketone **II-29** (18 mg, 0.054 mmol, 19%).

CuCl /TEMPO oxidation of II-2

A mixture of **II-2** (122 mg, 0.365 mmol), TEMPO (17.1 mg, 0.11 mmol), CuCl (7.2 mg, 0.073 mmol) and pyridine (2 mL) was used. The products were purified by column chromatography on silica gel (hexane/ethyl acetate = 3:1) to give a yellow oil acid **II-12** (12.6 mg, 0.069 mmol, 19%) and aldehyde **II-13** (6.8 mg, 0.041 mmol, 11%). Chromatographically immobile material also observed.

CuCl /TEMPO oxidation of II-3

A mixture of **II-3** (75 mg, 0.24 mmol), TEMPO (11.2 mg, 0.072 mmol), CuCl (4.7 mg, 0.047 mmol) and pyridine (2 mL) was used. The products were purified by column chromatography on silica gel (hexane/ethyl acetate = 3:1) to give aldehyde **II-16** (10 mg, 0.032 mmol, 13%). Starting material **3** was also recovered (47 mg, 63%).

CuCl /TEMPO oxidation of II-4

A mixture of **II-4** (90 mg, 0.30 mmol), TEMPO (14 mg, 0.09 mmol), CuCl (5.9 mg, 0.06 mmol) and pyridine (3 mL) was used. The product mixture was chromatography immobile.

2.4.3 HBr treatment of II-3

A mixture of **II-3** (136 mg, 0.24 mmol), HBr (139 mg, 1.7 mmol) and 1,2-dichloroethane (5 mL) was stirred at 84 ^{o}C overnight. The solution was cooled, then neutralized with 1M aqueous NaOH to pH=7 and extracted with dichloromethane (3 x 10 mL). The combined organic layers were dried with Na_2SO_4 and evaporated in *vacuo*. Purification by column chromatography on silica gel (hexane: ethyl acetate=2:1) gave **II-33** as a brown oil (16 mg, 0.05 mmol, 12%). Multiple unisolatable trace products were detected as well.

^{1}HNMR (400 MHz, $CDCl_3$): 7.35 (2 H, s), 7.19 - 7.09 (2 H, m), 6.96 (1 H, d, J = 8.8 Hz), 6.80 (1 H, d, J = 7.8 Hz), 4.03 (3 H, s), 3.97 (3 H, s), 3.93 (3 H, s), 2.44 (3 H, s).

2.4.4 KOH treatment of II-4

A mixture of 4 mL 2 M KOH and **II-4** (130 mg, 0.43 mmol) in 5 mL 1,4-dioxane was stirred overnight at room temperature. The solution was neutralized by adding 2 M HCl then extracted with dichloromethane (3 x 10 mL). The combined organic layers were dried with Na_2SO_4 and evaporated in *vacuo*. Purification by column chromatography on silica gel (hexane: ethyl acetate=1:1) gave stilbene **II-36** as a yellow oil (trace). Starting material **II-4** was recovered as well (94 mg, 0.31mmol, 72%).

^{1}HNMR (400 MHz, $CDCl_3$): 7.25 - 7.29 (1 H, m), 7.17 (1 H, d, *J* = 8.1 Hz), 7.11 (2 H, d, *J* = 17.2 Hz), 7.04 (1 H, d, *J* = 8.0 Hz), 6.90 (1 H, d, *J* =8.1 Hz), 6.84 (1 H, t, *J* = 7.8 Hz), 6.76 (1 H, d, *J* = 7.8 Hz), 5.95 (1 H, s), 5.64 (1 H, s), 3.95 (3 H, s), 3.91 (3 H, s); ^{13}CNMR (100 MHz, $CDCl_3$): 146.7, 146.6, 145.4, 143.1, 130.5, 129.4, 123.9, 120.6, 120.6, 119.5, 118.6, 114.4, 109.0, 108.2, 56.1, 55.9.

Chapter 3. Dramatic simplification of lignin HSQC spectra from ring-puck milling followed by oxidation

Disclaimer: This chapter was taken from the following papers:
Z. Fang, J. K. Mobley and M. S. Meier. Energy Fuels, 2018, 32 (11), 11632–11638

3.1 Introduction

As one of the most commonly used milling processes, ball-milling has been used in many studies on lignin processing [92, 94, 96, 175, 176] and has been proven to be more energy-efficient than solvent-based strategies or microwave digestion techniques.[177] This method was also magnified at larger scales (hectograms and kilograms level) in mechanocatalytic degradation of lignocellulose.[97] Addition of a solid base such as NaOH into the milling progress has been shown to significantly increase the yield of monomeric products.[96]

In our previous study, kraft lignin was ball milled in a reciprocating ball-mill and then treated with the two-step oxidative degradation approach.[178] Extraction of the aqueous solution after the second oxidation step (B-V oxidation), a larger amount of ethyl acetate soluble material was obtained from the ball-milled kraft lignin than from non-mechanochemically-treated kraft lignin. Two major products (methyl vanillate and methyl 5-carbomethoxyvanillate, 10wt% combined) can be isolated after methylation of the ethyl acetate soluble mixture (Figure 3.1). However, this reciprocating ball mill could only accommodate lignin in small quantity (~2 g) and extensive time (48 h) was required.

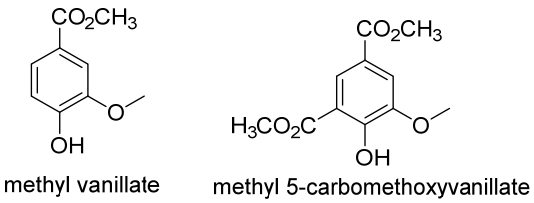

Figure 3. 1 Two major products isolated after methylation of the ethyl acetate soluble mixture

In contrast to results using a ball mill, a Spex Shatterbox mill with a ring-and-puck cell (Figure 3.2) can easily handle large quantity of samples (>100g) and reduce particle sizes in very short time. Therefore, we intend to treat kraft lignin with this Shatterbox mill in a

solvent-free system, following with porphyrin and B-V oxidations subsequently in order to compare how this more powerful technique would affect each oxidation step, compared to the ball mill.

Figure 3. 2 A Spex Shatterbox mill with a ring-puck cell

A reciprocating ball-mill, as we have used to carry out mechanochemical reactions of lignin,[178] can only be used on small quantities (*ca.* 1 g), making it difficult to produce quantities of lignin depolymerization products that are sufficient to explore potential applications of these compounds. In work by the Dabral group,[179] a Siebtechnik vibrating disc mill was used to produce cleavage of β-O-4 model compounds and to produce partial deconstruction of lignin on a 10g-scale. They also studied the HO-TEMPO/ oxone oxidation of lignin while milling. Inspired by that work, we have investigated another common milling method, using a Spex Shatterbox vibratory mill with KOH in a solvent-free system. Such mills can process relatively large quantities of sample (100 g) in a nesting, sliding ring-and-puck sample cell of a type that has been used in grinding nanotubes[180] as well as mineral samples.[181] In this work, we conducted the mechanochemical processing of lignin and the

oxidation steps separately in order to understand at which stage the most important reactions occur. Accordingly, kraft lignin (20 g) was milled in the Shatterbox and then subjected to a porphyrin-catalyzed oxidation, followed by Baeyer-Villiger oxidation. We find that each step in this process produced very different materials than we observed with lignin samples that had been subjected to ball-milling (scale of 2 g) followed by oxidation.[178]

In this study, a mixture of kraft lignin (KL, Indulin AT kraft lignin obtained from Ingevity, formerly MeadWestvaco) and KOH (lignin/KOH = 2:1 w/w) was milled in a Spex 8530 Shatterbox ring-and-puck mill for 4 different time intervals (15 mins, 1h, 2h, 3h). We then performed a two-step oxidative depolymerization approach on the mechanochemical-treated kraft lignin (Scheme 3.1),[115] starting with a porphyrin oxidation of the benzylic alcohols to corresponding ketones, and then followed by a Baeyer-Villiger (B-V) oxidation of the resulting ketones to esters with $HCOOH/H_2O_2$. We expect to produce a mixture of aromatic acids, phenols, and other monomers *via* hydrolysis of these esters.

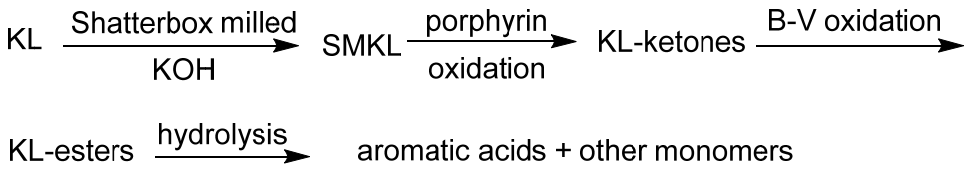

Scheme 3. 1 Two-step oxidative approach to depolymerize Shatterbox milled kraft lignin

The structures and functionalities of different lignin samples were monitored using 2D-^{1}H-^{13}C-HSQC NMR and ^{31}P NMR spectroscopy. The HSQC NMR spectrum showed minimal changes in kraft lignin after processing in the Shatterbox mill, but the subsequent porphyrin oxidation step resulted in a dramatic simplification of the aliphatic region of the HSQC spectrum. In addition, new and previously unobserved signals appeared in the downfield margin of the aromatic region. And more interestingly, the products formed in this

oxidation step could not be reduced back to the starting material by $NaBH_4$. We found that not only does the ring-and-puck mill induce significant changes more rapidly than does ball-milling, it also became clear that a significantly different set of reactions was occurring.

3.2 Results and Discussion

3.2.1 HSQC analysis

HSQC spectra of different lignin samples are shown in Figure 3.3. Frame I shows the spectrum of kraft lignin (KL), and resonances corresponding to β-O-4 (A), β-5 (B) and β-β (C) linkages are observed.[182, 183] After Shatterbox milling (SMKL, Frame II) it appears that structural units of lignin are still visible and few new signals appear, although the intensity of peaks corresponding to β-5 (B) are slightly lower than in the starting kraft lignin (Frame I). The decrease in intensity of resonances from β-5 units is potentially due to aromatization of the dihydrofuran ring during the milling progress, leading to a decreased peak intensity of B_α and B_β. Additionally, partial oxidation of the γ-OH to aldehydes would cause a reduction in the peak intensity of B_γ, and aromatization of the dihydrofuran ring and oxidation of γ-OH in a β-5 lignin model were observed in our previous project,[184] which is consistent with the observation in the HSQC spectrum.

It is surprising that after TPPFeCl/tBuOOH oxidation on the Shatterbox milled KL, all the units in the aliphatic region corresponding to β-O-4 (A), β-5 (B) and β-β (C) are absent (Frame III in Figure 3.3), indicating a number of reactions, presumably benzylic and γ-OH oxidations, aromatization of the dihydrofuran rings, or C-O bond cleavage have occurred that destroyed all these three linkages. This is quite different from what we saw in the case of

porphyrin oxidation of ball-milled lignin, where cross peaks associated with oxidized β-O-4 linkages are still present, though β-5 (B) and β-β (C) cross peaks disappeared as well in the previous study.[178] This result implies that the material produced by Shatterbox milling is significantly more reactive than material produced by ball milling.

To verify that lignin has been indeed oxidized, we treated the porphyrin oxidized Shatterbox milled KL (OSMKL) with $NaBH_4$. However, in striking contrast to our previous observations with oxidized ball-milled lignin,[178] none of the familiar resonances corresponding to these three linkages reappeared in the aliphatic region (Frame V in Figure 3.3). This result indicated that additional reactions occurred during the course of the oxidation, producing new structures that are not converted back to the original structures that were present before oxidation.

Wang[90] reported concerns over the effect of high temperatures generated during mechanical milling of lignin could potentially destroy linkages, and therefore they performed ball milling in 10 min intervals. Elevated temperatures can enable molecules to overcome the solid-solid diffusion barrier;[185] additionally, molecules can be deformed by mechanical impact into a more reactive energy state.[186] High temperatures may also drive elimination reactions, resulting in enol ethers which is not reducible by $NaBH_4$. Cleavage of C-O or C-C bonds might have already happened during the porphyrin oxidation step, causing an irreversible step. In contrast, oxidation of ball-milled lignin is reversible and the oxidized material can be easily reduced by $NaBH_4$ to reform the starting material.[178]

In our current work, we carried out the milling process in the Shatterbox mill for a continuous 2h period, and we observed that the temperature of the sample cell increased

during the run. Indeed, the sample cell rose from an initial temperature of 21 °C to 84 °C after 2h (temperature of the steel cell, observed with an optical thermometer). However, it seems unlikely that this temperature is high enough to cause significant structural changes on the lignin. Therefore, mechanical impact is likely the primary contributor to the observed changes.

The positions of cross-peaks in the aromatic region of the HSQC spectrum (Figure 3.4) are sensitive to the oxidation state of the α-carbon, and thus give direct evidence of oxidation of the α-carbon. Cross-peaks corresponding to the oxidized guaiacyl units (G': G'2, G'5, and G'6) appear in much higher intensity after Shatterbox milling (Frame II') than those in unmodified kraft lignin (Frame I'), especially G'6, which is nearly absent for unmodified KL but significantly present for Shatterbox milled KL. This observation suggests that some oxidations had happened during the milling process, analogous to the oxidation that we observed during ball-milling of lignin.[178] It is striking that almost all of the cross-peaks associated with *p*-hydroxyphenyl and guaiacyl units disappeared after porphyrin oxidation. While we do not observe the products formed from these moieties, it is possible that those aromatic rings were converted to water-soluble dicarboxylic acids *via* oxidative hydroxylation of the rings, followed by ring opening.[187, 188]

The dramatic simplification of the HSQC spectrum, with few, narrow resonances rather than large numbers of cross peaks or broad "bands," suggests that a smaller number or a more narrow range of structures are present. Two new cross-peaks at *ca*. 130/8.5 ppm (δ_C/δ_H) and 130/8.8 ppm (δ_C/δ_H) are present in the HSQC spectrum of porphyrin-oxidized Shatterbox-milled kraft lignin (Frame III' in Figure 2) but both disappeared after $NaBH_4$

reduction (Frame V' in Figure 3.4). Protons in such uncommon chemical shift area (8.5 and 8.8 ppm) indicate that the products of Shatterbox milled material are very different from materials produced by ball-milling, and that subsequent oxidation takes a dramatically different path. $NaBH_4$ reduction does not regenerate the spectrum of the material prior to oxidation, indicating that unlike in ball-milled material, the oxidation is accompanied by reactions that are not reversed by simple hydride reduction. And more interestingly, disappearance of these two unusual peaks (cross-peaks at *ca*. 130/8.5 ppm (δ_C/δ_H) and 130/8.8 ppm (δ_C/δ_H)) after reduction is not accompanied by formation of identifiable aromatic structures.

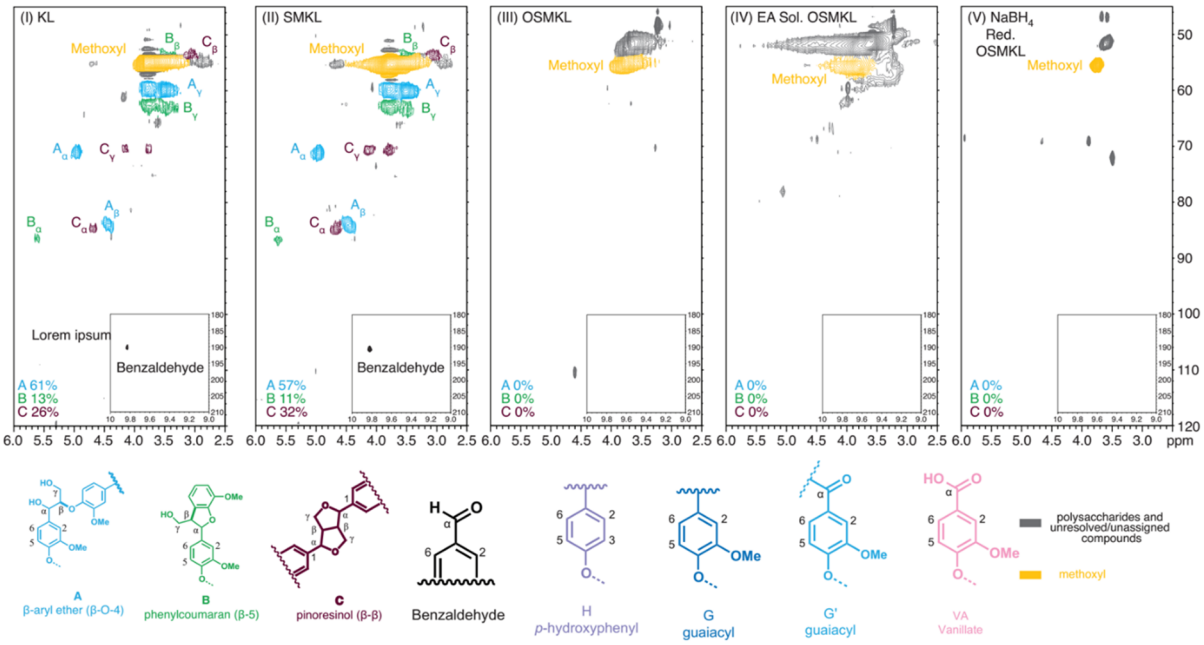

Figure 3. 3 HSQC spectra of different lignin samples (Aliphatic regions)

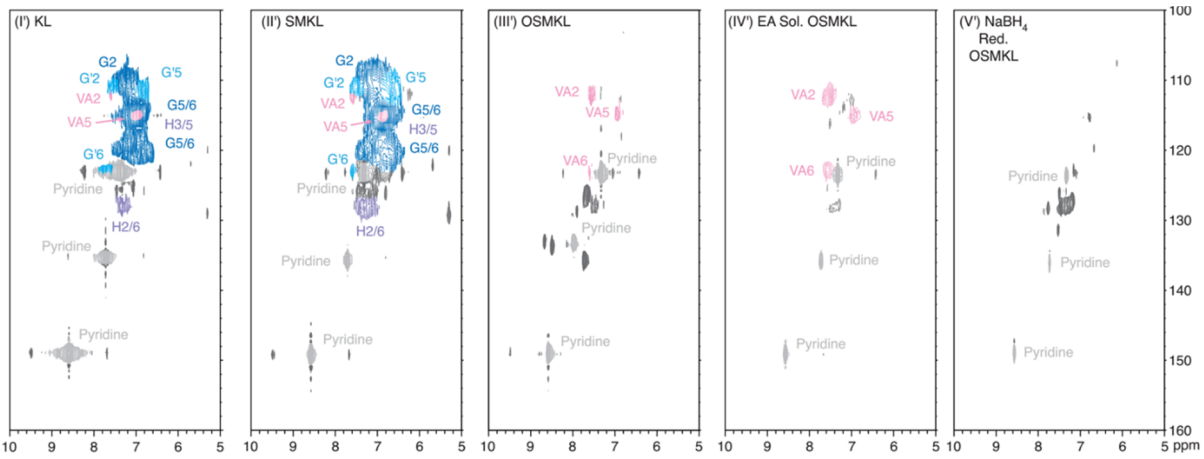

Figure 3. 4 HSQC spectra of different lignin samples (Aromatic regions)

Tran[41] reported a C-H proton at 8.21 ppm (in DMSO) in a pyran-4-one structure which was produced from the DDQ oxidation of a β-β model compound (see Figure 3.5). Unfortunately, the chemical shift of carbon of this cross-peak at 147.3/8.21 ppm (δ_C/δ_H) in Tran's HSQC spectrum is quite far away from what we observed (δ_C = 130 ppm). Another proton that can be at such downfield was from a ring-opened dicarboxylic acid product (δ_H = 8.50 ppm),[189] which has been produced by oxidization of a β-5 model (Scheme 3.2) with an iron complex in t-BuOOH (similar to our porphyrin oxidation system). We suspect that structures similar to the pyran-4-one structure are formed in our case since dramatic decrease of phenol content and no significant growth of acid content were observed from the ^{31}P NMR experiment (see Section 3.2.2 and Table 3.1, below); indicating that formation of diacids from the opening of the aromatic ring is unlikely to have occurred.

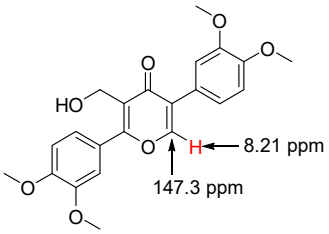

Figure 3. 5 Pyran-4-one structure reported by Tran[41]

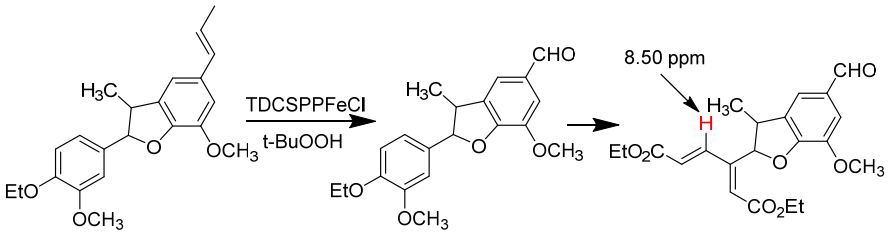

Scheme 3. 2 Ring-cleaved product from iron-complex oxidation of β-5 model compounds[189]

Remarkably, other than cross peaks corresponding to methoxy groups (Frame IV in Figure 3.3), no resonances from the familiar lignin structural units or linkages could be identified in the aliphatic region of the HSQC spectrum of the ethyl acetate-soluble fraction of the Baeyer-Villiger reaction mixture. Structural units associated with simple aromatic oligomers (vanillic acid and other unknown oligomers) were observed in the aromatic region (Frame IV' in Figure 3.4) which suggested that after Shatterbox milling and the two-step oxidative process, very little recognizable lignin structure remains. It is notable that new correlation peaks at *ca*. 70/3.9 (δ_C/δ_H) and 73/3.5 (δ_C/δ_H) appeared after $NaBH_4$ reduction of the porphyrin oxidized Shatterbox milled kraft lignin (Frame V in Figure 3.3) Neither of these two peaks were observed in the HSQC spectrum of the similarly-treated ball-milled samples.

3.2.2 ^{31}P NMR analysis

The content and type of hydroxyl groups in lignin (phenols, 1° or 2° alcohols) can be quantified *via* ^{31}P NMR after treatment of lignin with a phosphitylation reagent (2-chloro-4,4,5,5-tetramethyl-1,3,2-dioxaphospholane) (see Scheme 3.3).[190] Derivatization and ^{31}P NMR were performed to analyze the content of hydroxyl groups in a set of milled and milled/oxidized samples (Figure 3.6), and the results from each lignin sample are summarized in Table 3.1.

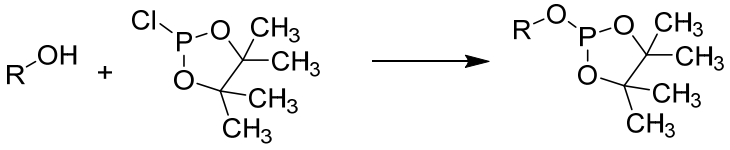

Scheme 3. 3 phosphitylation reaction of different types of hydroxyl groups

After Shatterbox milling for 2h, the content of aliphatic hydroxyl groups and phenols were significantly increased (Table 3.1). This observation is consistent with the fact that cleavage of β-O-4 linkages dominated when lignin was milled in the presence of solid base[96] such as NaOH or KOH. Growth in the acid content is presumably due to air oxidation of lignin during the milling process. Not surprisingly, the content of aliphatic hydroxyl groups and phenols decreased dramatically after the porphyrin oxidation step. Lower acid content after oxidation was not expected, nor was the lack of signals in the aliphatic region in ^{31}P NMR spectrum (see blue trace in Figure 3.6) after the $NaBH_4$ reduction. Notable growth in the acid content was observed in the ethyl acetate-soluble portion after the porphyrin and Baeyer-Villiger oxidations (Table 3.1), although the ethyl acetate-soluble portion (EA Sol. OSMKL) no longer shows obvious features of lignin (see Frame IV in Figure 3.3 and Frame IV' in Figure 3.4).

Table 3. 1 Hydroxyl group contents of different lignin samples

	Hydroxyl group contents (mmol/g)		
	Aliphatic	Phenol	acid
KL	2.869	4.056	0.095
SMKL-2h	4.042	10.015	1.096
OSMKL-2h	0.412	0.974	0.081
Red. OSMKL-2h	n/a	n/a	n/a
EA Sol. OSMKL	1.092	2.190	2.156

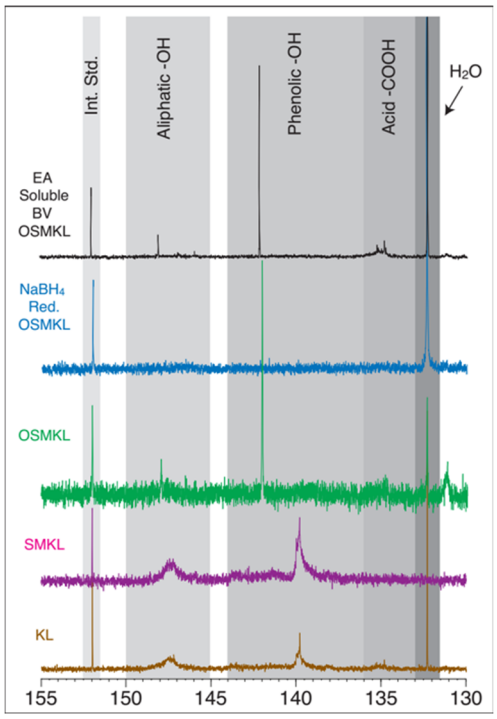

Figure 3. 6 ^{31}P spectra of different lignin samples

3.2.3 Baeyer-Villiger oxidation and derivatization

Each sample of porphyrin-oxidized Shatterbox milled lignin (milled for 15 min, 1h, 2h, and 3h) was subjected to Baeyer-Villiger oxidation with H_2O_2 and HCOOH at room temperature for 48 h. The mixtures were filtered by gravity filtration and both the water-soluble and water-insoluble (the filter cake) fractions were extracted with ethyl acetate. Therefore, four fractions were produced from each Baeyer-Villiger reaction mixture: material that is only water soluble, material that is only ethyl acetate soluble, material that is both water and ethyl acetate soluble, and material is that not soluble in either water or ethyl acetate. The amount of each fraction is given in Table 3.2. Yields in the table represent weight percentages which are calculated based on the masses of lignin produced from the porphyrin oxidation step (OSMKL). Kraft lignin and ball-milled kraft lignin (milled for 48 h) were also

treated under these two oxidation steps (porphyrin and Baeyer-Villiger oxidation) in previous study,[178] and materials obtained from untreated kraft lignin and from the Baeyer-Villiger (B-V) oxidation of the porphyrin-oxidized ball-milled lignin were also isolated by solubility into these above 4 categories. The amount of material in each fraction is also given (see Table 2) for comparison.

Table 3. 2 Fractionation of B-V oxidation mixtures from Shatterbox milled lignin samples by solubility

Milling time	Only H_2O soluble	Both H_2O and EA soluble	Only EA soluble	insoluble
OSMKL-15 min	23.2%	18.9%	10.4%	6.5%
OSMKL-1h	21.1%	22.9%	14.3%	3.5%
OSMKL-2h	19.7%	22.2%	15.8%	3.6%
OSMKL-3h	21.7%	24.3%	16.6%	4.8%
Porp-oxidized KL	65%	19%	7%	12%
Porp-oxidized BMKL	44%	19%	6%	32%

The amount of lignin that remains insoluble after shatter milling (even only Shatterbox milled after 15 mins) is quite low (below 10%). In comparison, more than 30% of the lignin mass remained insoluble after extended ball-milling. The ethyl acetate-soluble portion from shatter-milled lignin has significantly increased to 10%-16%, compared to only 0.2% produced from kraft lignin and 6% from ball-milled lignin, indicating that shatter-mill process has more significantly changed the structure of lignin. The fraction of shatter-milled material that is both water-soluble and ethyl acetate soluble was similar to the fraction of

material from ball-milling, but we obtained a smaller fraction of material that was only water-soluble from shatter-milled lignin than from KL or from ball-milled lignin. While this could be a direct result of the chemistry that occurs during the milling step, some or all of this difference could be the result of different reaction temperatures in the B-V oxidation step. In previous ball-milling project we heated the B-V oxidation solution mixture to 50 ^{o}C for 70h but for the experiments summarized in table 3.2, we carried out the reaction at room temperature over 48h to avoid decomposition of H_2O_2 or oxidation of aromatic rings. Hydroxylation and oxidative opening of aromatic rings to form carboxylic acids at elevated temperature was reported by Yin[187] who found that 4-carbon dicarboxylic acids were generated in up to 41% yield from a lignin model compound catechol when using 50% H_2O_2 at 260 ^{o}C in just 60s at pressures of 9-17 MPa. Since oxidation conditions were more harsh in previous ball milling case, higher yields of water-soluble portion should be expected.

We also investigated the quantities of small aromatic molecules that can be isolated from the ethyl acetate-soluble fraction, so these fractions were combined and derivatized with $BF_3 \cdot OEt_2$ in MeOH to esterify any formed carboxylic acids. As we have previously observed after the ball-milling process,[178] two major products (see Figure 3.7), methyl 5-carbomethoxy-vanillate and methyl vanillate (**3-I** and **3-II**) were isolated from each mixture. Yields of **3-I** and **3-II** from derivatization of ethyl acetate-soluble portion were shown in Table 3.3.

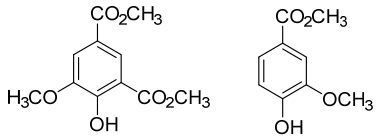

3-I **3-II**

Figure 3. 7 Structures of **3-I** and **3-II**

Table 3. 3 Yields of **3-I** and **3-II** from derivatization after Baeyer-Villiger oxidation

Milling time	**3-I**	**3-II**
15 min	0.6%	2%
1h	0.7%	1.4%
2h	0.7%	4.0%
3h	0.6%	3.5%
Porp-oxidized KL	0.2%	1.5%
Porp-oxidized BMKL	2.2%	7.8%

3.3 Conclusions

In this study we applied a mechanochemical approach, using ring-and-puck milling in a Shatterbox with KOH in a solvent-free system to promote lignin degradation. In order to analyse how milling time affects the structure changes during milling progress, different lignins were isolated from four-time intervals (15 min, 1h, 2h, 3h). We investigated how large-scale ring-and-puck milling would affect the success of a two-step oxidative lignin deconstruction strategy which we previously employed small-scale ball-milling. We monitored changes in lignin structure and functionality using 2D-^{1}H-^{13}C-HSQC and ^{31}P NMR spectroscopy.

^{31}P NMR indicated that 2 hours of ring-and-puck milling can generate significant amounts of aliphatic OH's and phenols, which is consistent with the fact that milling in the presence of KOH can cleave a significant number of the β-O-4 linkages. The content of aliphatic hydroxyl groups and phenols decreased dramatically after TPPFeCl/t-BuOOH oxidation, although we were surprised that the acid content does not increase significantly. Shatterbox milling followed by porphyrin oxidation yielded a structural change which cannot

be reversed by $NaBH_4$ reduction. After Baeyer-Villiger oxidation, the ethyl acetate-soluble portion of the mixture gave higher acid content, though less features of lignin remained.

The absence of cross-peaks associated with aliphatic units, and the notable disappearance of signals in the aromatic region in the HSQC Shatterbox milling indicates a significantly different set of reactions than does ball-milling. In addition, subsequent Baeyer-Villiger oxidation produced a remarkable increase of the ethyl acetate-soluble portion and a decrease in the amount of insoluble solid. Moreover, the amount of each fraction (both soluble and insoluble portions) tend to be constant with respect to time. Extending the milling time from 1 h to 3 h did not give significant growth of each fraction, indicating that the structural change was probably complete within 1 h. A short 2-hour period of Shatterbox milling produced nearly the half the amount of vanillic acid (isolated as the methyl ester) as an extended 26-hour period of ball-milling.

3.4 Experimental Section

3.4.1 Mechanochemical treatment of KL to SMKL

Milling was carried out in a SPEX 8530 Shatterbox equipped with a ring-and-puck milling sample container. Kraft lignin (12 g) was milled with KOH (6 g) (KL/KOH = 2:1 w/w). Certain amounts of Shatterbox milled kraft lignin were taken out after 15min (3.67 g), 1h (3.75 g), 2h (4.74 g), and 3h (4.52 g), respectively. These Shatterbox milled lignin's were dispersed in water and then acidified with 0.2 M HCl until precipitates appear. The precipitated lignins were recovered by vacuum filtration, washed with deionized water until pH was 7, and then dried in a vacuum oven at 80 ^{o}C for 14 h. The amount of recovered

Shatterbox milled lignins were as follows: 15 min (2.31 g), 1 h (2.31 g), 2 h (2.80g), and 3 h (2.59 g). Total mass recovery: 16.68 g, 92.6%; Lignin recovery: 10.01 g, 83%.

3.4.2 Porphyrin oxidation of Shatterbox milled lignin

A mixture consisting of TPPFeCl (26 mg), t-BuOOH (70% in water, 10 mL), phosphate buffer (pH 3, 30 mL), and 30 mL MeCN for every 1 g of Shatterbox milled lignin was stirred overnight at room temperature. The mixture was acidified with 0.2 M HCl until precipitate appeared. The precipitate was washed with deionized water until the pH of washing solutions was 7, and then dried in a vacuum oven at 80 ^{o}C for 14 h.

15 min: 2 g of Shatterbox milled lignin was used, 1.30 g oxidized lignin recovered, yield 65%.

1h: 2 g of Shatterbox milled lignin was used, 1.55 g oxidized lignin recovered, yield 78%.

2h: 2 g of Shatterbox milled lignin was used, 1.90 g oxidized lignin recovered, yield 95%.

3h: 2.09 g of Shatterbox milled lignin was used, 1.43 g oxidized lignin recovered, yield 71%.

3.4.3 Reduction of porphyrin-oxidized Shatterbox milled lignin

A mixture consisting of 1.4 g porphyrin-oxidized 2h-Shatterbox milled kraft lignin, and 1.36 g $NaBH_4$ was stirred at room temperature for 24 h in methanol. HCl (0.2 M) was added to quench the reaction until precipitate appeared. The precipitate was washed with

deionized water until the pH of washing solutions was 7, and then dried in a vacuum oven at 80 ^{o}C for 14 h. Reduced lignin: 0.78 g, 56%.

3.4.4 Baeyer-Villiger oxidation

A mixture consisting of 3.4 mL H_2O_2 (30%), 2 mL HCOOH (95%), and 2.7 mL H_2O for every 1 g of porphyrin-oxidized Shatterbox milled lignin was stirred at room temperature for 48 h. Deionized water was added until the pH was 4, and the mixture was filtered by gravity filtration. Water-insoluble and water-soluble portions were each extracted with ethyl acetate (3 x 30 mL). The residue from ethyl acetate extraction of the water-insoluble fraction was filtered by gravity filtration, washed with ethyl acetate, then dried in a vacuum oven at 80 ^{o}C for 14 h.

The combined ethyl acetate-soluble layers were dried with anhydrous Na_2SO_4 and evaporated in *vacuo* to produce a crude brown oil, then the resulting oil was derivatized with $BF_3{\cdot}OEt_2$ (0.2 mL) in MeOH (20 mL) for every mmol substrate (calculated based on methyl vanillate) at 80 ^{o}C for 6 h. Water was added after evaporation of solvent and the solution was extracted with ethyl acetate (3 x 30 mL). The combined organic layers were dried with anhydrous Na_2SO_4, evaporated in *vacuo* and purified by chromatography on silica gel (hexane/ethyl acetate = 3:1) to give **3-I** and **3-II**, respectively. Yields were calculated based on the mass of the amount of porphyrin-oxidized Shatterbox milled lignin used.

15 min: 1 g of porphyrin-oxidized Shatterbox milled lignin was used, **3-I** (6 mg, 0.6%),**3-II** (20 mg, 2%) were produced.

1h: 1 g of porphyrin-oxidized Shatterbox milled lignin was used, **3-I** (7 mg, 0.7%), **3-II** (14 mg, 1.4%) were produced.

2h: 1.5 g of porphyrin-oxidized Shatterbox milled lignin was used, **3-I** (7 mg, 0.7%), **3-II** (40 mg, 4%) were produced.

3h: 1 g of porphyrin-oxidized Shatterbox milled lignin was used, **3-I** (6 mg, 0.6%), **3-II** (35 mg, 2%) were produced.

3.4.5 HSQC

$^{1}H^{13}C$-gradient heteronuclear single quantum coherence spectra (gHSQC) were collected at 400 MHz (and 100 MHz ^{13}C) on a Varian 400 MR NMR spectrometer (Varian-Agilent, Palo Alto CA) equipped with a ATB 5 mm probe at room temperature. The $^{13}C^{1}H$ correlation experiment was collected using the Agilent pulse program 'gHSQC' which implements a gradient-selected phase-sensitive heteronuclear single quantum coherence spectrum. Spectra were collected with spectral widths of 4800 Hz (^{1}H) and 22 KHz (^{13}C) using an acquisition time of 150 ms (F2, 721 complex points for ^{1}H) and 150 ms (F1, 128 increments for the ^{13}C dimension). At least 392 scans were taken per increment using a delay of 0.65 s.

Data were processed using TopSpin (Mac version 4.0.3). Processing used typical sine bell (90º) in F2 and squared sine-bell (90º) in F1. The DMSO solvent peak was used as an internal reference (δ_C 39.5 ppm, δ_H 2.5 ppm) and spectra are displayed in absolute value mode and color coded (in Adobe Illustrator CC 2018) using authentic or literature reference standards. In all cases lignin samples were made using >100 mg of sample and ~1 mg $Cr(acac)_3$ dissolved in ~750 µL DMSO-d6/Pyridine-d5 (4:1). Relative linkage percentages were determined via volume integration of the αC-H.

3.4.6 ^{31}P NMR experimental

^{31}P NMR was carried out on a Varian (Agilent) Inova 400 MHz spectrometer equipped with a ASW (4Nuc) probe tuned to 162 MHz. The acquisition time was set to 81 ms and the relaxation delay was set to 25 s in order to ensure complete relaxation of the nuclei between scans. In all cases, 16-32 scans were collected and the spectra were reference to the phosphitylated internal standard (152 ppm). Integration regions were held standard for each sample and were as follows: internal standard (152.5-151.5 ppm), aliphatic alcohol (150-145 ppm), phenolic hydroxyl (145-136 ppm), carboxylic acid (136-133 ppm).

Samples were prepared as follows: To an NMR tube 40 mg of lignin (accurately weighed) was added along with 500 μL of pyridine-d_5: $CDCl_3$ (1.6/1 v/v). Then 200 μL of internal standard solution (endo-N-hydroxy-5-norbornene-2,3-dicarboximide, 50 mmol/L in pyridine-d_5/$CDCl_3$ 1.6/1 v/v) and 50 μL of $Cr(acac)_3$ solution (11.4 mg/mL in pyridine-d_5/$CDCl_3$ 1.6/1 v/v) were added to the NMR tube. Once the lignin samples were dissolved (*via* sonication and mild heating), 100 μL of phosphytilation reagent (2-chloro-4,4,5,5-tetramethyl-1,3,2-dioxaphospholane) was added. In the case of oxidized lignins, 40 mg of oxidized lignin (accurately weighed) was added to 300 μL of DMF and 200 μL of pyridine-d5. Then 200 μL of internal standard solution, 50 μL of $Cr(acac)_3$ solution, and 125 μL of $CDCl_3$ were added. Once the lignin samples were dissolved, 100 μL of phosphytilation agent was added. Note, NMR spectra were collected within 1 hour of addition of the phosphytilation reagent in order to ensure that the sample had not degraded.

Chapter 4 Toward valorisation of lignin: Investigation of lignin and lignin derived materials as building blocks for epoxy resins

Disclaimer: Portions of this chapter was taken from the following paper:

Z. Fang, M. C. Weisenberger and M. S. Meier. Towards valorisation of lignin: Investigation of lignin and lignin-derived materials as building blocks for epoxy resins (*ACS Sustainable Chem. Eng., submitted*)

4.1 Introduction

Epoxy resins have been widely used as structural adhesives, protective coatings, and in other applications due to their excellent thermal and mechanical performance. Bisphenol A (BPA) is the most widely used building block in the epoxy resin industry[103] but recently, concerns about the potential toxicity associated with BPA have limited its application. BPA is suspected to be an endocrine disruptor[104] and it can increase incidence of obesity, heart disease, diabetes and other diseases.[105] Therefore, replacement of bisphenol A-based epoxy resins with less hazardous monomers, especially monomers derived from sustainable and renewable resources rather petroleum-derived materials, is strongly preferred as production of BPA heavily relies on substantial petroleum-derived products.[106]

Thermosetting materials derived from renewable sources,[191] especially from feedstocks composed of aromatic units[111] have drawn great attention recently because the stability and rigidity of aromatic monomers would contribute to the high thermal and mechanical performance of thermosets.[112] Lignin, the most abundant natural biopolymer composed of aromatic units, is one of the most attractive renewable materials. Lignin is a three-dimensional polymer produced from through three building blocks, known as syringyl (S), guaiacyl (G), and *p*-hydroxyphenyl (H) units (Fig. 1.3).[10, 16]

Multiple functional groups are usually present in raw lignin including phenols, aliphatic hydroxyls and carboxylic acids,[16] and many of these can used to introduce epoxides.[192] Thermal and mechanical studies of thermosets utilizing raw and functionalized lignin,[10, 108, 193] and degraded lignin[194] have been reported. Although the high molecule mass

and poor solubility of raw lignin usually limits its utilization, application of monomer streams obtained from lignin degradation is both environmentally and economically feasible in epoxy resins preparation since these monomer streams usually carry hydroxyl groups[8, 10] (phenols, carboxylic acids) that are reactive in epoxide synthesis.

Earlier studies have reported the synthesis and characterization of epoxy resins from lignin and lignin-derived materials. Lignin has been exploited as the precursors of different types of polymeric materials such as polyesters,[102, 195, 196] polyurethanes,[100, 197, 198] and epoxies.[192-194, 199-203].[204, 205] Investigation of the properties of epoxy resins from model compounds that potentially can be obtained from decomposition of lignin have been reported, where model compounds including vanillin,[111, 112] 2-methoxy-4-propylphenol (iso-eugenol),[206, 207] lignin-derived phenols[202, 208] and C2-acetals.[209] These are very reasonable model systems, considering that in work by several groups,[8, 10, 16, 117] including our previous work on cleavage of β-O-4 model compounds[121] and on ball milled kraft lignin,[178, 210] various phenols (i.e. guaiacol, vanillic alcohol, syringol) or phenolic acids (i.e. vanillic acid, veratric acid), or mixtures of aromatic streams are typically formed. However, the economics of lignin utilization improve if the cost of pre-treatments (deconstruction, chemical modification) can be held to a minimum, and this argues for the development of uses for raw lignin or for uses of lignin that has been subject to the fewest, least expensive modifications.

In this study, kraft lignin (KL) was Shatterbox-milled (with a ring-and-puck Spex 8530 Shatterbox) for 15 minutes, as mechanochemical pre-treatment is known to increase the hydroxyl content in lignin.[210] Both KL and Shatterbox-milled KL (SMKL) were treated with epichlorohydrin to produce the corresponding glycidyl ether, KL-epoxide and SMKL-

epoxide, respectively (Fig 4.1). We then prepared blends of these materials with a commercial BPA-based resin (EPON 826), curing agent (NMA), and an amine initiator (BDMA), as shown in Fig 4.1. Cured samples of these mixtures were then examined to determine how the substitution of lignin-derived material affected the thermal and mechanical properties.

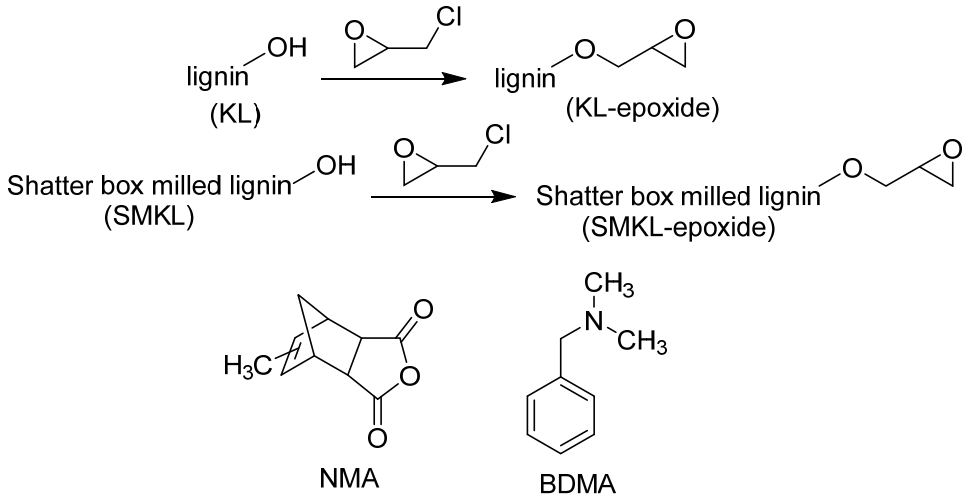

Figure 4. 1 Formation of KL-epoxide, SMKL-epoxide and structures of NMA and BDMA

Earlier, we determined that mechanochemical processing can significantly increase the yield of monomeric products from the two-step oxidative deconstruction of lignin ,[178, 210] so we used this approach to prepare samples of oxidized lignin for use in epoxy resins. Shatterbox milled kraft lignin was subjected to the two-step oxidative degradation strategy (FeTPP/tBuOOH, followed by Baeyer-Villiger oxidation with formic acid and hydrogen peroxide), and the resulting ethyl acetate soluble portion was treated with epichlorohydrin to produce corresponding epoxides (glycidyl ethers). Thermal and mechanical properties studies of thermosets prepared from these epoxides were also investigated and compared with BADGE-based resins.

We also focussed on utilization of three representative monomers that can be produced after more complete lignin deconstruction: vanillic acid (**IV-1**), 3,4-dimethoxybenzoic acid (**IV-2**) and *p*-hydroxybenzoic acid (**IV-3**) (see Scheme 4.1). These three acids were treated with epichlorohydrin to produce corresponding epoxides (see Scheme 4.1) and these were blended with NMA and BDMA (see Fig. 4.1) to prepare different thermosets.

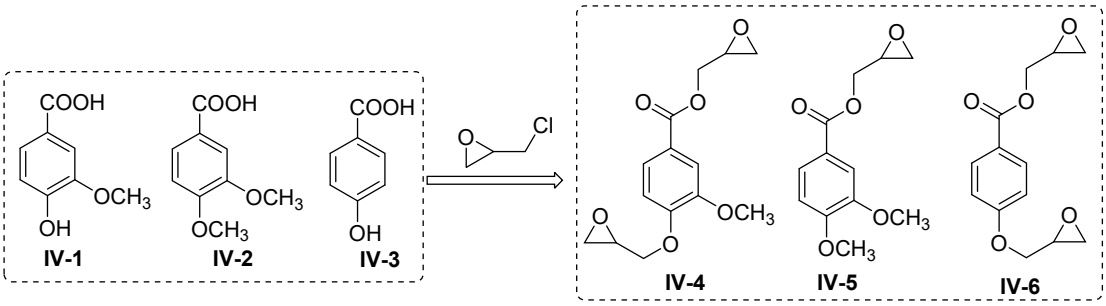

Scheme 4. 1 Model compounds (**IV-1, IV-2, IV-3**) and corresponding epoxides (**IV-4, IV-5, IV-6**)

Differential scanning calorimetry (DSC), thermogravimetric analyses (TGA) and dynamic mechanical analysis (DMA) were performed to examine both the thermal and mechanical properties of the resulting polymers. Bisphenol A diglycidyl ether (BADGE) based epoxy resins (EPON 826) were used for comparison to investigate how the properties of the cured resins differed from commercial epoxy systems. We hoped to identify whether materials prepared from these mono-aromatic epoxides can partially (or fully) substitute for BADGE-based materials in epoxy resins. Thermal and mechanical properties of thermosets composed of different combinations of those epoxides (**IV-4**, **IV-5**, **IV-6**) were examined as well, since a mixture of monomeric compounds with different functional groups usually exist in the products stream of lignin degradation, therefore we can understand whether isolation

and purification of each component in the monomers stream is essential or if it can be avoided.

In addition, we investigated the preparation of BPA and BPF analogues, using lignin-derived aromatics as the starting material rather than phenol. The structures of commercial BPA or BPF-based resins suggest the importance of the "bridge" between the two aromatic rings in determining material properties (Fig. 4.2), as either the isopropyl bridge or the methylene bridge affects the degree of mobility and rotational freedom of the polymer backbone.[113, 211]

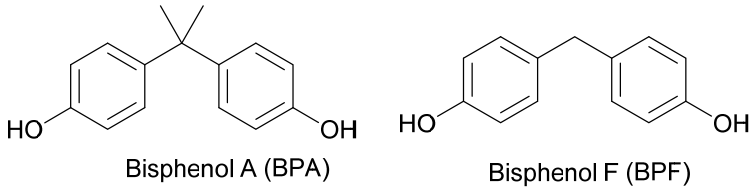

Figure 4. 2 Structures of BPA and BPF

Therefore, beginning from acids **IV-1 - IV-3**, bis-aromatic acids consisted of "bridge" were synthesized in our study. These BPA and BPF analogues were utilized to compare to commercial products and we also investigated how polymers from bis-aromatic epoxides differ from polymers from mono-aromatic epoxides **IV-4** – **IV-6**.

4.2 Materials and methods

4.2.1 Synthesis of model epoxides

Followed the procedures of Fache,[111] epoxides **IV-4 - IV-6** were prepared from glycidylation of aromatic acids **IV-1 - IV-3** with epichlorohydrin.

Conventional synthesis of bisphenol (BPA or BPF) involves an excess amount of phenol and a bridging molecule (acetone or formaldehyde), as shown in Scheme 4.2.

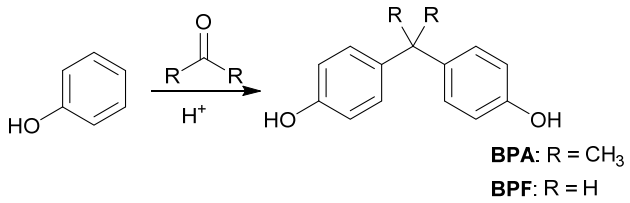

Scheme 4. 2 Conventional synthesis of bisphenols

Availability of the position *para*- to the phenolic hydroxyl group is essential in generation of BPA analogues. Removal of carboxylates in this position can be achieved decarboxylation of acid **IV-2** (vanillic acid) to guaiacol and of acid **IV-3** (*p*-hydroxybenzoic acid) to phenol can be achieved with cucumber juice (obtained from cutting the fresh green cucumbers into slices, followed with grinding and filtration) in 80% and 75% yield, respectively.[212] Bisphenols formed from guaiacol with isopropylene bridges[213] and with methylene bridges[211], and properties of epoxy resins based on these resulting bisphenols have been reported as well. Alternatively, conversion of vanillic acid into creosol by reducing the carboxylic acid to a methyl group[214] facilitated the formation of the dimeric compound.[215] Bisphenol compounds **IV-7** and **IV-9** (see Scheme 4.3) were previous reported[216-218] but epoxy resins prepared from these bisphenols were not reported. Following these ideas, we prepared two BPF-type diglycidyl ethers **IV-8** and **IV-10** (see Scheme 4.3).

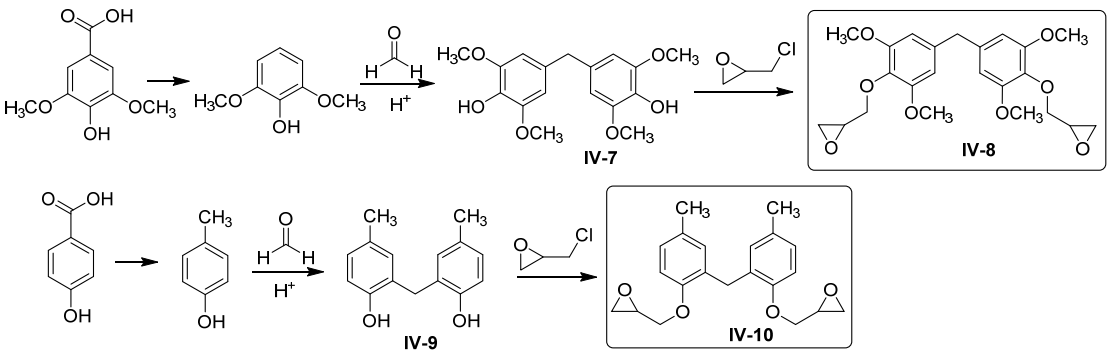

Scheme 4. 3 Synthesis of diglycidyl ether **IV-8** and **IV-10**

4.2.2 Preparation of epoxy thermosets

KL, SMKL, KL-epoxide, SMKL-epoxide were each blended to replace 50% (w/w) BADGE resin, mixed with NMA and BDMA in a mass ratio 1:0.8:0.08, then hand-stirred at room temperature for 1 min. The glycidyl ether of the ethyl acetate soluble portion (GE-EAS) derived from Shatterbox-milled kraft lignin after the two-step oxidative approach was prepared and utilized as a partial replacement for BADGE resin as well.

A group of epoxy thermosets prepared from epoxides **IV-4** - **IV-6** were prepared[207] to compare their thermal properties to commercial BADGE-based epoxy (EPON 826). Individual epoxides **IV-4** - **IV-6** and BADGE were each mixed with NMA and BDMA in a molar ratio of 1/0.8/0.08 and then hand-stirred at room temperature to obtain a homogenous mixture. In addition, a 1:1:1 molar mixture of **IV-4 - IV-6** was mixed with NMA and BDMA in an effort to determine whether it is necessary to isolate pure individual monomers from complex product streams from deconstructed lignin, since purification can be difficult and costly. We also replaced 50% (molar ratio) of BADGE with compounds **IV-4** - **IV-6** to study how the thermal properties change. Similarly, thermosets consisting of diglycidyl ethers **IV-8**

and **IV-10** were prepared to compare to a commercial BPF-based resin (EPON 862). EPON 862 was blended (50% molar ratio) with diglycidyl ether **IV-8** and with **IV-10** to investigate how the properties of the cured resins were affected.

DSC analyses of these thermosets was performed immediately after mixing. The rest of the uncured materials were poured into a Teflon mold (length: 35 mm, width 5 mm, thickness: 5 mm). Any trapped air was removed *in vacuo* overnight, and then all thermosets were cured at 150 ºC for 1h and post-cured at 100 ºC for 1h. Cured samples were cut and shaped into desired dimensions (length: 30 mm, width 5 mm, thickness: 1.5 mm) for DMA analysis. The remaining portions of cured samples were used for further DSC and TGA analysis.

4.2.3 Test methods

(1) Differential scanning calorimetry (DSC):

The curing behaviour of all thermosets was evaluated on the TA Q20 calorimeter under N_2 flow (50 mL/min) from -20 to 250.00 °C at a heating rate of 10.00 °C/min. A heat-cool-heat method was used from -20 to 180 °C at the same heating rate to determine the glass transition temperatures (T_g) for specific samples.

(2) Thermogravimetric analyses (TGA):

Weight loss of all cured thermosets was evaluated on a TA Q5000 thermogravimetric analyser under air flow (25 mL/min) from room temperature to 700.00 °C at a heating rate of 20.00 °C/min in a platinum pan.

(3) Dynamic Mechanical Analyses (DMA):

Dynamic mechanical analyses were conducted in single cantilever mode on a TA Q800 instrument under an N_2 atmosphere from room temperature to 225 °C at a heating rate of 3.00 °C/min with a constant frequency of 1 Hz. Glass transition temperatures (T_g) were determined as the peak temperature of tan δ curves.

4.3 Results and discussion

For convenience, DSC, TGA and DMA analysis of BPA-typed epoxy resins (prepared from KL, SMKL, KL-epoxide, SMKL-epoxide, GE-EAS and epoxides **IV-4**, **IV-5**, **IV-6**) and BPF-typed epoxy resins (prepared from epoxides **IV-8** and **IV-10**) was discussed below separately.

4.3.1 Epoxy resins prepared from KL and Shatterbox milled KL (SMKL)

4.3.1.1 DSC analysis

DSC data including the temperatures of polymerizations (T_p) and enthalpies of reactions (ΔH) were recorded.

In all cases, when 50% (w/w) of BADGE resin was replaced by KL, SMKL, KL-epoxide and SMKL-epoxide, they still cured with NMA and BDMA (See Fig. 4.3). The enthalpies (ΔH, obtained by integration of the exothermic peaks using TA Universal Analysis software) of each curing reaction were significantly lower than the enthalpy observed in curing reactions with neat BADGE resin, NMA, and BDMA, which indicated a considerable drop in the number of cross-links formed during curing (Table 4.1).

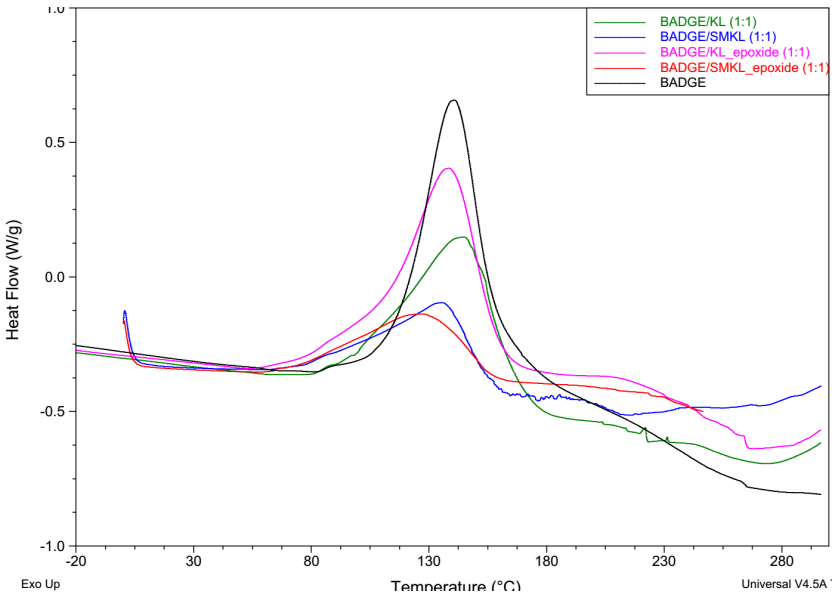

Figure 4. 3 DSC analysis of curing reaction from thermosets constituted of KL and SMKL

Table 4. 1 DSC data of different lignins cured with NMA and BDMA

Monomers	T_p (° C)	ΔH (J/g)
BADGE	141	213
BADGE/KL	145	156
BADGE/SMKL	136	76
BADGE/KL-epoxide	139	173
BADGE/SMKL-epoxide	127	70

4.3.1.2 TGA analysis

TGA analysis of these thermosets in air flow were performed to evaluate the thermal stability. Degradation temperatures of each thermoset corresponding to 5% weight loss ($T_{5\%}$) and maximum degradation rate (T_{max}) are summarized in Table 4.2 and Fig. 4.4.

Thermal stability of thermosets from raw lignin samples (Table 4.2) was measured in an air atmosphere over a temperature range of 0 ˚C to 700 ˚C. Multiple processes, manifest as more “inflections,” were observed from the thermal degradation curves, (Fig. 4.4) reflecting

decomposition of different functionalities existing in these lignin materials compared to neat BADGE-based resins, although all samples generally followed a 2-step degradation profile.

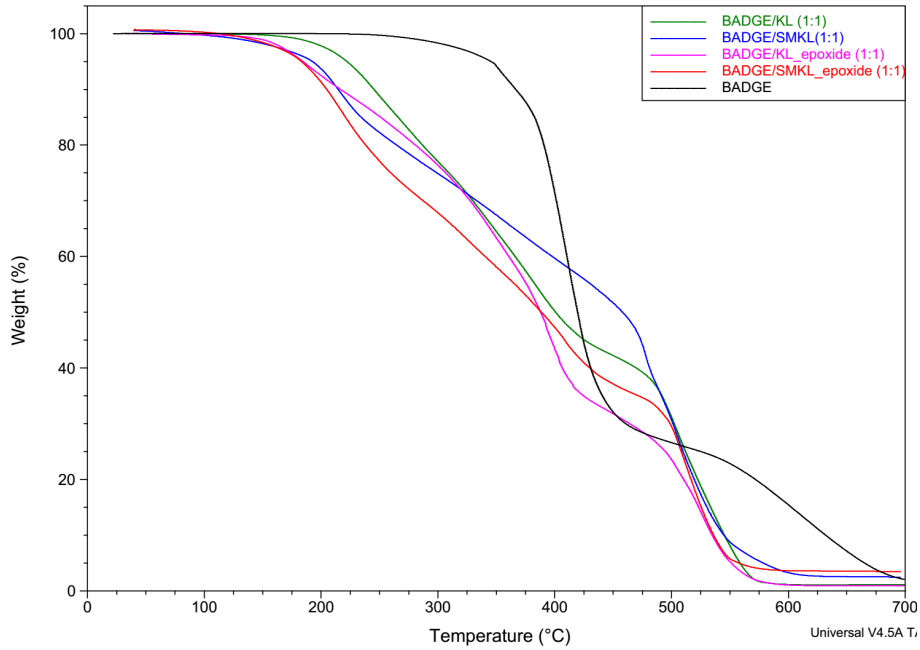

Figure 4. 4 Thermal degradation of different lignin samples cured with NMA and BDMA

In general, the lignin- and lignin-derived materials led to thermosets that began to decompose at lower temperatures than thermosets made from the commercial BADGE resin and throughout most of the temperature range, the thermosets composed of the commercial resin retained more mass than did the blends. This is likely due to the abundance of aliphatic alcohols and other lignin-derived structures that can thermally decompose and oxidize readily, combined with the lower crosslink density that produces a more flexible material that can be more easily accessed by oxygen.

Table 4. 2 Temperatures of thermal degradation ($T_{5\%}$ and T_{max}) of thermosets prepared from different monomers

Monomers	$T_{5\%}$ (°C)	T_{max} (°C)
BADGE	345	410
BADGE/KL	222	506
BADGE/SMKL	192	478
BADGE/KL-epoxide	184	392
BADGE/SMKL-epoxide	182	512

4.3.1.3 DMA analysis

In general, modulus can be defined in the context of Hooke's law as Modulus = Stress/Strain. Depending on the nature of the deformation, it can be a tensile modulus, bending modulus, or shear modulus.[219] Storage modulus reflects the elastic response characteristics of the material, while loss modulus reflects the viscous response. The ratio of the two is equal to tan δ which reflects overall damping properties. A typical curve to show the modulus and tan δ from DMA test are shown in Fig 4.5 and Fig 4.6.[219] A typical single cantilever[220] is shown in Fig. 4.7.

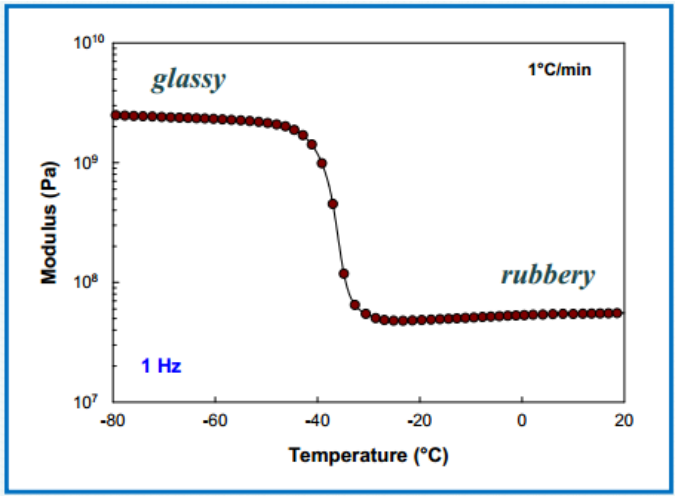

Figure 4. 5 A typical modulus curve from DMA test

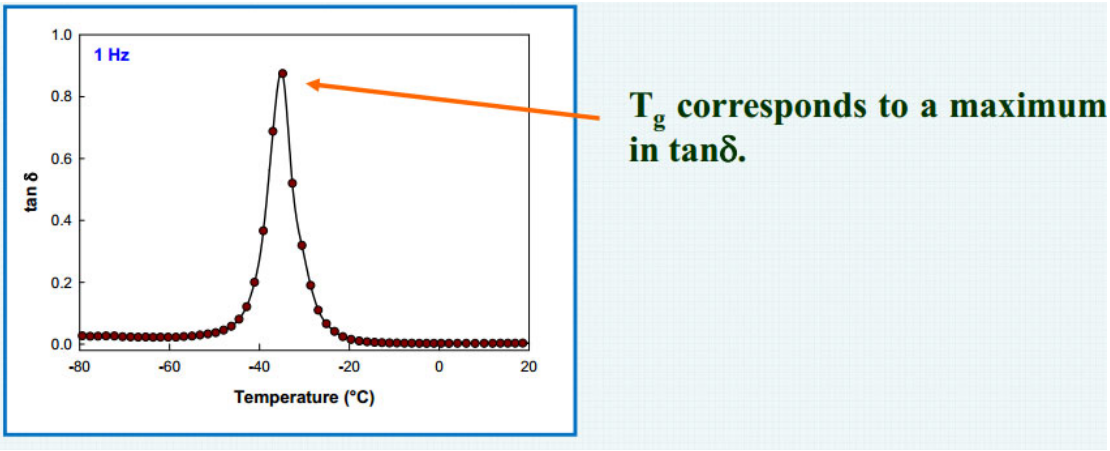

Figure 4. 6 A typical tan δ curve from DMA test

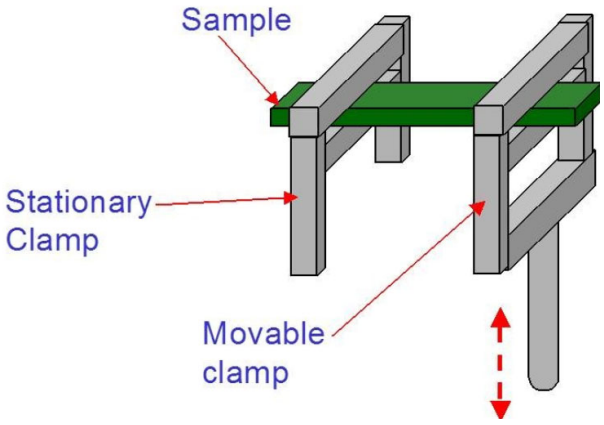

Figure 4. 7 A schematic image of single cantilever

Cured polymers based on EPON 826 and KL and on EPON 826 and SMKL were too delicate to be cut and shaped into desired dimensions for DMA testing, and this fragility is likely another manifestation of a low degree of crosslinking. As a result, the storage modulus (E') could not be observed from these materials. Glass transition temperature (T_g) was recorded by DSC using a heat-cool-heat method over a temperature range of -20 to 180 °C at a heating rate of 10 ºC/min.

Not surprisingly, thermosets prepared from the highly optimized commercial BADGE-based resin system show a much higher glass transition temperature (146 ºC) than

any of the lignin-based or synthesized monomer-based resins. Replacement of BADGE resin with 50% (w/w) KL, SMKL, KL-epoxide or SMKL-epoxide dramatically dropped the glass transition temperatures and interestingly all of their T_g were around 74-75 ^oC (Table 4.3).

Table 4. 3 Glass transition temperatures (T_g) of thermosets prepared from KL and SMKL

Monomers	T_g (^oC)
BADGE	146
BADGE/KL	74
BADGE/SMKL	74
BADGE/KL-epoxide	75
BADGE/SMKL-epoxide	75

4.3.2 Epoxy resins prepared from GE-EAS

4.3.2.1 DSC analysis

In contrast, compared to thermosets from KL and SMKL, lower curing temperatures and slightly higher ΔH were recorded (Table 4.4) when using GE-EAS or a mixture of BADGE/GE-EAS. More reactive sites should have generated after two-step oxidative approach.

Table 4. 4 DSC analysis of thermosets from GE-EAS

Monomers	T_p (^oC)	ΔH (J/g)
BADGE	141	213
GE-EAS	115	181
BADGE/GE-EAS (1:1)	121	179

4.3.2.2 TGA analysis

Though thermal stability is still much poorer than commercial BADGE-based epoxy resin, slightly higher $T_{5\%}$ was observed when utilizing the mixture of BADGE/GE-EAS compared to utilization of KL and SMKL.

Polymers composed of glycidyl ethers of the lignin-derived ethyl acetate soluble fractions (GE-EAS) are less thermally stable, even when 50% (molar ratio) of BADGE was blended into the GE-EAS portion. The lack of stability suggests poor cross-linking density due to very low hydroxyl content left in the ethyl acetate soluble portion after kraft lignin was Shatterbox milled and treated with the two-step oxidative approach.[210] Multiple-step degradation events in these non-rigid structures were taking place in these thermosets at 200-600 ºC, as more peaks and shoulders indicated in the TGA curve (see Fig. 4.8).

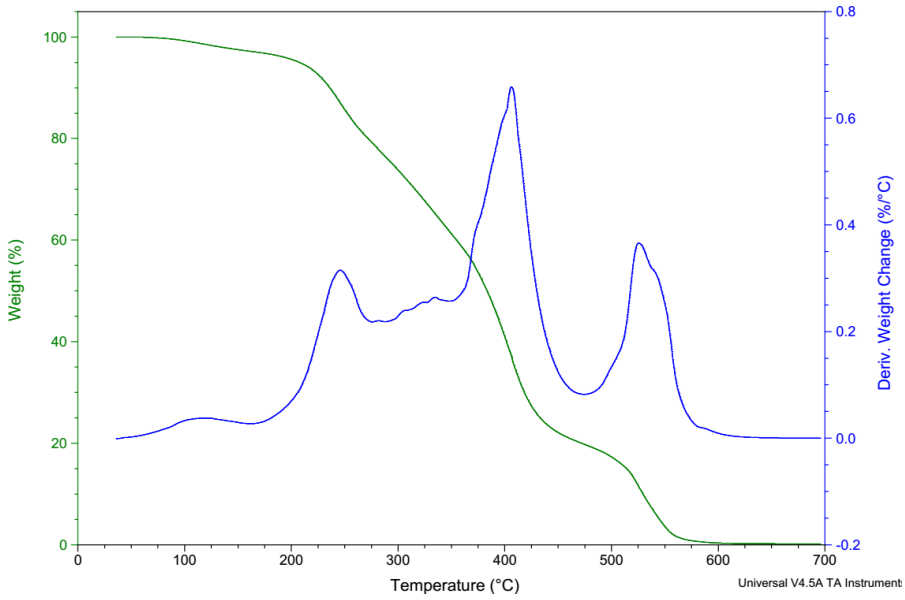

Figure 4. 8 Thermal degradation of thermoset from GE-EAS

Table 4. 5 Thermal degradation of thermosets from GE-EAS

Monomers	$T_{5\%}$ (°C)	T_{max} (°C)
BADGE	345	410
GE-EAS	206	405
BADGE/GE-EAS	242	412

4.3.2.3 DMA analysis

Similarly, cured thermosets from GE-EAS is too delicate to be shaped into desired dimensions to test storage modulus, so does even when using the mixture of BADGE/GE-EAS (50/50, w/w). Glass transition temperatures (T_g) of these materials were determined by DSC as well. In contrast, blending 50% (w/w) GE-EAS into BADGE gave much higher T_g (101 °C) than from those KL or SMKL based thermosets.

Table 4. 6 Glass transition temperatures of thermosets from GE-EAS

Monomers	T_g (°C)
BADGE	146
GE-EAS	57
BADGE/GE-EAS	101

4.3.3 BPA-type epoxy resins prepared from monomeric materials (IV-4, IV-5 and IV-6)

4.3.3.1 DSC analysis

All the resin mixtures, including BADGE, showed very similar curing behaviour, with peaks at similar temperatures, as shown in Table 4.7, suggesting that the underlying epoxy resin chemistry is essentially unchanged. Exothermic processes associated with polymerization are between 130-142 °C and slightly vary with the specific epoxies used but are very close to the temperature of the polymerization reaction of neat BADGE (T_p=141 °C).

Thermosets composed of epoxide **IV-4** displayed endothermic peaks around 45-70 ºC (see Fig. 4.9) which is assigned to the melting progress of monomer **IV-4** (m.p. 77 ºC).[111] Blending monomer **IV-4** with the curing agents afforded a non-homogenous mixture initially and an obvious exothermic peak was observed once the mixture became homogenous at high temperatures.

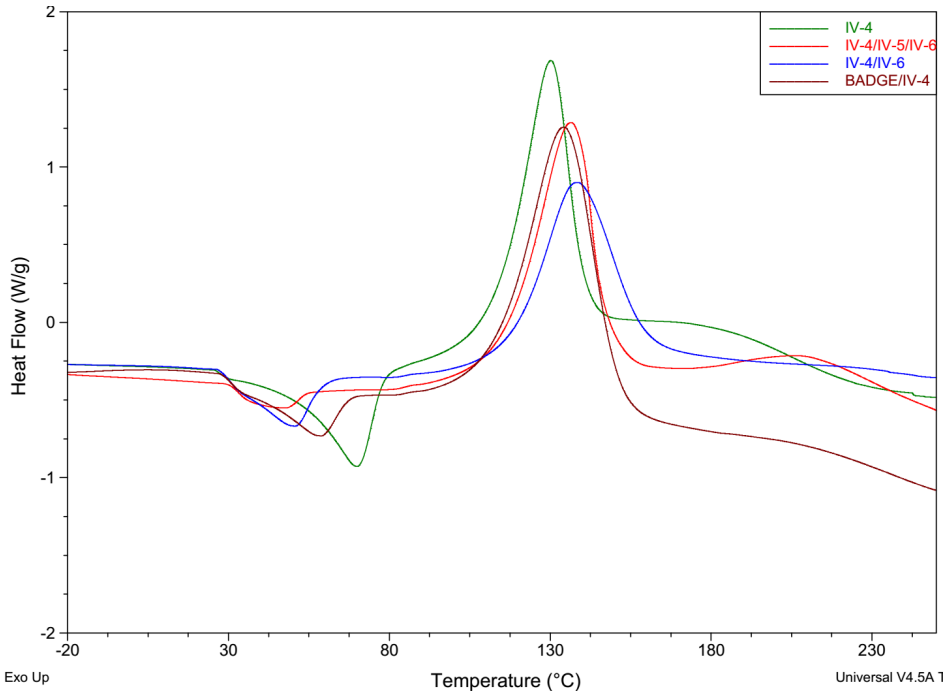

Figure 4. 9 DSC analysis of curing reaction from thermosets constituted epoxide **IV-4**

Table 4. 7 DSC data of different epoxies cured with NMA and BDMA

Monomers	T_p (°C)		ΔH (J/g)	
BADGE	141		213	
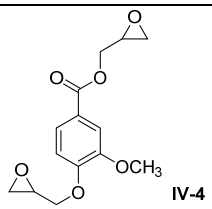 IV-4	130		199	
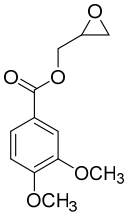 IV-5	142		159	
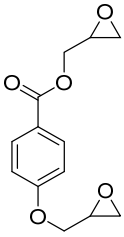 IV-6	130	195[a]	238	30[a]
BADGE/ **IV-4** (1:1)	135		276	
BADGE/ **IV-5** (1:1)	133		131	
BADGE/ **IV-6** (1:1)	136		227	
IV-4/ **IV-5**/ **IV-6** (1:1:1)	136	209[a]	215	20[a]
IV-4/ **IV-6** (1:1)	138		200	

[a]T_g and ΔH for a second, higher temperature process that was observed in these samples.

Enthalpies of polymerization reactions are shown in Table 4.7. Due to fewer cross-linking sites in mono-epoxide resins **IV-5** (163 J/g) and BADGE/ **IV-5** (131 J/g), polymerization enthalpies are lower in these cases when compared to samples prepared from bis-epoxide resins or neat BADGE. Much lower heat of reaction was also observed from

curing of **IV-6** (41 J/g) and **IV-4**/ **IV-5**/ **IV-6** (25 J/g), at exothermic temperature of 196 ºC and 210 ºC, respectively (see Table 4.7). The multiple peaks are associated with different reactions during curing progress.[221] Interestingly, this phenomenon was not observed in other samples. It's important to know that exothermic peaks and heat of polymerization from mixed bis-epoxides resins or from BADGE-blended resins do not differ dramatically from those observed from curing of resins containing neat BADGE, and even significant higher enthalpies of reaction were detected from polymer resins prepared from BADGE/ **IV-4** (1:1). Lower enthalpies would indicate a lower degree of cross-linking and ΔH's were observed in similar range (except for the mono-epoxide case) again imply that the underlying epoxy resin chemistry is unchanged.

4.3.3.2 TGA analysis

All of these new thermosets are stable in air until 230 ºC, at which point they undergo rapid oxidation (combustion) and leave almost no residue by 700 ºC. Most of the resin mixtures that include lignin-derived material virtually indistinguishable from the commercial epoxy resin system. All the thermosets exhibit a 2-step degradation profile: one process in the range of 230 - 450 ˚C and another in the range of 450 - 650 ºC, as shown in Fig. 4.10. The first degradation, producing a dramatic 60% weight loss is likely associated with the breaking of aliphatic chains and loss of water, carbon monoxide, carbon dioxide or other pyrolysis products.[222] The second weight loss (> 450 ºC) is presumably due to the oxidation of C-C linkages between lignin units and functional groups (such as carbonyls, phenolic hydroxyl groups),[223] or related to destruction of aromatic rings.[222]

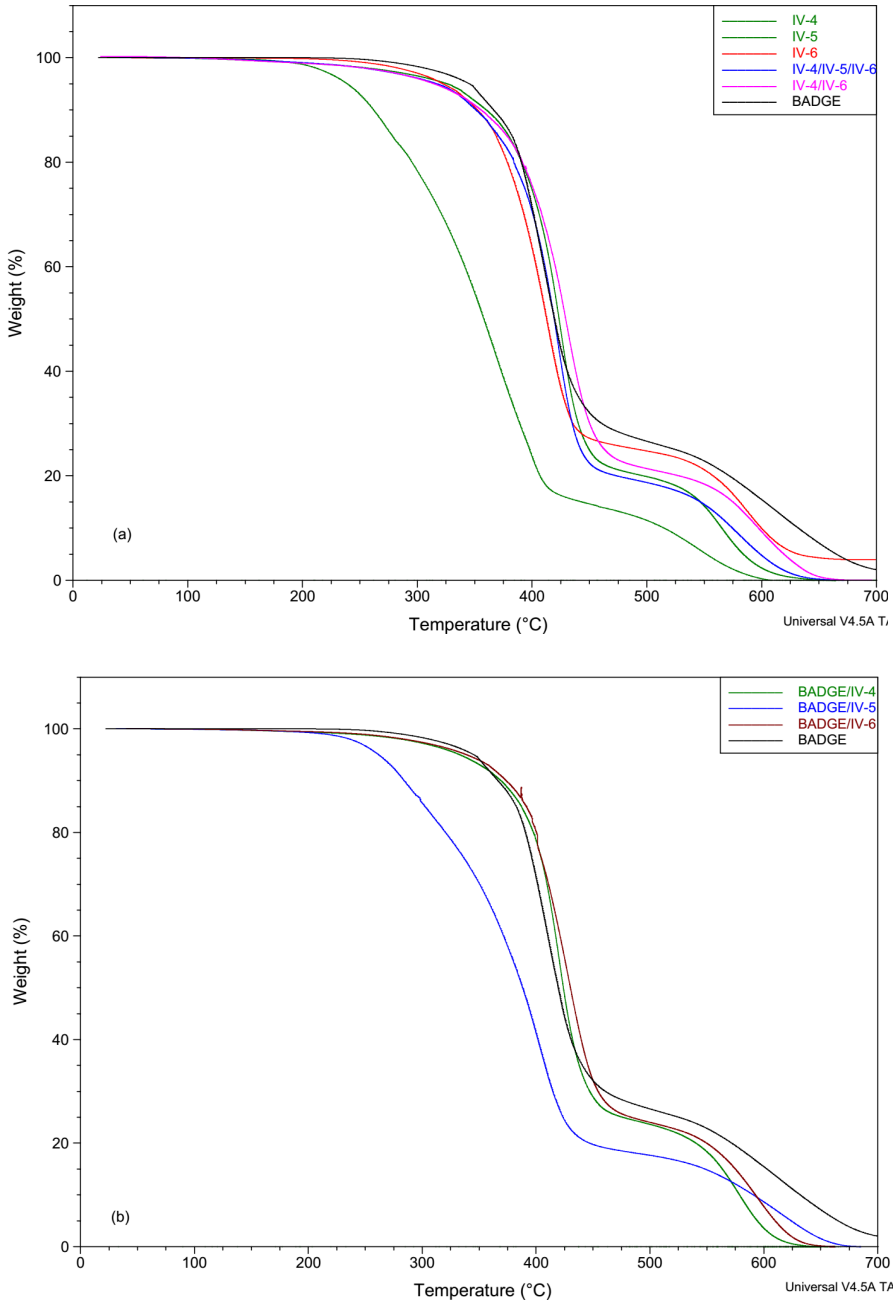

Figure 4. 10 Thermal degradation ($T_{5\%}$ and T_{max}) of monomers cured with NMA and BDMA, measured in an air atmosphere.

Again, not surprisingly, thermosets made from resins that included mono-epoxide **IV-5**, including the mixture **IV-4**/ **IV-5**/ **IV-6** (in Fig. 4.10a), mono-epoxide **IV-5** alone, and the mixture BADGE/ **IV-5**, (in Fig. 4.10b) are the least thermally stable of the thermosets studied, presumably due fewer cross-links than found of other bis-epoxide based resins.[112]

Degradation temperatures of these three thermosets corresponding to 5% weight loss are less than 300 ºC, while that of the rest are all higher than 300 ºC. Material with lower cross-link density requires less energy to destroy the structures, yielding lower degradation temperatures. The thermal stability of resins based on bis-epoxides is comparable with commercial BADGE-based resin (EPON 826, Miller-Stephenson) though their degradation temperatures associated with 5% weight loss are slightly lower. T_{max} degradation temperatures of these polymers are in the range 369-413 ºC.

4.3.3.3 DMA analysis

The temperature dependence of the storage modulus (E') and tan δ are shown in Fig. 4.11 and Fig. 4.12. The glass transition temperatures (T_g) were recorded as the peak temperature of the tan δ curve and are summarized in Table 4.8.

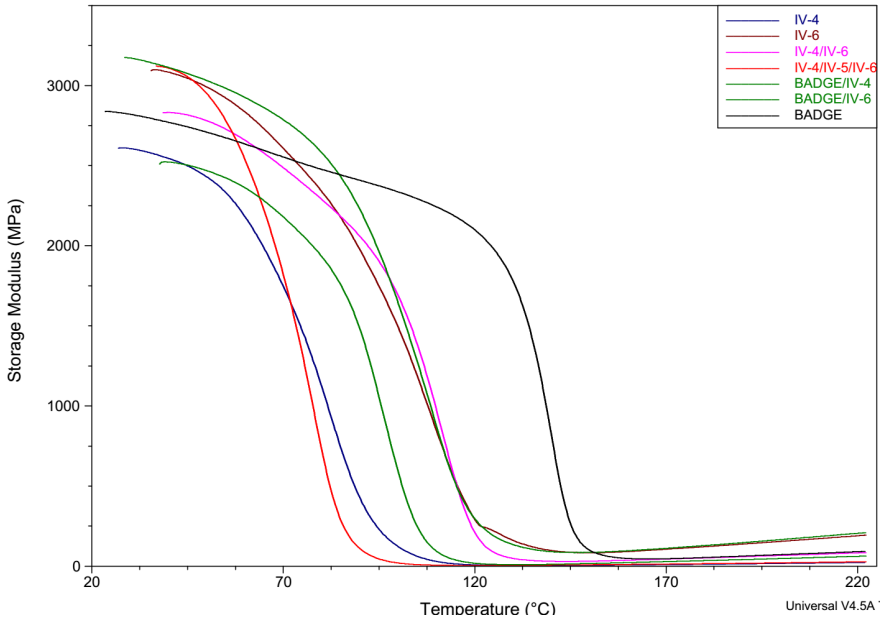

Figure 4. 11 Storage modulus of thermosets from different monomers

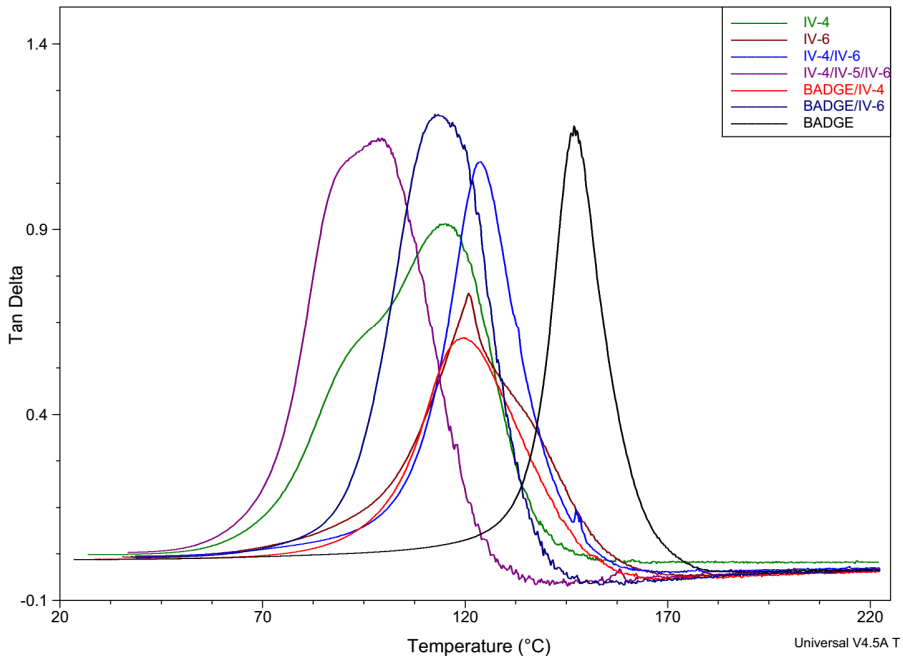

Figure 4. 12 Tan δ curves of thermosets from different monomers

Table 4. 8 Glass Transition temperatures (T_g) of thermosets from different monomers

Monomer	T_g (°C)
BADGE	146
IV-4	115
IV-5*	55
IV-6	120
BADGE/ **IV-4** (1:1)	119
BADGE/ **IV-5** (1:1) *	58
BADGE/ **IV-6** (1:1)	113
IV-4/ **IV-5**/ **IV-6** (1:1:1)	98
IV-4/ **IV-6** (1:1)	123

*: T_g was determined by DSC

The storage modulus (E') of all the resins was located between 2.5 to 3.3 GPa at room temperature (25 °C) and dropped to near 0 at temperatures between 80 °C and 150 °C.

The storage modulus of the BADGE-based resin was relatively stable until about 125 ^{o}C, while the storage modulus of all other resins dramatically decreased to almost 0 by this temperature, at which they essentially lost all tendencies to return to the original shape.

Not surprisingly, the highly optimized commercial BADGE-based resin has a much higher glass transition temperature (146 ^{o}C) than all of the lignin-based or synthetic monomer-based resins. It is interesting that neat **IV-4**-based resin has slightly lower glass transition temperature than **IV-6**-based polymer. The only difference between monomers **IV-4** and **IV-6** is the presence of a methoxy group *ortho*- to the glycidyl ethers in **IV-4**, but it has been reported that an *ortho*-methoxy group can lead to a decrease in T_g due to more rotational freedom of polymer backbone during heating as the extra methoxy group produces a relatively poorer "packing" order.[211] Bis-epoxide **IV-4**, prepared from vanillic acid, has a higher melting point (77 ^{o}C) and this led to poor miscibility with NMA and finally yielded an inhomogeneous and pliable structure with a relatively slightly low T_g.

Sample homogeneity is reflected in the width of the tan δ peak; the narrower and sharper the peak, the more homogeneous the sample. It is clear from Fig. 4.12 that the commercial BPA-based resin has a sharp, symmetrical tan δ peak, indicating its high homogeneity. Rest of the samples all exhibit relatively broad peaks, especially the peak from **IV-4**-based polymer. The breadth of the tan δ peak in the **IV-4**-based polymer is likely due to the poor dispersion of **IV-4** in the curing agent, leading to a less homogeneous polymer.

The resins that composed of neat mono-epoxide **IV-5** and GE-EAS were too delicate to be cut into the required rectangular dimensions for DMA measurements, and replacement of 50% of the **IV-5** with BADGE did not harden the sample sufficient for cutting. This

behaviour is consistent with low molecular weight material. Accordingly, the T_g of thermosets prepared from **IV-5**, BADGE/ **IV-5** and GE-EAS were identified by DSC (as a reversible heat flow that is not a melting process using a heat-cool-heat method) and unsurprisingly, these samples exhibited very low T_g's. A high viscosity mixture was obtained when BADGE/GE-EAS (1:1) was cured with NMA and removal of trapped air became difficult even the resulting mixture was set in *vacuo* at 50 ^oC overnight so the T_g of materials from BADGE/GE-EAS was also identified by DSC analysis.

The polymer prepared from a mixture of **IV-4**, **IV-5** and **IV-6** exhibited a low T_g (98 ^oC) which is significantly lower than the T_g observed in neat **IV-4-** or **IV-6-**based resins. In contrast, materials from **IV-4** and **IV-6** with the absence of **IV-5** exhibit an outstanding T_g (123 ^oC) as shown in Table 4.8. This suggests that utilization of mixed product streams from lignin deconstruction need to be treated to either remove mono-functional products or to introduce additional functionality.

4.3.4 BPF-type epoxy resins prepared from monomeric materials (IV-8 and IV-10)

4.3.4.1 DSC analysis

DSC data of curing reaction of thermosets prepared from **IV-8**, **IV-10** and EPON 862 is summarized in Fig. 4.13 and Table 4.9. The endothermic processes below 100 ˚C are attributed to the melting of undissolved monomer **IV-10** (m.p. 103 ^oC) present in the sample. Compared to commercial EPON 862, lower ΔH's (ΔH was determined as the integral of the exothermal peak in TA Universal Analysis software) were observed in these curing reactions of thermosets from synthetic monomers which suggested a lower degree of cross-linking

occurred. There are no obvious residual exothermic peaks once all the samples were cured, indicating curing reactions were already complete after 2h at 150 ºC.

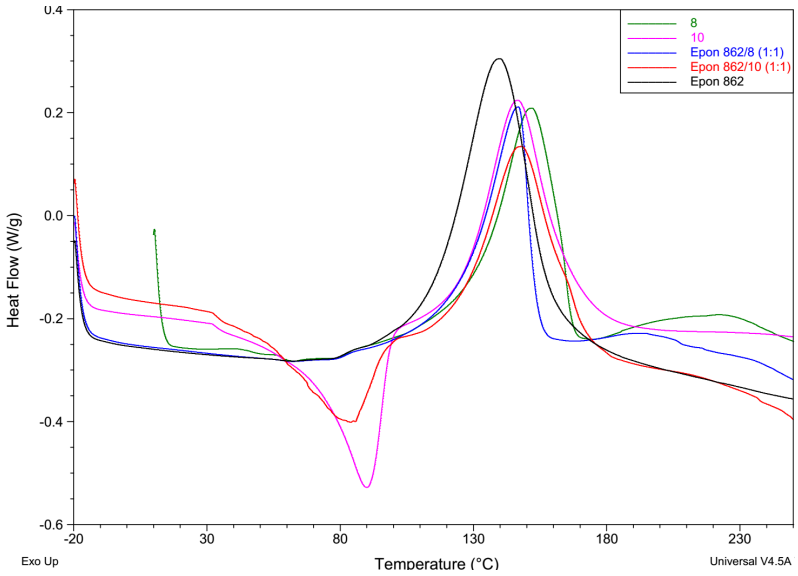

Figure 4. 13 DSC analysis of curing reaction of thermosets from **IV-8** and **IV-10**

Table 4. 9 DSC data of different monomers cured with NMA and BDMA

Monomers	T_p (ºC)	ΔH (J/g)
IV-8	146	73
IV-10	151	76
EPON 862/ **IV-8** (1:1)	146	62
EPON 862/ **IV-10** (1:1)	148	71
EPON 862	139	113

4.3.4.2 TGA analysis

Resin polymers cured with lignin-derived BPF-analogues are less thermally stable (see Table 4.10) than materials made with commercial EPON 862 based resin. A two-step degradation profile at 200-450 and 450-650 ºC was observed as well. It is interesting that blending EPON 862 into monomer **IV-8** or **IV-10** led a drop of the $T_{5\%}$ compared to thermosets constituted of neat **IV-8** or **IV-10**.

Table 4. 10 Temperatures of thermal degradation ($T_{5\%}$ and T_{max}) of thermosets from monomers **IV-8** and **IV-10**

Monomers	$T_{5\%}$ (°C)	T_{max} (°C)
IV-8	314	395
IV-10	285	422
EPON 862/ **IV-8**	300	411
EPON 862/ **IV-10**	264	427
EPON 862	340	424

4.3.4.3 DMA analysis

As observed with samples cured from **IV-5**, thermosets cured from monomers **IV-8** and **IV-10** are too delicate to be cut into desired bars, even when blended with 50% EPON 862. Therefore, T_g was identified by DSC (see Table 4.11). The cured thermosets listed in Table 4.11 all exhibited a much lower T_g than the thermoset produced by curing the commercial EPON system, presumably due to a lower degree of cross-linking and to increased rotational freedom in the polymer backbone.[224] BPF-type resins exhibited lower T_g's than BPA-type resins as the methylene spacer in BPF resins leads to greater rotational freedom in the framework relative to the isopropylidene spacer in BPA resins.[224, 225] Compared the methylene bridge in BPF, the isopropylidene bridge in BPA decreases the mobility and rotational freedom of the backbone, leading to a higher glass transition temperature.

Table 4. 11 T_g from DSC of thermosets prepared from **IV-8** and **IV-10**

Monomers	T_g
IV-8	57
IV-10	43
EPON 862/ **IV-8**	42
EPON 862/ **IV-10**	53
EPON 862	139

4.4 Conclusions

Commercial BADGE-based epoxy resin (EPON 826) was replaced by 50% (w/w) different lignin samples (KL, SMKL, KL-epoxide and SMKL-epoxide) then cured with NMA and BDMA. Both the thermal and the mechanical properties of the resulting thermosets are inferior to thermosets based on neat BADGE-based resins. To determine if lower molecular weight lignin-derived materials would produce better thermosets, we investigated mixtures of epoxy resin with mechanochemically treated and oxidized lignin. Mechanochemically-treated kraft lignin was processed with a two-step oxidative approach and the ethyl acetate soluble fractions were treated with epichlorohydrin to generate corresponding glycidyl ethers (GE-EAS). Compared to thermosets from lignin samples, thermal stability of BADGE/GE-EAS (50/50, w/w) based thermoset is obviously improved, although compared to BADGE-based resin, all of these thermosets exhibit low glass transition temperatures.

Utilization of monomeric samples (**IV-4**, **IV-5**, **IV-6**) produced thermosets with better thermal and mechanical properties than when lignin samples or GE-EAS were used. Mono-epoxide **IV-5** leads to lower glass transition temperatures and thermal stability,

compared to bis-epoxide **IV-4** and **IV-6**. In order to achieve better properties, mono-functional products should be removed from the product streams.

The ubiquitous use of BPA or BPF in commercial epoxy resin systems suggested importance of isopropyl and methylene bridges between aromatic rings. We synthesized two BPF-type monomers (**IV-8** and **IV-10**) from compounds that can be produced from lignin and cured them with NMA and BDMA. Using the same formula, these BPF-type thermosets exhibit much lower glass transition temperatures compared to BPA-type thermosets prepared from monomeric epoxides **IV-4 - IV-6**, although they are much more thermally stable than from lignin-based or GE-EAS based materials.

4.5. Experimental

Column chromatography was performed using silica gel-60 (Supelco) and preparative TLC was carried out with 1 mm plates (Merck). ^{1}H and ^{13}CNMR spectra were obtained at room temperature on a Varian INOVA 400 MHz spectrometer, with chemical shifts (δ) referenced to the residual solvent signal. EPON 826 and EPON 862 were purchased from Miller-Stephenson. NMA (≥ 95%) and BDMA (> 99.5%) were purchased from Sigma Aldrich. All other chemicals were purchased from commercial vendors and directly used without further purification.

4.5.1 Synthesis of bisphenol IV-7

A mixture of Syringol (5 g, 32.5 mmol) and 37wt% formaldehyde (1.2 mL, 16.3 mmol) in 60% H_2SO_4 (25 mL) was stirred overnight at 90 °C. The mixture was cooled and extracted with ethyl acetate (3 x 20 mL) and the combined organic layers were dried over

Na_2SO_4 and concentrated under vacuum. The crude products were purified by column chromatography on silica gel (hexane/ethyl acetate = 2:1) to give **IV-7** (2.47 g, 7.7 mmol, 47%) as yellow solid.

^{1}HNMR (400 MHz, $CDCl_3$): 6.56 - 6.49 (4 H, m), 3.90 (2 H, s), 3.79 (12 H, d, *J* = 2.4 Hz). ^{13}CNMR (101 MHz, $CDCl_3$): 146.3, 145.4, 138.6, 127.2, 120.0, 106.4, 60.3, 56.1, 28.9

4.5.2 Synthesis of diglycidyl ether IV-8

A mixture of bisphenol **IV-7** (2.28 g, 7.1 mmol), TBAB (0.04g) and epichlorohydrin (5.4 mL, 71.5 mmol) was stirred at 80 ºC for 3h. The mixture was cooled and NaOH (5 M, 5.4 mL) was added then continued to stir for 1h. Ethyl acetate (20 mL) and water (20 mL) was added and the mixture was stirred for another 30 min. The organic layer was isolated and the aqueous solution was extracted with ethyl acetate (3 x 20 mL). The combined organic layers were dried over Na_2SO_4 and concentrated under vacuum. The crude products were purified by column chromatography on silica gel (hexane/ethyl acetate = 2:1) to give diglycidyl ether **IV-8** (2.85 g, 6.6 mmol, 93%) as yellow oil.

^{1}HNMR (400 MHz, $CDCl_3$): 6.68 (2 H, d, *J* = 8.5 Hz), 6.52 (2 H, d, *J* = 8.6 Hz), 4.14 (2 H, dd, *J* = 11.2 Hz, 3.5 Hz), 3.91 (2 H, dd, *J* = 11.3 Hz, 6.1 Hz), 3.79 (2 H, s), 3.75 (6 H, s), 3.73 (6 H, s), 3.30 (2 H, m), 2.76 (2 H, dd, *J* = 5.0 Hz, 4.2 Hz), 2.59 (2 H, dd, *J* = 5.0 Hz, 2.7 Hz). ^{13}CNMR (101 MHz, $CDCl_3$): 152.1, 151.9, 141.0, 127.3, 124.8, 107.2, 74.1, 60.8, 55.9, 50.5, 44.5, 29.2. HRMS (ESI) m/z $[M + H]^+$ *calcd* for $C_{23}H_{28}O_8$ 433.1862, found 433.1858.

4.5.3 Synthesis of bisphenol IV-9

A mixture of *p*-Cresol (5 g, 46.3 mmol) and 37wt% formaldehyde (1.7 mL, 23.2 mmol) in 60% H_2SO_4 (25 mL) was stirred overnight at 90 ºC. The mixture was cooled and extracted with ethyl acetate (3 x 20 mL) and the combined organic layers were dried over Na_2SO_4 and concentrated under vacuum. The crude products were purified by column chromatography on silica gel (hexane/ethyl acetate = 2:1) to give bisphenol **IV-9** (5.2 g, 2.3 mmol, 98%) as white solid.

^{1}HNMR (400 MHz, $CDCl_3$): 7.10 - 7.03 (2 H, m), 6.89 - 6.82 (2 H, m), 6.69 (2 H, dd, *J* = 7.4 Hz, 4.8 Hz), 3.83 (2 H, s), 2.24 (6 H, d, *J* = 5.2 Hz). ^{13}CNMR (101 MHz, $CDCl_3$): 150.2, 131.27, 130.7, 128.5, 126.9, 115.8, 31.1, 20.5, 20.5

4.5.4 Synthesis of diglycidyl ether IV-10

A mixture of bisphenol **IV-9** (5 g, 21.9 mmol), TBAB (0.10 g) and epichlorohydrin (16.5 mL, 22.2 mmol) was stirred at 80 ºC for 3h. The mixture was cooled and NaOH (5 M, 16.5 mL) was added then continued to stir for 1h. Ethyl acetate (20 mL) and water (20 mL) was added and the mixture was stirred for another 30 min. The organic layer was isolated and the aqueous solution was extracted with ethyl acetate (3 x 20 mL). The combined organic layers were dried over Na_2SO_4 and concentrated under vacuum. The crude products were purified by column chromatography on silica gel (hexane/ethyl acetate = 2:1) to give diglycidyl ether **IV-10** (3.25 g, 9.5 mmol, 44%) as white solid.

^{1}HNMR (400 MHz, $CDCl_3$): 6.94 (4 H, d, *J* = 6.9 Hz), 6.73 (2 H, d, *J* = 8.9 Hz), 4.14 (2 H, dd, *J* = 11.5 Hz, 5.7 Hz), 3.97 (1 H, dd, *J* = 5.3 Hz, 2.5 Hz), 3.96 - 3.93 (3 H, m), 3.34 - 3.27 (2 H, m), 2.85 (2 H, t, *J* = 4.6 Hz), 2.69 (2 H, dd, *J* = 5.0 Hz, 2.6 Hz), 2.22 (3 H, s).

^{13}CNMR (101 MHz, $CDCl_3$): 154.4, 131.5, 130.2, 129.5, 127.3, 111.7, 69.1, 50.3, 44.7, 29.9, 20.5. HRMS (ESI) m/z $[M + H]^+$ *calcd* for $C_{21}H_{24}O_4$ 341.1753, found 341.1748.

Chapter 5 Conclusions and Future directions

5.1 Conclusions

In this work we studied oxidative degradation of lignin through a two-step oxidation approach and investigated utilization of lignin-derived materials (monomers and oligomers) as building blocks for epoxy resin. We conducted oxidation of lignin models under both stoichiometric and aerobic catalytic systems to see how different lignin linkages respond under same conditions. Mechanochemical pre-treatment on lignin was applied to facilitate the two-step oxidative depolymerization. To investigate a potential use of these oxidized materials, epoxy thermosets were prepared from a set of lignin-derived aromatic acids as well as from the ethyl acetate soluble fractions after the two-step oxidation of the mechanochemical treated kraft lignin. Future research can now focus on formulation of epoxy resins that are both thermally and mechanically competitive with commercialized but that employ little-to-no BPA/BPF-based resins, avoiding both the health hazards of these materials and the fossil resources used to make them.

There have been numerous reports on methods for the oxidative cleavage of β-O-4 linkages in lignin model compounds, but relatively few reports of how those methods affect other linkages that are present in lignin. In this dissertation we investigated the effect of several of these oxidation methods on the β-1 and the β-5 lignin linkages, using four β-1 and β-5 model compounds. Interestingly, different TEMPO-based oxidation systems produced different arrays of products. Based on the result reported here, it is clear that the 're-oxidants' used ($NaNO_2/O_2$, $Fe(NO_3)_3/O_2$, and $CuCl/O_2$) are not completely innocent - they play roles as oxidants beyond just the re-oxidation of TEMPO. We observed that direct oxidative cleavage

of C-C bonds occurs in metal-catalyzed TEMPO oxidation systems and with iron porphyrin oxidations, neither of which had produced C-C bond cleavage in similar oxidations of β-O-4 models. The β-5 linkage proved to be largely resistant to all of these oxidative systems, but the dihydrofuran ring in the β-5 model **3** was opened when treated with $KMnO_4$ at elevated temperature. The most promising reaction we found was the oxidation of β-1 model **2** with DDQ, which produced the benzylic ketone in high yield (84%), as it does in reactions with β-O-4 models. This reaction exhibits selectivity for the benzylic position as well as compatibility with phenols, characteristics that are highly desirable for a two-step, benzylic oxidation/Baeyer-Villiger route to cleavage of lignin.

Conversion of biomass into usable fuels and chemicals, especially under very low-cost processing, remains a major challenge. Mechanochemical treatment of lignin can greatly improve the yield of monomer products that can be obtained by oxidative deconstruction. In this study we applied a mechanochemical approach, using ring-and-puck milling with KOH in a solvent-free system to promote lignin degradation. We investigated how milling with this larger-scale method would affect the success of a two-step oxidative lignin deconstruction strategy in which we previously employed small-scale ball milling. We monitored changes in lignin structure and functionality using HSQC and ^{31}P NMR spectroscopy.

^{31}P NMR indicated that 2 hours of ring-and-puck milling can generate significant amounts of aliphatic OH's and phenols. Dramatic simplification of the HSQC spectra and a pronounced downfield shift in NMR resonances (to δH = 8.5 and 8.8 ppm) after porphyrin oxidation suggests that ring-and-puck milling produced a significantly different set of reactions and products than is produced by the ball-milling technique we used in a previous

study. Also in contrast to our findings with ball-milled material, porphyrin oxidation of the ring-and-puck milled material produced new products that could not be reduced with $NaBH_4$ to reform the starting material. In addition, Baeyer-Villiger oxidation produced a remarkable increase in the amount of the ethyl acetate-soluble portion, as well as a decrease in the insoluble solid, as compared to the amounts obtained from the ball-milling process. A short 2-hour period of ring-and-puck milling produced nearly half the amount of vanillic acid (isolated as the methyl ester) as was previously isolated after an extended (48 hour) period of ball-milling. The significant changes in the HSQC spectrum, the irreversibility of the oxidation step, as well as the dramatic increase in ethyl acetate soluble products suggest that previously unobserved chemistry is taking place.

Different reactivity of β-1 and β-5 from β-O-4 linkages under the same oxidative conditions could significantly impact the formation and distribution of monomers. In an oxidation-reduction lignin decomposition strategy, Li and coworkers[226] found that DDQ pretreated lignin led to lower yield of monomers and soluble aromatic fractions when using W_2C/AC and 4 other catalysts. Although β-O-4 linkages were oxidized into corresponding carbonyl-containing structures, these β-5 linkages remained robust and were converted into α, β-unsaturated phenylcoumarans, which were even more difficult to cleave. This result again implies that only breaking the dominate β-O-4 linkages can not liberate large quantities of monomers, and oxidation of other linkages should also be important.

Kraft lignin is usually processed in harsh conditions which leads to irreversible and severe structures changes and this highly modified lignin is hydrophobic but possess lower molecular weight than raw lignin though.[16] Oxidative approaches of kraft lignin degradation

were widely reported. For instance, Rohr and coworkers[227] obtained vanillin and methyl vanillate in 5 wt% yield (based on kraft lignin) and *ca*. 60% oligomeric materials when using $H_3PMo_{12}O_{40}$ in methanol at 170 ^oC in 20 mins. Co(salen)/Y-IM was applied to convert kraft pulp lignin to guaiacol in 46% yield in water/MeOH with peracetic acid by Zhou.[228] Gao and coworkers obtained monomers including syringaldehyde, vanillin and 2,6-dimethoxyphenol in 23.3% yield using H_2O_2 as the oxidant with a Cu(salen) powder with an interconnected 3D-network.[229] Shatterbox milling was initially designed to grind large quantities of coals and rocks; the great force impact and shear forces generated between metal parts and lignin powders demonstrated that novel chemistry occurred during milling progress. Employing this Shatterbox milling, followed by our two-step oxidative lignin degradation approach, in our study we can isolate 3.1 wt % of methyl vanillate from the 2h-Shatterbox-milled KL and 45% of soluble fractions (both based on dry kraft lignin).[210]

5.2 Future work

Lignin is a three-dimensional bio-polymer that consists of complicated linkages, while all the model compounds we studied possess only one representative linkage (β-1, β-5 or β-O-4). The selectivity of oxidations of trimers or tetramers composed of more than one type of linkages should be investigated as lignin-derived fragments usually possess multiple linkages. Such a study would provide additional insight in the relative reactivity of the different linkages.

Large quantities of free phenols exist in lignin and DDQ exhibited surprising compatibility with all β-1, β-5 and β-O-4 phenolic model compounds in our studies. We

applied iron (III) porphyrin oxidations in our previous ball-milled kraft lignin and in Shatterbox milled kraft lignin in this study, although iron (III) porphyrin seems not to be an entirely compatible oxidant since oxidation of phenolic model linkages all gave chromatographically immobile materials. In contrast, during our two-step oxidative depolymerization approach, future work should consider using DDQ-based oxidation on mechanochemically treated kraft lignin, with the hopes of increasing the monomer yields.

Epoxy resins prepared from lignin-derived materials are thermally competitive though much worse mechanically. To achieve higher glass transition temperature, modifications such as the introduction of long linear chains is helpful as backbone rotational freedom degree can be decreased. Our work showed that replacement of BPA or BPF with 50% lignin-derived materials dramatically decreases the storage modulus and T_g of the cured thermosets. Experiments at lower levels of substitution of lignin-derived materials for BPA/BPF (5%, 10%, 20%...) would provide insight into how much lignin-derived material can be incorporated while in retaining useful thermal and mechanical properties in the resulting thermoset.

References

1. http://biomasspower.gov.in/document/Reports/BP%20statistical%20review-2015.pdf (accessed February 26, 2019).
2. International Energy Agency http://www.worldenergyoutlook.org/media/weowebsite/2008-1994/weo_2007.pdf (accessed February 26, 2019).
3. The Renewable Energy Policy Network for the 21st Century http://www.ren21.net/wp-content/uploads/2016/10/REN21_GSR2016_FullReport_en_11.pdf (accessed February 26, 2019).
4. C. H. Zhou, J. N. Beltramini, Y. X. Fan, G. Q. Lu, *Chem. Soc. Rev.*, 2008**, 37**, 527-549.
5. T. E. Amidon, S. Liu, *Biotechnol. Adv.*, 2009**, 27**, 542-550.
6. Z. Zhang, M. D. Harrison, D. W. Rackemann, W. O. S. Doherty, I. M. O'Hara, *Green Chem.*, 2016**, 18**, 360-381.
7. V. Balan, *ISRN Biotechnol*, 2014**, 2014**, 463074.
8. J. Zakzeski, P. C. Bruijnincx, A. L. Jongerius, B. M. Weckhuysen, *Chem. Rev.*, 2010**, 110**, 3552-3599.
9. R. Shalini, D. Gupta, *J. Food Sci. Technol.*, 2010**, 47**, 365-371.
10. B. M. Upton, A. M. Kasko, *Chem. Rev.*, 2015**, 116**, 2275-2306.
11. L. Hu, H. Pan, Y. Zhou, M. Zhang, *BioResources*, 2011**, 6**, 3515-3525.
12. A. V. a. A. Kraslawski, *BioResources*, 2011**, 6**, 3547-3568.
13. R. Davis, L. Tao, E. Tan, M. Biddy, G. Beckham, C. Scarlata, J. Jacobson, K. Cafferty, J. Ross, J. Lukas *Process design and economics for the conversion of lignocellulosic biomass to hydrocarbons: dilute-acid and enzymatic deconstruction of biomass to sugars and biological conversion of sugars to hydrocarbons*; NREL/TP-5100-62498; National Renewable Energy Laboratory, 2013, 10.2172/1107470: 2013.
14. D. Carpenter, T. L. Westover, S. Czernik, W. Jablonski, *Green Chem.*, 2014**, 16**, 384-406.
15. W.-J. Liu, H. Jiang, H.-Q. Yu, *Green Chem.*, 2015**, 17**, 4888-4907.
16. C. Li, X. Zhao, A. Wang, G. W. Huber, T. Zhang, *Chem. Rev.*, 2015**, 115**, 11559-11624.
17. F. G. Calvo-Flores, J. A. Dobado, *ChemSusChem*, 2010**, 3**, 1227-1235.
18. E. Adler, *Wood Sci. Technol.*, 1977**, 11**, 169-218.
19. E. Dorrestijn, L. J. Laarhoven, I. W. Arends, P. Mulder, *J. Anal. Appl. Pyrolysis*, 2000**, 54**, 153-192.
20. D. V. Evtuguin, C. P. Neto, A. M. Silva, P. M. Domingues, F. M. Amado, D. Robert, O. Faix, *J. Agric. Food. Chem.*, 2001**, 49**, 4252-4261.
21. P. Gallezot, *Catal. Today*, 2007**, 121**, 76-91.
22. C. Awungacha Lekelefac, N. Busse, M. Herrenbauer, P. Czermak, *Int. J. Photoenergy*, 2014**, 2015**, 1-18.
23. R. Ma, M. Guo, X. Zhang, *Catal. Today*, 2018**, 302**, 50-60.

24. M. P. Pandey, C. S. Kim, *Chem. Eng. Technol.*, 2011**, 34**, 29-41.
25. V. Taraban'ko, N. Koropatchinskaya, A. Kudryashev, B. Kuznetsov, *Russ. Chem. Bull.*, 1995**, 44**, 367-371.
26. P. C. Rodrigues Pinto, E. A. Borges da Silva, A. r. E. d. Rodrigues, *Ind. Eng. Chem. Res.*, 2010**, 50**, 741-748.
27. A. J. Fatiadi, *Synthesis*, 1987**, 1987**, 85-127.
28. D. Lee, Hydrocarbon oxidation using transition metal compounds. Dekker: New York: 1969; Vol. 1, pp 1-51.
29. K. Stärk, N. Taccardi, A. Bösmann, P. Wasserscheid, *ChemSusChem*, 2010**, 3**, 719-723.
30. W. Partenheimer, *Adv. Synth. Catal.*, 2009**, 351**, 456-466.
31. B. P. Joshi, A. Sharma, A. K. Sinha, *Tetrahedron*, 2006**, 62**, 2590-2593.
32. L. Liu, P. E. Floreancig, *Org. Lett.*, 2009**, 11**, 3152-3155.
33. K. Peng, F. Chen, X. She, C. Yang, Y. Cui, X. Pan, *Tetrahedron Lett.*, 2005**, 46**, 1217-1220.
34. K. Mori, K. Koseki, *Tetrahedron*, 1988**, 44**, 6013-6020.
35. M. A. Rahim, S. Matsumura, K. Toshima, *Tetrahedron Lett.*, 2005**, 46**, 7307-7309.
36. G. Sharma, B. Srinivas, P. R. Krishna, *Tetrahedron Lett.*, 2003**, 44**, 4689-4691.
37. D. Cheng, W. Bao, *J. Org. Chem.*, 2008**, 73**, 6881-6883.
38. D. Ramesh, U. Ramulu, S. Rajaram, P. Prabhakar, Y. Venkateswarlu, *Tetrahedron Lett.*, 2010**, 51**, 4898-4903.
39. W. Tu, P. E. Floreancig, *Angew. Chem.*, 2009**, 121**, 4637-4641.
40. J. Chang, K. Zhao, S. Pan, *Tetrahedron Lett.*, 2002**, 43**, 951-954.
41. F. Tran, C. S. Lancefield, P. C. J. Kamer, T. Lebl, N. J. Westwood, *Green Chem.*, 2015**, 17**, 244-249.
42. C. S. Lancefield, O. S. Ojo, F. Tran, N. J. Westwood, *Angew. Chem., Int. Ed.*, 2015**, 54**, 258-262.
43. L. Wang, J. Li, H. Yang, Y. Lv, S. Gao, *J. Org. Chem.*, 2012**, 77**, 790-794.
44. P. J. Figiel, A. Sibaouih, J. U. Ahmad, M. Nieger, M. T. Räisänen, M. Leskelä, T. Repo, *Adv. Synth. Catal.*, 2009**, 351**, 2625-2632.
45. R. A. Sheldon, I. W. Arends, G.-J. ten Brink, A. Dijksman, *Acc. Chem. Res.*, 2002**, 35**, 774-781.
46. F. Minisci, F. Recupero, G. F. Pedulli, M. Lucarini, *J. Mol. Catal. A: Chem.*, 2003**, 204**, 63-90.
47. G. Csjernyik, A. H. Éll, L. Fadini, B. Pugin, J.-E. Bäckvall, *J. Org. Chem.*, 2002**, 67**, 1657-1662.
48. J. Muzart, *Tetrahedron*, 2003**, 59**, 5789-5816.
49. X. Wang, R. Liu, Y. Jin, X. Liang, *Chem.–Eur. J*, 2008**, 14**, 2679-2685.
50. C. L. Hill, *Angew. Chem.*, 2004**, 116**, 406-408.
51. A. Rahimi, A. Azarpira, H. Kim, J. Ralph, S. S. Stahl, *J. Am. Chem. Soc.*, 2013**, 135**, 6415-6418.
52. A. Rahimi, A. Ulbrich, J. J. Coon, S. S. Stahl, *Nature*, 2014**, 515**, 249-252.

53. M. Wang, J. Lu, X. Zhang, L. Li, H. Li, N. Luo, F. Wang, *ACS Catal.*, 2016**, 6**, 6086-6090.
54. E. Hagglund, C. Bjorkman, *Biochem. Z*, 1924**, 147**, 74.
55. V. Roberts, S. Fendt, A. A. Lemonidou, X. Li, J. A. Lercher, *Applied Catalysis B: Environmental*, 2010**, 95**, 71-77.
56. M. Meshgini, K. V. Sarkanen, Synthesis and kinetics of acid-catalyzed hydrolysis of some α-aryl ether lignin model compounds. 1989.
57. V. M. Roberts, R. T. Knapp, X. Li, J. A. Lercher, *ChemCatChem*, 2010**, 2**, 1407-1410.
58. J. B, G. MIKSCHE, *Acta Chem. Scand.*, 1972**, 26**, 289.
59. S. Jia, B. J. Cox, X. Guo, Z. C. Zhang, J. G. Ekerdt, *ChemSusChem*, 2010**, 3**, 1078-1084.
60. K. V. Sarkanen, L. H. Hoo, *J. Wood Chem. Technol.*, 1981**, 1**, 11-27.
61. T. Imai, T. Yokoyama, Y. Matsumoto, *Journal of wood science*, 2011**, 57**, 219-225.
62. T. Yokoyama, *J. Wood Chem. Technol.*, 2015**, 35**, 27-42.
63. O. Karlsson, *Acta Chem Scand B*, 1988**, 42**, 48-51.
64. W. Schutyser, T. Renders, S. Van den Bosch, S. F. Koelewijn, G. T. Beckham, B. F. Sels, *Chem. Soc. Rev.*, 2018**, 47**, 852-908.
65. M. M. Hepditch, R. W. Thring, *Can. J. Chem. Eng.*, 2000**, 78**, 226-231.
66. H. Yu, J. Hu, J. Fan, J. Chang, *Ind. Eng. Chem. Res*, 2012**, 51**, 3452-3457.
67. P. J. Deuss, M. Scott, F. Tran, N. J. Westwood, J. G. de Vries, K. Barta, *J. Am. Chem. Soc.*, 2015**, 137**, 7456-7467.
68. B. J. Cox, S. Jia, Z. C. Zhang, J. G. Ekerdt, *Polym. Degrad. Stab.*, 2011**, 96**, 426-431.
69. B. J. Cox, J. G. Ekerdt, *Bioresour. Technol.*, 2012**, 118**, 584-588.
70. S. Jia, B. J. Cox, X. Guo, Z. C. Zhang, J. G. Ekerdt, *Ind. Eng. Chem. Res*, 2010**, 50**, 849-855.
71. C. W. Lahive, Deuss, P.J., Lancefield, C.S., Sun, Z., Cordes, D.B., Young, C.M., Tran, F., Slawin, A.M., de Vries, J.G., Kamer, P.C. and Westwood, N.J., *J. Am. Chem. Soc.*, 2016**, 138**, 8900-8911.
72. P. J. Deuss, Lahive, C.W., Lancefield, C.S., Westwood, N.J., Kamer, P.C., Barta, K. and de Vries, J.G., *ChemSusChem*, 2016**, 9**, 2974-2981.
73. V. Roberts, V. Stein, T. Reiner, A. Lemonidou, X. Li, J. A. Lercher, *Chem. Eur. J*, 2011**, 17**, 5939-5948.
74. A. Toledano, L. Serrano, J. Labidi, *J. Chem. Technol. Biotechnol.*, 2012**, 87**, 1593-1599.
75. J. E. E. Miller, L.; Littlewolf, A.; Trudell, D. E., *Fuel*, 1999**, 78**, 1363-1366.
76. F. S. Chakar, A. J. Ragauskas, *Ind Crops Prod.*, 2004**, 20**, 131-141.
77. J. Gierer, *Wood Sci. Technol.*, 1985**, 19**, 289-312.
78. J. Gierer, *Holzforschung*, 1982**, 36**, 43-51.
79. S. Jia, B. J. Cox, X. Guo, Z. C. Zhang, J. G. Ekerdt, *Holzforschung*, 2010**, 64**, 577-580.

80. K. E. Achyuthan, A. M. Achyuthan, P. D. Adams, S. M. Dirk, J. C. Harper, B. A. Simmons, A. K. Singh, *Molecules*, 2010**, 15**, 8641-8688.
81. M. J. Taherzadeh, K. Karimi, *Int. J. Mol. Sci.*, 2008**, 9**, 1621-1651.
82. A. Tolbert, H. Akinosho, R. Khunsupat, A. K. Naskar, A. J. Ragauskas, *Biofuels, Bioprod. Bioref.*, 2014**, 8**, 836-856.
83. Y. Sun, J. Cheng, *Bioresour. Technol.*, 2002**, 83**, 1-11.
84. V. S. Chang, M. T. Holtzapple, *Appl. Biochem. Biotechnol.*, 2000**, 84**, 5-37.
85. A. Guerra, I. Filpponen, L. A. Lucia, C. Saquing, S. Baumberger, D. S. Argyropoulos, *J. Agric. Food. Chem.*, 2006**, 54**, 5939-5947.
86. A. Björkman, *Nature*, 1954**, 174**, 1057.
87. Z. Hu, T.-F. Yeh, H.-m. Chang, Y. Matsumoto, J. F. Kadla, *Holzforschung*, 2006**, 60**, 389-397.
88. S. A. Wu, D. S. , *J. Pulp. Pap. Sci.*, 2003**, 29**, 235-240.
89. T. Ikeda, K. Holtman, J. F. Kadla, H.-m. Chang, H. Jameel, *J. Agric. Food. Chem.*, 2002**, 50**, 129-135.
90. H.-M. Wang, B. Wang, J.-L. Wen, T.-Q. Yuan, R.-C. Sun, *ACS Sustainable Chem. Eng.*, 2017**, 5**, 11618-11627.
91. H.-m. Chang, E. B. Cowling, W. Brown, *Holzforschung*, 1975**, 29**, 153-159.
92. Y. Qu, H. Luo, H. Li, J. Xu, *Biotech. Rep.*, 2015**, 6**, 1-7.
93. T. De Vrije, G. De Haas, G. Tan, E. Keijsers, P. Claassen, *Int. J. Hydrogen Energy*, 2002**, 27**, 1381-1390.
94. A. Fujimoto, Y. Matsumoto, H.-M. Chang, G. Meshitsuka, *J. Wood Sci.*, 2005**, 51**, 89-91.
95. Z. Yuan, S. Cheng, M. Leitch, C. C. Xu, *Bioresour. Technol.*, 2010**, 101**, 9308-9313.
96. T. Kleine, J. Buendia, C. Bolm, *Green Chem.*, 2013**, 15**, 160-166.
97. M. D. Kaufman Rechulski, M. Käldström, U. Richter, F. Schüth, R. Rinaldi, *Ind. Eng. Chem. Res.*, 2015**, 54**, 4581-4592.
98. Z. Sun, B. Fridrich, A. de Santi, S. Elangovan, K. Barta, *Chem. Rev.*, 2018**, 118**, 614-678.
99. L. D. Duong, G.-Y. Nam, J.-S. Oh, I.-K. Park, N. D. Luong, H.-K. Yoon, S.-H. Lee, Y. Lee, J.-H. Yun, C.-G. Lee, S.-H. Hwang, *BioResources*, 2014**, 9**, 2359-2371.
100. B.-L. Xue, J.-L. Wen, R.-C. Sun, *ACS Sustainable Chem. Eng.*, 2014**, 2**, 1474-1480.
101. H. W. Chung, N. R., *ACS Appl. Mater. Interfaces*, 2012**, 4**, 2840-2846.
102. N. T. Thanh Binh, N. D. Luong, D. O. Kim, S. H. Lee, B. J. Kim, Y. S. Lee, J.-D. Nam, *Compos. Interfaces*, 2009**, 16**, 923-935.
103. R. Auvergne, S. Caillol, G. David, B. Boutevin, J. P. Pascault, *Chem. Rev.*, 2014**, 114**, 1082-1115.
104. P. Fenichel, N. Chevalier, F. Brucker-Davis, *Annales d'endocrinologie*, 2013**, 74**, 211-220.
105. J. Michalowicz, *Environ. Toxicol. Pharmacol.*, 2014**, 37**, 738-758.
106. M. Green, H. Wittcoff, *Organic chemistry principles and industrial practice*, Wiley-VCH, Weinheim, 2003.

107. G. Engelmann, J. Ganster, *Holzforschung*, 2014**, 68**, 435-446.
108. L. C. Over, E. Grau, S. Grelier, M. A. R. Meier, H. Cramail, *Macromol. Chem. Phys.*, 2017**, 218**, 1600411.
109. A. G. Llevot, E.; Carlotti, S.; Grelier, S.; Cramail, H., *Macromol. Rapid Commun.*, 2016**, 37**, 9-28.
110. E. A. B. d. Silva, M. Zabkova, J. D. Araújo, C. A. Cateto, M. F. Barreiro, M. N. Belgacem, A. E. Rodrigues, *Chem. Eng. Res. Des.*, 2009**, 87**, 1276-1292.
111. M. Fache, E. Darroman, V. Besse, R. Auvergne, S. Caillol, B. Boutevin, *Green Chem.*, 2014**, 16**, 1987-1998.
112. M. Fache, B. Boutevin, S. Caillol, *Green Chem.*, 2016**, 18**, 712-725.
113. S. Zhao, M. M. Abu-Omar, *Macromolecules*, 2017**, 50**, 3573-3581.
114. C. Aouf, J. Lecomte, P. Villeneuve, E. Dubreucq, H. Fulcrand, *Green Chem.*, 2012**, 14**, 2328.
115. N. D. Patil, S. G. Yao, M. S. Meier, J. K. Mobley, M. Crocker, *Org. Biomol. Chem.*, 2015**, 13**, 3243-3254.
116. A. Sakakibara, *Wood Sci. Technol.*, 1980**, 14**, 89-100.
117. R. Rinaldi, R. Jastrzebski, M. T. Clough, J. Ralph, M. Kennema, P. C. Bruijnincx, B. M. Weckhuysen, *Angew. Chem. Int. Ed. Engl.*, 2016**, 55**, 8164-8215.
118. C. Crestini, M. D'Auria, *Tetrahedron*, 1997**, 53**, 7877-7888.
119. C. Amen-Chen, H. Pakdel, C. Roy, *Bioresour. Technol.*, 2001**, 79**, 277-299.
120. Y. S. Kim, H.-m. Chang, J. F. Kadla, *Holzforschung*, 2008**, 62**, 38-49.
121. N. D. Patil, S. G. Yao, M. S. Meier, J. K. Mobley, M. Crocker, *Org. Biomol. Chem.*, 2015**, 13**, 3243-3254.
122. D. W. Cho, R. Parthasarathi, A. S. Pimentel, G. D. Maestas, H. J. Park, U. C. Yoon, D. Dunaway-Mariano, S. Gnanakaran, P. Langan, P. S. Mariano, *J. Org. Chem.*, 2010**, 75**, 6549-6562.
123. G. Brunow, K. Lundquist, *Acta Chem. Scand. 1984, B38, 335-336.*, 1984**, 38**, 335-336.
124. G. Tojo, M. I. Fernández, *Oxidation of alcohols to aldehydes and ketones: a guide to current common practice*. Springer Science & Business Media: 2006.
125. L. Paquette, M. Earle, G. Smith, *Organic syntheses*, 1996**, 73**, 36-43.
126. Y. Tu, M. Frohn, Z. X. Wang, Y. Shi, *Org. Synth.*, 2003**, 80**, 1-8.
127. L. Paquette, T. Heidelbaugh, *Org. Synth.*, 1996**, 73**, 44-49.
128. J. March, *Advanced organic chemistry: reactions, mechanisms, and structure*. John Wiley & Sons: 1992.
129. J. Villar, A. Caperos, F. Garcia-Ochoa, *Wood Sci. Technol.*, 2001**, 35**, 245-255.
130. T. Mallat, A. Baiker, *Chem. Rev.*, 2004**, 104**, 3037-3058.
131. I. E. Marko, A. Gautier, R. Dumeunier, K. Doda, F. Philippart, S. M. Brown, C. J. Urch, *Angew. Chem. Int. Ed.*, 2004**, 43**, 1588-1591.
132. K. M. Gligorich, M. S. Sigman, *Angew. Chem. Int. Ed.*, 2006**, 45**, 6612-6615.
133. M. Wang, L. Li, J. Lu, H. Li, X. Zhang, H. Liu, N. Luo, F. Wang, *Green Chem.*, 2017**, 19**, 702-706.
134. B. Sedai, C. Díaz-Urrutia, R. T. Baker, R. Wu, L. A. P. Silks, S. K. Hanson, *ACS Catal.*, 2013**, 3**, 3111-3122.

135. S. K. Bose, R. C. Francis, M. Govender, T. Bush, A. Spark, *Bioresour. Technol.*, 2009**, 100**, 1628-1633.
136. F. M. Menger, D. W. Carnahan, *J. Org. Chem.*, 1985**, 50**, 3927-3928.
137. R. DiCosimo, H. C. Szabo, *J. Org. Chem.*, 1988**, 53**, 1673-1679.
138. E. A. I. Heiba, R. M. Dessau, W. J. Koehl Jr, *J. Am. Chem. Soc.*, 1969**, 91**, 6830-6837.
139. C. C. Cosner, P. J. Cabrera, K. M. Byrd, A. M. A. Thomas, P. Helquist, *Org. Lett.*, 2011**, 13**, 2071-2073.
140. Z. Shen, J. Dai, J. Xiong, X. He, W. Mo, B. Hu, N. Sun, X. Hu, *Adv. Synth. Catal.*, 2011**, 353**, 3031-3038.
141. W. Zhang, H. Ma, L. Zhou, Z. Sun, Z. Du, H. Miao, J. Xu, *Molecules*, 2008**, 13**, 3236-3245.
142. W. Wang, T. Li, G. Attardo, *J. Org. Chem*, 1997**, 62**, 6598-6602.
143. P. G. Wang, M. Xian, X. Tang, X. Wu, Z. Wen, T. Cai, A. J. Janczuk, *Chem. Rev.*, 2002**, 102**, 1091-1134.
144. H. Guo, Daniel M. Miles-Barrett, A. R. Neal, T. Zhang, C. Li, N. J. Westwood, *Chem. Sci.*, 2018**, 9**, 702-711.
145. A. T. Radosevich, C. Musich, F. D. Toste, *J. Am. Chem. Soc.*, 2005**, 127**, 1090-1091.
146. C.-T. Chen, J.-Q. Kao, S. B. Salunke, Y.-H. Lin, *Org. Lett.*, 2010**, 13**, 26-29.
147. Q.-X. Guo, Z.-J. Wu, Z.-B. Luo, Q.-Z. Liu, J.-L. Ye, S.-W. Luo, L.-F. Cun, L.-Z. Gong, *J. Am. Chem. Soc.*, 2007**, 129**, 13927-13938.
148. S. K. Hanson, R. T. Baker, J. C. Gordon, B. L. Scott, A. D. Sutton, D. L. Thorn, *J. Am. Chem. Soc.*, 2008**, 131**, 428-429.
149. S. Son, F. D. Toste, *Angew. Chem. Int. Ed.*, 2010**, 49**, 3791-3794.
150. S. K. Hanson, R. Wu, L. A. Silks, *Angew. Chem. Int. Ed.*, 2012**, 51**, 3410-3413.
151. J. M. Chan, S. Bauer, H. Sorek, S. Sreekumar, K. Wang, F. D. Toste, *ACS Catal.*, 2013**, 3**, 1369-1377.
152. Y. Ma, Z. Du, J. Liu, F. Xia, J. Xu, *Green Chem.*, 2015**, 17**, 4968-4973.
153. R. Liu, X. Liang, C. Dong, X. Hu, *J. Am. Chem. Soc.*, 2004**, 126**, 4112-4113.
154. Y. Xie, W. Mo, D. Xu, Z. Shen, N. Sun, B. Hu, X. Hu, *J. Org. Chem*, 2007**, 72**, 4288-4291.
155. T. Miyazawa, T. Endo, S. Shiihashi, M. Okawara, *J. Org. Chem*, 1985**, 50**, 1332-1334.
156. D. Hunter, D. Barton, W. Motherwell, *Tetrahedron Lett.*, 1984**, 25**, 603-606.
157. B. Sedai, C. Díaz-Urrutia, R. T. Baker, R. Wu, L. P. Silks, S. K. Hanson, *ACS Catal.*, 2011**, 1**, 794-804.
158. N. D. Patil, N. Yan, *Tetrahedron Lett.*, 2016**, 57**, 3024-3028.
159. C. Díaz-Urrutia, B. Sedai, K. C. Leckett, R. T. Baker, S. K. Hanson, *ACS Sustain. Chem. Eng.*, 2016**, 4**, 6244-6251.
160. J. M. Hoover, B. L. Ryland, S. S. Stahl, *ACS Catal.*, 2013**, 3**, 2599-2605.
161. J. M. Hoover, S. S. Stahl, *J. Am. Chem. Soc.*, 2011**, 133**, 16901-16910.
162. B. Sedai, R. T. Baker, *Adv. Synth. Catal.*, 2014**, 356**, 3563-3574.

163. S. Ma, J. Liu, S. Li, B. Chen, J. Cheng, J. Kuang, Y. Liu, B. Wan, Y. Wang, J. Ye, *Adv. Synth. Catal.*, 2011**, 353**, 1005-1017.
164. S. G. Yao, M. S. Meier, R. B. Pace Iii, M. Crocker, *RSC Adv.*, 2016**, 6**, 104742-104753.
165. S. K. Boovanahalli, D. W. Kim, D. Y. Chi, *J. Org. Chem*, 2004**, 69**, 3340-3344.
166. J. Li, G. Henriksson, G. Gellerstedt, *Bioresour. Technol.*, 2007**, 98**, 3061-3068.
167. K. Okuda, M. Umetsu, S. Takami, T. Adschiri, *Fuel Process. Technol.*, 2004**, 85**, 803-813.
168. U. Wongsiriwan, Y. Noda, C. Song, P. Prasassarakich, Y. Yeboah, *Energy Fuels*, 2010**, 24**, 3232-3238.
169. J. Long, Y. Xu, T. Wang, Z. Yuan, R. Shu, Q. Zhang, L. Ma, *Applied Energy*, 2015**, 141**, 70-79.
170. J. Ralph, S. Quideau, J. H. Grabber, R. D. Hatfield, *J. Chem. Soc., Perkin Trans. 1*, 1994, 3485-3498.
171. C. Crestini, A. Pastorini, P. Tagliatesta, *J. Mol. Catal. A: Chem.*, 2004**, 208**, 195-202.
172. C. Crestini, M. Crucianelli, M. Orlandi, R. Saladino, *Catal. Today*, 2010**, 156**, 8-22.
173. K. Alagiri, K. R. Prabhu, *Tetrahedron*, 2011**, 67**, 8544-8551.
174. H. Zhao, Q. Chen, L. Wei, Y. Jiang, M. Cai, *Tetrahedron*, 2015**, 71**, 8725-8731.
175. A. D. Brittain, N. J. Chrisandina, R. E. Cooper, M. Buchanan, J. R. Cort, M. V. Olarte, C. Sievers, *Catal. Today*, 2018**, 302**, 180-189.
176. U. Mais, A. R. Esteghlalian, J. N. Saddler, S. D. Mansfield, *Appl. Biochem. Biotechnol.*, 2002**, 98**, 815.
177. F. Schneider, T. Szuppa, A. Stolle, B. Ondruschka, H. Hopf, *Green Chem.*, 2009**, 11**, 1894-1899.
178. S. G. Yao, J. K. Mobley, J. Ralph, M. Crocker, S. Parkin, J. P. Selegue, M. S. Meier, *ACS Sustainable Chem. Eng.*, 2018**, 6**, 5990-5998.
179. S. Dabral, H. Wotruba, J. G. Hernández, C. Bolm, *ACS Sustainable Chem. Eng.*, 2018**, 6**, 3242-3254.
180. D. A. Pienkowski, R. J. Andrews U.S. 6599961B1, 2003.
181. V. A. Gostin, P. W. Haines, R. J. Jenkins, W. Compston, I. S. Williams, *Science*, 1986**, 233**, 198-200.
182. T. Q. Yuan, S. N. Sun, F. Xu, R. C. Sun, *J. Agric. Food. Chem.*, 2011**, 59**, 10604-10614.
183. J. C. del Rio, J. Rencoret, G. Marques, J. Li, G. Gellerstedt, J. Jimenez-Barbero, A. T. Martinez, A. Gutierrez, *J. Agric. Food. Chem.*, 2009**, 57**, 10271-10281.
184. Z. Fang, M. S. Meier, *Org. Biomol. Chem.*, 2018**, 16**, 2330-2341.
185. S. L. James, C. J. Adams, C. Bolm, D. Braga, P. Collier, T. Friscic, F. Grepioni, K. D. Harris, G. Hyett, W. Jones, A. Krebs, J. Mack, L. Maini, A. G. Orpen, I. P. Parkin, W. C. Shearouse, J. W. Steed, D. C. Waddell, *Chem. Soc. Rev.*, 2012**, 41**, 413-447.

186. F. Schüth, R. Rinaldi, N. Meine, M. Käldström, J. Hilgert, M. D. K. Rechulski, *Catal. Today*, 2014**, 234**, 24-30.
187. G. Yin, F. Jin, G. Yao, Z. Jing, *Ind. Eng. Chem. Res.*, 2015**, 54**, 68-75.
188. D. R. Vardon, M. A. Franden, C. W. Johnson, E. M. Karp, M. T. Guarnieri, J. G. Linger, M. J. Salm, T. J. Strathmann, G. T. Beckham, *Energy Environ. Sci.*, 2015**, 8**, 617-628.
189. F. Cui, D. Dolphin, *Biorg. Med. Chem.*, 1994**, 2**, 735-742.
190. D. S. Argyropoulos, *J. Wood Chem. Technol.*, 1994**, 14**, 45-63.
191. J.-M. Raquez, M. Deléglise, M.-F. Lacrampe, P. Krawczak, *Prog. Polym. Sci.*, 2010**, 35**, 487-509.
192. N. E. El Mansouri, Yuan, Q., , F. Huang, *BioResources*, 2011**, 6**, 2492-2503.
193. G. H. Delmas, B. Benjelloun-Mlayah, Y. L. Bigot, M. Delmas, *J. Appl. Polym. Sci.*, 2013**, 127**, 1863-1872.
194. J. Sun, C. Wang, J. C. C. Yeo, D. Yuan, H. Li, L. P. Stubbs, C. He, *Macromol. Mater. Eng.*, 2016**, 301**, 328-336.
195. N. D. Luong, N. T. T. Binh, L. D. Duong, D. O. Kim, D.-S. Kim, S. H. Lee, B. J. Kim, Y. S. Lee, J.-D. Nam, *Polym. Bull.*, 2011**, 68**, 879-890.
196. D. Evtugin, A. Gandini, *Acta Polym.*, 1996**, 47**, 344-350.
197. G. Griffini, V. Passoni, R. Suriano, M. Levi, S. Turri, *ACS Sustainable Chem. Eng.*, 2015**, 3**, 1145-1154.
198. B.-L. Xue, J.-L. Wen, M.-Q. Zhu, R.-C. Sun, *RSC Adv.*, 2014**, 4**, 36089-36096.
199. F. Ferdosian, Z. Yuan, M. Anderson, C. Xu, *RSC Adv.*, 2014**, 4**, 31745-31753.
200. A. Maiorana, A. F. Reano, R. Centore, M. Grimaldi, P. Balaguer, F. Allais, R. A. Gross, *Green Chem.*, 2016**, 18**, 4961-4973.
201. P.-Y. Kuo, M. Sain, N. Yan, *Green Chem.*, 2014**, 16**, 3483-3493.
202. S. Zhao, M. M. Abu-Omar, *ACS Sustainable Chem. Eng.*, 2017**, 5**, 5059-5066.
203. C. François, S. Pourchet, G. Boni, S. Rautiainen, J. Samec, L. Fournier, C. Robert, C. M. Thomas, S. Fontaine, Y. Gaillard, V. Placet, L. Plasseraud, *C. R. Chimie*, 2017**, 20**, 1006-1016.
204. Y.-L. Chung, J. V. Olsson, R. J. Li, C. W. Frank, R. M. Waymouth, S. L. Billington, E. S. Sattely, *ACS Sustainable Chem. Eng.*, 2013**, 1**, 1231-1238.
205. C. Wang, R. A. Venditti, *ACS Sustainable Chem. Eng.*, 2015**, 3**, 1839-1845.
206. S. Zhao, M. M. Abu-Omar, *Biomacromolecules*, 2015**, 16**, 2025-2031.
207. C. François, S. Pourchet, G. Boni, S. Fontaine, Y. Gaillard, V. Placet, M. V. Galkin, A. Orebom, J. Samec, L. Plasseraud, *RSC Adv.*, 2016**, 6**, 68732-68738.
208. A. Salanti, L. Zoia, M. Orlandi, *Green Chem.*, 2016**, 18**, 4063-4072.
209. A. Kaiho, D. Mazzarella, M. Satake, M. Kogo, R. Sakai, T. Watanabe, *Green Chem.*, 2016**, 18**, 6526-6535.
210. Z. Fang, J. K. Mobley, M. S. Meier, *Energy & Fuels*, 2018**, 32**, 11632-11638.
211. E. D. Hernandez, A. W. Bassett, J. M. Sadler, J. J. La Scala, J. F. Stanzione, *ACS Sustainable Chem. Eng.*, 2016**, 4**, 4328-4339.
212. H. S. Maity, K. Misra, T. Mahata, A. Nag, *RSC Adv.*, 2016**, 6**, 24446-24450.
213. M. Ochi, Shiba, T., Takeuchi, H., Yoshizumi, M. and Shimbo, M., *Polymer*, 1989**, 30**, 1079-1084.

214. H. Le Deit, Cron, S. and Le Corre, M., *Tetrahedron Lett.*, 1991**, 32**, 2759-2762.
215. B. a. R. McKague, D.W., *Environ. Sci. Technol.*, 1994**, 28**, 573-576.
216. B. Roth, Strelitz, J.Z. and Rauckman, B.S., *J. Med. Chem*, 1980**, 23**, 379-384.
217. E. Nifant'ev, A. Teleshev, A. Zhdanov, *Russ. J. Gen. Chem.*, 2002**, 72**, 903-908.
218. M. Li, D. Liu, X.-S. Cong, J.-H. Wu, C.-C. Wu, W. Xia, *Energy Fuels*, 2016**, 30**, 10950-10953.
219. S. Kalakkunnath, D. S. Kalika, H. Lin, B. D. Freeman, *Macromolecules*, 2005**, 38**, 9679-9687.
220. https://www.google.com/search?q=single+cantilever+dma&tbm=isch&tbo=u&source=univ&sa=X&ved=2ahUKEwjFrIXxmYzeAhVJ94MKHUfOAukQsAR6BAgDEAE&biw=1280&bih=597#imgrc=0NTQTAXxEW0VBM: (accessed February 26, 2019).
221. J. Qin, H. Liu, P. Zhang, M. Wolcott, J. Zhang, *Polym. Int.*, 2014**, 63**, 760-765.
222. H. Pan, G. Sun, T. Zhao, G. Wang, *Polym. Eng. Sci.*, 2015**, 55**, 924-932.
223. J. Domínguez, M. Oliet, M. Alonso, M. Gilarranz, F. Rodríguez, *Ind. Crop. Prod.*, 2008**, 27**, 150-156.
224. F. Hu, J. J. La Scala, J. M. Sadler, G. R. Palmese, *Macromolecules*, 2014**, 47**, 3332-3342.
225. F. Hu, S. K. Yadav, J. J. La Scala, J. M. Sadler, G. R. Palmese, *Macromol. Chem. Phys.*, 2015**, 216**, 1441-1446.
226. H. Guo, D. M. Miles-Barrett, B. Zhang, A. Wang, T. Zhang, N. J. Westwood, C. Li, *Green Chemistry*, 2019**, 21**, 803-811.
227. T. Voitl, P. Rudolf von Rohr, *ChemSusChem*, 2008**, 1**, 763-769.
228. X. F. Zhou, *J. Appl. Polym. Sci.*, 2014**, 131**, 40809.
229. J. Dai, A. F. Patti, K. Saito, *Tetrahedron Lett.*, 2016**, 57**, 4945-4951.

Vita

Zhen Fang

Education

M.S., Chemistry, Nankai University, Tianjin, China 2013

B.S., Chemistry, Linyi University, Linyi, China 2010

Professional Positions

Research Assistant (Aug. 2014-present)

University of Kentucky, Lexington, KY, 40503

Research Assistant (Sep. 2010-Jun.2013)

Nankai University, Tinajin, China

Publications and Patents

Zhen Fang, M. C. Weisenberger and M. S. Meier. Towards valorisation of lignin: Investigation of lignin and lignin-derived materials as building blocks for epoxy resins (*ACS Sustainable Chem. Eng., submitted*)

Zhen Fang, M. S. Meier, J. K. Mobley. Effect of a ring-and-puck mill on the two-step oxidative lignin deconstruction approach (Energy Fuels, 2018, **32** (11), 11632–11638)

Zhen Fang, M.S. Meier. Toward the Oxidative Deconstruction of Lignin: Oxidation of β-1 and β-5 Linkages (Org. Biomol. Chem., 2018, **16**, 2330-2341)

Zhen Fang, et al, Preliminary studies on the biological activity and mode of action of wq-C-13. The Proceedings of the 9th National Novel Pesticide Development Conference, April 24-27, 2011, Yangzhou, Jiangsu, China, 40-42.

Y.D. Li, **Zhen Fang**, et al. The Proceedings of the 9th National Novel Pesticide Development Conference, April 24-27, 2011, Yangzhou, Jiangsu, China, 34-36.

S.-X. Wang, **Zhen Fang***, et al. Synthesis of tetrazole containing 1,2,3-thiadiazole derivatives via U-4CR and their anti-TMV activity. Chinese Chemical Letters. 2013, 24: 889-892. (*: co-first author)

S.-X. Wang, **Zhen Fang**, et al. Chin. J. Org. Chem. 2013, 33 (11), 2367-2375.

X.Y. Chen, **Zhen Fang**, et al. Chinese Journal of Pesticide Science. 2013, 15(2), 140-144.

Zhijin Fan, **Zhen Fang**, et al. CN Pat., 201310155458.X. 2013-05-02

Zhijin Fan, **Zhen Fang**, et al. CN Pat., 201310134915.7, 2013-04-18

Zhijin Fan, **Zhen Fang**, et al. CN Pat., CN102174030A. 2011-09-07

Zhijin Fan, **Zhen Fang**, et al. CN Pat., CN102174029A, 2011-09-07

Conferences

Oral presentations at ACS National Meeting

- Effect of a ring-and-puck mill on the two-step oxidative lignin deconstruction approach. (Boston, MA, August 20, 2018)
- Toward the Oxidative Deconstruction of Lignin: Oxidation of β-1 and β-5 Linkages. (New Orleans, LA, March 18, 2018)

China's first pesticide Forum National Conference (Hangzhou, China, 2012)

National 973 pesticides Conference; The Proceedings of the 9th National Novel Pesticide Development Conference (Oral presented, Yangzhou, China, 2011)

Annual Meeting of Element Organic State Key Laboratory of Nankai University (Tianjin, 2010, 2011)

Award

Dissertation Year Award (2018)

Research Challenge Trust Fund (RCTF) scholarship (2017)

Third-class scholarship (2010-2013); Wan Xiang Meeting Scholarship (2011)

Third-class scholarship (2007)